Measurement and Communication Uncertainty in Automated Aircraft Separation Management

A THESIS SUBMITTED TO
THE SCIENCE AND ENGINEERING FACULTY
OF QUEENSLAND UNIVERSITY OF TECHNOLOGY
IN FULFILMENT OF THE REQUIREMENTS FOR THE DEGREE OF
MASTER OF PHILOSOPHY

Jiezhen Sean Fan

Principal Supervisor: Dr. Jason J. Ford

Associate Supervisor: Dr. Felipe L. Gonzalez

Australian Research Centre for Aerospace Automation
Electrical Engineering and Computer Science School
Science and Engineering Faculty
Queensland University of Technology

2016

Copyright in Relation to This Thesis

Statement of Original Authorship

The work contained in this thesis has not been previously submitted to meet requirements for an award at this or any other higher education institution. To the best of my knowledge and belief, the thesis contains no material previously published or written by another person except where due reference is made.

Signature:

Date: 21/05/2016

Abstract

The primary purpose of the air traffic management system (ATM) is to organize and expedite the flow of traffic and to prevent a collision between aircraft operating in the system [1]. However, in recent years, air traffic management systems have faced increasing levels of air traffic. As the airspace has become more congested and ATM operational errors have become problematic, there has been increasing motivation to improve the efficiency and safety of the air traffic management process by investigating the use of automation technologies.

One key characteristic of an automated air traffic management system is the ability to perform automated aircraft traffic separation management. In order to improve safety and efficiency, conflict detection and conflict resolution processes that are within the separation management system need to be robust in an uncertain environment.

The issue of an uncertain environment in the separation management has been tackled in a number of different ways, but in this thesis, we aim to focus on the impact of different measurement uncertainty models on the estimated risk of conflict, where the risk of conflict is considered as a primary measurement to be used for early conflict detection. Measurement uncertainty models can be used to represent different sensor accuracy and sensor choices. This thesis demonstrates the value of modelling measurement uncertainty in the conflict risk estimation problem and presents techniques for assessing sensor requirements to achieve desired conflict detection performance.

Additional insights into the uncertain environment problem were brought forth by a comparison of separation performance behavior of several popular algorithms in an uncertain communication environment. In this study, uncertain communication environments will be represented by periods of information loss. In this thesis, a comparison is initially conducted through simulation studies, then followed by flight tests. Simulation results suggest that communication

failure can cause the performance of these separation management algorithms to degrade significantly. To overcome the degraded performance problems in uncertain environments, a new type of automated separation management algorithm that utilizes inter-aircraft communication and a track file manager (or bank of Kalman filters) is proposed. The proposed separation management algorithm is tested in a range of flight scenarios during periods of communication failure, in both simulation and flight test (flight tests were conducted as part of the Smart Skies project[1]). The purpose of flight tests was to investigate the benefits of using inter-aircraft communication to provide an extra layer of safety protection in support of air traffic management during periods of failure of the communication network. The ability of the proposed separation management system to resolve potential conflict during a period of central communication failure is confirmed.

This thesis achieves its overall aim of investigating the impact of uncertain environment on air traffic management systems.

[1]Refer to website for details: http://www.arcaa.net/research/smart-skies-project/

Keywords

Separation Management, Conflict Detection and Resolution, Risk of Conflict, Uncertainty, Communication Breakdown, Inter-aircraft Communication

Acknowledgments

I would like to express my gratitude to my principal supervisor, Dr. Jason Ford, for his patient help and support throughout these years. Without his guidance, this research would not have been possible. Also, I would like to express my thanks to my associate supervisor Dr. Felipe Gonzalez, fellow staff members and researchers at QUT and at ARCAA for their help in the last few years of my studies.

I would also like to thank all my friends for emotional support. Lastly, I would like to thank my family for their unwavering support throughout my life.

Table of Contents

Nomenclature

6DOF	Six Degree of Freedom
ADS-B	Automatic Dependent Surveillance-Broadcast
AILS	Airborne Information for Lateral Spacing
ATC	Air Traffic Controller
ATM	Air Traffic Management
Auto ACAS	Automatic Air Collision Avoidance System
CASA	Civil Aviation Safety Authority
CCA	Causal Chain Analysis
CLMC	Coarse-Level Markov Chain
CPE	Conflict Probability Estimation
CTAS	Centre TRACON Automation System
DDE	Double-Double Exponential
DRCA	Decentralized Reactive Collision Avoidance Approach
FAA	Federal Aviation Authority
FAST	Final Approach Spacing Tool
FLMC	Fine-Level Markov Chain

GA	Genetic Algorithm
GPS	Global Positioning System
JAA	Joint Aviation Authorities
MDP	Markov Decision Process
MEBRA	Multi objective Evolutionary-Based Risk Assessment
MIP	Mixed Integer Programming
ML	Multi-level
MPC	Model Predictive Control
NEXTGen	The Next Generation Air Transportation System
NMAC	Near Mid-Air-Collision
POMDP	Partially Observable Markov Decision Process
PRA	Probabilistic Risk Analysis
RAS	Radar Advisory Service
RNP	Required Navigation Performance
SDP	Semi Definite Programming
SESAR	Single European Sky ATM Research
TCAS	Traffic and Collision Avoidance System
TOPAZ	Traffic Organization and Perturbation AnalyZer
TRUST	Terminal Routing Using Speed Control Techniques
UAV	Unmanned aerial vehicle

List of Figures

List of Tables

Chapter 1

Introduction

1.1 Background

In recent years, air traffic management systems have faced increasing levels of air traffic. With air traffic expected to grow from roughly 45,000 daily flights to 61,000 daily flights in the next ten years, there is increasing motivation to improve the efficiency of the air traffic management process. Air traffic demand has resulted in increased air traffic density. Increased air traffic density, on one hand increases the traffic throughput, but on the other hand will affect the safety of aircraft operations due to the increased risk of air traffic conflicts. Prevot [4] indicates that if current airspace operations remain unchanged, increasing traffic demands are expected to compromise both on-time performance and safety. The aim of this research is to investigate air traffic management safety and efficiency through evaluation of impacts of uncertainty on risk of air traffic conflicts and air traffic separation management performance.

The air traffic management system (ATM) aims firstly to organize the flow of traffic and to prevent a collision between aircraft operating in the system [1]. In many countries, ATM services are provided throughout the majority of airspace, and its services are available to all users. When controllers are responsible for separating some or all aircraft, such airspace is called “controlled airspace” in contrast to “uncontrolled airspace” where aircraft may fly without the use of the ATM. Depending on the type of flight and the class of airspace, Air traffic controllers (ATC) may issue instructions that pilots are required to follow, or merely issue flight information to assist pilots operating in the airspace.

The major problems faced by the ATM system looking into the future will be primarily

related to the volume of air traffic demand placed on the system, with an expected 3%-5% air traffic growth rate for the next 10 years [5]. Current solutions to congestion problems have included building more facilities, hiring more controllers and expanding existing air traffic control technologies. These patchwork solutions have been only marginally effective, at a huge cost. Automation technologies greatly improve the efficiency of the air traffic management process. However, automation technologies have been mostly relegated to an advisory role in the current ATM systems. For example, Ground based systems such as TRUST (Terminal Routing Using Speed Control Techniques), FAST (Final Approach Spacing Tool) and CTAS (Centre TRACON Automation System) assist human controllers by providing sequencing and vectoring information. AILS (Airborne Information for Lateral Spacing) and TCAS (Traffic and Collision Avoidance System) alerts pilots about potential collisions and advise procedural maneuvers. Automated air traffic management will play a crucial role in the next generation air traffic management systems.

Boarder automation approaches for safer and more efficient air traffic systems are currently being developed with the support of various governments and industry partners. Two examples of these programs are the SESAR project in Europe and the NextGen project in US. These two projects are different in scope. However, they share the common understanding of future air traffic management capability, which is to include automated functions to assist air traffic controllers in decision making as well as providing situation awareness to all aircraft. The concept of situation awareness is generally accepted as referring to the perception of elements in the environment within a volume of time and space, the comprehension of their meaning, and the projection of their status in the near future. However, if these automated concepts are to be adopted, some of the safeguards, which were built according to the old operational procedures, will no longer exist. Therefore, a higher level of assurance for safety will be required for these systems.

Automated air traffic management also plays an important part in the UAV industry. In the past few years, technology involving UAVs has experienced rapid growth, applications emerging in areas such as military combat, surveillance, reconnaissance, and many more. However, the potential of UAV technology cannot be fully realised until this technology is proven to have the ability to operate safely in civilian airspace with other types of aircraft. In fact, it has been proposed by Federal Aviation Authority (FAA) and other civil aviation regulatory bodies including Civil Aviation Safety Authority (CASA), that UAV must demonstrate an equivalent

level of safety to that of manned aircraft. Without such evidence of guaranteed performance, aviation regulation authorities (CASA, FAA, JAA, etc.) are unlikely to agree to let UAVs fly in the same airspace as other aircraft. This provides an additional motivation to develop an automated air traffic management system, as it will not only prevent aircraft collisions within the defined airspace, but also help provide safe trajectories for UAVs.

1.1.1 Current Separation Management Approach Problem

Safety in air traffic management is generally understood to involve five layers of safety processes and systems that are shown in the Figure 1.1. These five layers provide multiple levels of collision protection and, as such, each of these layers would have to fail in order for a mid-air collision to occur. This layered approach starts in Layer 1 which contains the basic procedures and structures of airspace management (aspects such as predefined operational altitudes and predefined flight routes) that provide the basic framework for air-traffic operation. In the 2nd and 3rd layers, a centrally located air traffic management system (human operators and ground-based radar systems) performs aircraft traffic separation management. Layers 4 and 5 relate to emergency safety systems. This thesis is specifically focused on (automated) separation management (in the 2nd and 3rd layers) which has the task of maintaining safe separation distances between aircraft and, in the event of a potential conflict arising, this system also has the task of resolving conflicts in a safe manner.

One key characteristic of an automated air traffic management system is the ability to perform automated aircraft traffic separation management. During the operation of air traffic separation management processes, the traffic environment must be first monitored, then appropriate aircraft state information must be collected and disseminated using sensors and appropriate communication equipment. The collected state information provides an estimate of the current traffic situation. However, there is generally some uncertainty in the values of the collected aircraft states. In order to improve the safety and efficiency of the separation management system, conflict detection and conflict resolution processes within the separation management system need to be robust to account for uncertainty in the values collected for each aircraft state.

Most proposed automated separation management approaches over the last decades assume an exact knowledge of all aircraft state. However, in realistic environments where uncertainty

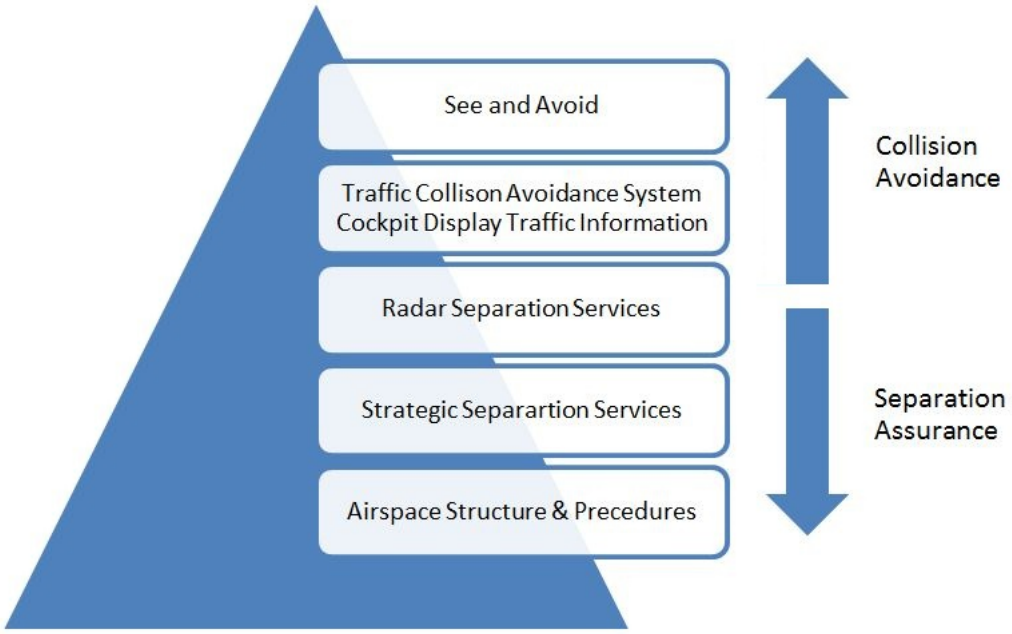

Figure 1.1: Safety in air traffic management

exists, these idealized assumptions are not valid. Furthermore, uncertainties which are common in realistic environments can potentially lead to information mishandling in the separation management process, increasing the risk of mid-air collision. The uncertainty in aircraft location and states can occur due to various reasons, including measurement noise and special cases when communication failure occurs. One of the possible sources of uncertainty from measurement noise is due to sensor accuracy. While it has been demonstrated that high measurement noise in sensors does have an effect on separation management performance [6], the level of impact from different sensor accuracy and sensor choices on the risk of conflict is yet to be determined. Communication failure events can also be treated as special cases of measurement uncertainty. They occur when communication equipment breaks down or when there is congestion in the communication network. Thus, there is an urgent need for new automated ATM systems with robust behavior against uncertainties within realistic environments.

To address the issue of automated ATM taking into account uncertainty, this thesis investigates different types of uncertainty in air traffic management and concentrate on quantifying risk of conflict from uncertainty in measurement information which occurs consistently. In addressing the issue, the thesis proposes and tries to provide an answer to the following research questions.

1.2 Research Questions

Question 1: How does some information about measurement uncertainty (such as sensor accuracy and choices) impacts the quality of our estimates of the risk of mid-air collision? The following sub question is also considered:

(i) If additional information about uncertainty (sensors) helps to reduce the risk, does it perform differently in different conflict scenarios?

Another problem regarding the uncertainty in air traffic management system is in the area of communication uncertainty. This uncertainty can be treated as a special case of measurement uncertainty when the measurement is invalid and cannot be used. This leads to the second research question:

Question 2: Can inter-aircraft communication be used to improve separation performance in uncertain communication environments (e.g. communication failure)? The following sub-questions are considered:

(i) If low-bandwidth communication between nearby aircraft is assumed, can requested information be used to reduce uncertainty?

(ii) Can an integrated solution based on the triggering concept or low bandwidth inter-aircraft communication be build? What possible issues can arise using this approach?

1.3 Research Objectives

The main objective of this research is to investigate separation management approaches that are robust and mitigate uncertainty in sensor or communication failure raised by the next generation of air traffic management approaches. We have identified the following sub-objectives:

1. Identify several types of uncertainty issues and determine a realistic representation of uncertainty in a simulation environment.

2. Investigate the influence of measurement uncertainty on the risk of conflict.

3. Identify the key elements and metrics to determine the performance of separation management approaches. Compare the performance with existing approaches.

4. Investigate novel separation management approaches that mitigate uncertainty in communication based on requesting information via inter-aircraft communication link.

1.4 Key Contributions of Research

The significant original contribution of the thesis are:

- Knowledge:
  - Influence of measurement choices on estimated risk of conflict is explained.
  - Influence of measurement accuracy on estimated risk of conflict is explained.
  - The impact on risk ratio of variation in the accuracy of different types of sensor information (e.g. Radar range, radar bearing, radar elevation, etc.)
  - Sensor accuracy requirement derived from a risk of conflict modelling.
- Tools and Methods:
  - The use of more general aircraft models to represent the aircraft dynamics in the problem of estimating the risk of conflict.
  - A methodology for realizing the risk of conflict benefits by combining ADS-B and radar measurements.
  - Use of particle filters in determining the risk ratio of a particular situation to a nominal situation.
  - Using risk ratio in determining impact on risk of conflict from measurement accuracy.
- Outputs:
  - A new risk-ratio based approach for assessing the impact of sensor accuracy and sensor choice on the ability to accurately predict conflicts is presented.
  - Comparisons of the impact of communication loss on several existing automated separation management approaches.

- A new safety augmentation system using a decentralised separation management system that involves a track file manager, an on-board conflict detection system, and a separation manager based on a modified satisficing approach is proposed.

The outcomes of this research will help to understand automated air traffic management system operating in realistic environments. Automated ATM systems not only offer potential benefits to the general aviation industry but may also facilitate Unmanned Aerial Vehicle (UAV) entering service in civilian airspace.

1.5 Overview of the Thesis

Chapter 2 introduces the mathematical framework which will be used in the later chapters and provides the mathematic language in which the research problems are posed. Chapter 2 first details the aircraft dynamic models which include both three degree-of-freedom (3DOF) model and six degree-of-freedom (6DOF) model. The chapter then describes the aircraft measurement models, briefly introduces the particle filtering techniques and Kalman filtering techniques used in this thesis. The second half of Chapter 2 contains necessary mathematic background information on satisficing separation management approach and the Decentralized Reactive Collision Avoidance approach (DRCA).

Chapter 3 provides a literature review of aircraft conflict risk modelling tools. Chapter 3 first defines the concept of risk of conflict and other related terms, then the chapter discusses different risk of conflict models. Next, the chapter explains other aspects of the problem such as conflict risk estimation. Finally, Chapter 3 provides a summary of the literature review on the topic of conflict risk.

Chapter 4 presents an overview of separation management approaches used for air traffic management. Chapter 4 first defines the concept of automated aircraft separation management and other related terms. Then the chapter compares different separation management approaches in two different categories: centralized separation management and decentralized separation management. Finally, a comprehensive summary of the literature findings related to separation management system approaches and their robustness towards uncertainty is presented.

Chapter 5 proposes a novel approach to assessing the impact of different measurement

uncertainty models on the estimated risk of conflict. Chapter 5 first discusses the existing uncertainty problem in separation management, it then introduces the risk of conflict model. Later, Chapter 5 discusses the methodology used in modelling risk of conflict and compares different sets of sensor configurations using risk ratio concept: Range, bearing, longitude and latitude accuracy. Chapter 5 then evaluates the benefit of using additional sensor information to better quantify the risk of conflict and presents three different test cases. Finally, a comparative analysis of the simulation results is presented.

Chapter 6 examines and evaluates the separation performance behavior of several algorithms. Chapter 6 first examines the separation performance of the algorithms in an uncertain communication environment where periods of communication breakdown occur. Then the chapter discusses the communication uncertainty problem and compares the separation performance through simulation studies. These simulation studies suggest that communication failure can cause the performance of these separation management approaches to degrade significantly.

Chapter 7 proposes a new type of automated separation management algorithm that utilizes inter-aircraft communication and a track file manager that is capable of resolving conflicts in an uncertain communication environment where periods of communication failure occur. Chapter 7 first details the proposed separation management algorithm in a range of flight scenarios in a simulation study. Then Chapter 7 discusses the conducted flight test environment and flight test results. Finally, Chapter 7 concludes that the proposed separation management system was able to resolve potential conflict during a period of central communication failure with the help of inter-aircraft communication.

Chapter 8 provides the main conclusions of thesis with some recommendations for future work, where a measurement and communication uncertainty model can potentially be incorporated into separation management approaches to strengthen the safety aspects of future automatic air traffic management system in regard to uncertainties.

Chapter 2

Background Material: Dynamics, Estimation, and Separation Management Mathematics

---

Chapter 2 introduces the mathematical framework and provides the mathematical language which will be used in the following chapters. This mathematical framework includes models of aircraft dynamics, aircraft measurement process models, filtering techniques and mathematical background of separation management approaches. The chapter is organized as follows: Section 2.1 describe the aircraft models. Section 2.2 describe the measurement models. Section 2.3 describes the filtering techniques. Section 2.4 details the filtering techniques in aircraft conflict problems. Section 2.5 describes the mathematical background for some of the separation management approaches. Section 2.6 draws some conclusions.

2.1 Aircraft Dynamic Models

Aircraft dynamic models are the basis for all aircraft simulations. There are two types of aircraft dynamic models involved in this project: 3DOF and 6DOF.

2.1.1 Aircraft 3DOF Models

3DOF Aircraft models are used in the simulations throughout the thesis. 3DOF models are used for representing simple 2D kinematics of aircraft. In a 3DOF aircraft model, the dynamics of

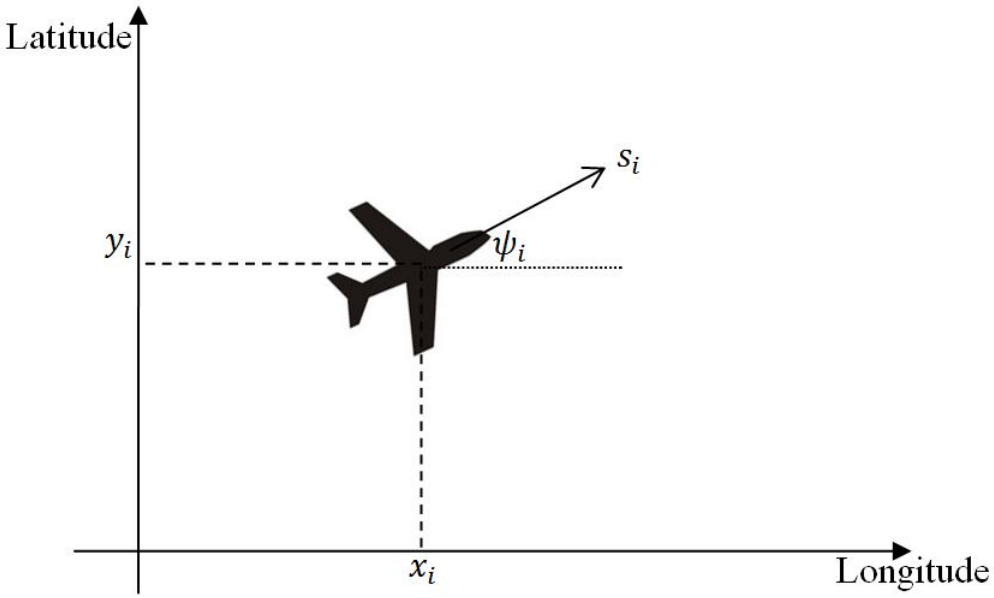

Figure 2.1: Aircraft 3DOF representation

i^{th} aircraft can be represented using simple 2D kinematics, see Figure 2.1.

$$\frac{d}{dt}\begin{bmatrix} x_i \\ y_i \\ \psi_i \end{bmatrix} = \begin{bmatrix} s_i \cos(\psi_i) \\ s_i \sin(\psi_i) \\ u_i \end{bmatrix} \tag{2.1}$$

Where s_i is the speed of i^{th} aircraft, ψ_i is bearing angle of i^{th} aircraft and u_i is the heading change of i^{th} aircraft. In a 3DOF aircraft model, x_i is defined as the longitude of i^{th} aircraft. y_i is defined as the latitude of i^{th} aircraft.This can then be further discretised with a sampling time T_s

$$\begin{aligned} x_i(k+1) &= x_i(k) + T_s s_i \cos(\psi_i(k)) \\ y_i(k+1) &= y_i(k) + T_s s_i \sin(\psi_i(k)) \\ \psi_i(k+1) &= \psi_i(k) + u_i \end{aligned} \tag{2.2}$$

The inputs are restricted to a constrained domain by the limitation of vehicle: $u_{i,min} \leq u_i \leq$

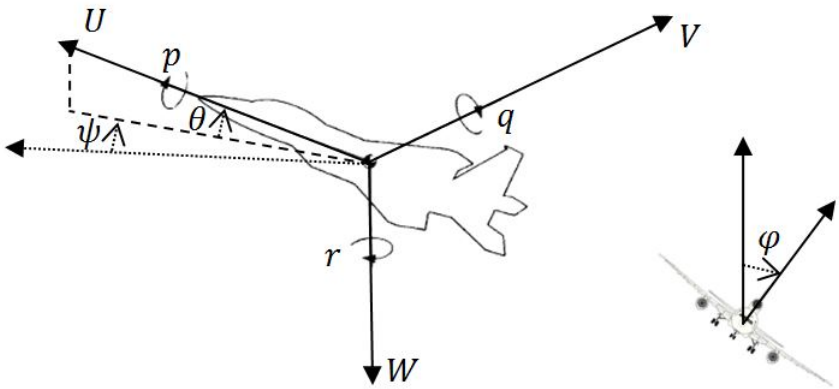

Figure 2.2: Aircraft 6DOF representation

$u_{i,max}$.

2.1.2 Aircraft 6DOF Models

6DOF Aircraft models are used in the C172 aircraft simulator which developed by the University of Sheffield. The C172 simulator will be used in our flight tests to simulate the dynamics of the aircraft. The 6DOF equations arise from understanding the equations of motion that govern an aircraft, these equations describe how the state of the aircraft dependents on the aerodynamic forces, moments and thrust that act on the aircraft. These forces and moments are driven by the control surface deflections, aircraft geometry, mass properties, and airflow about the body of aircraft. The following list and Figure 2.2 contains the notation that are used in the equations.

U: True airspeed, forward direction

V: True airspeed, starboard direction

W: True airspeed, down direction

θ: Pitch angle

ψ: Yaw angle

φ: Roll angle

g_0: Local level gravity constant

r: Angular yaw rate

p: Angular roll rate

q: Angular pitch rate

The equation are written in terms of the body frame translational velocity vector components (U, V, W), body frame angular velocity vector components (p, q, r), gravity (g), external forces (F_x, F_y, F_z) and body mass (m).

$$\frac{d}{dt}\begin{bmatrix} U \\ V \\ W \end{bmatrix} = \begin{bmatrix} rV - qW - g_0 \sin\theta + \frac{F_x}{m} \\ -rU + pW + g_0 \sin\varphi \cos\theta + \frac{F_y}{m} \\ qU - pV + g_0 \cos\varphi \cos\theta + \frac{F_z}{m} \end{bmatrix} \tag{2.3}$$

These forces are often characterized in the form of dimensionless coefficients, understanding and being able to characterize these dimensionless aerodynamic coefficients is the main problem in the development of the mathematical 6DOF model. Expressions for these dimensionless aerodynamic coefficients are not the focus of this project. Further details on 6DOF and how to obtain these dimensionless coefficients can be found in [7].

2.2 Aircraft Measurement Models

Aircraft measurement models are used to model the measurements obtained through various sensors. In this thesis, aircraft is classified into two basic types, observer aircraft and target aircraft. By convention, the observer aircraft is the first aircraft (1) in the description, with the state of the observer aircraft denoted as $x_t^1 \in \mathbb{R}^4$. N targets within the target aircraft set are denoted as $\mathcal{T}_N := \{2, ..., N+1\}$. Each target aircraft $r \in \mathcal{T}_N$, is described by:

$$\dot{x}_t^r = f(x_t^r) + v_t^r, \tag{2.4}$$

where $x_t^r \in \mathbb{R}^4$ is the target aircraft state. $x_t^r(q)$ denotes the q^{th} element of the state of target aircraft r. Here $x_t^r = \begin{bmatrix} x_t^r(1) & x_t^r(2) & x_t^r(3) & x_t^r(4) \end{bmatrix}^\top$, where $x_t^r(1)$ and $x_t^r(3)$ denote x, y directions respectively and $x_t^r(2) = \dot{x}_t^r(1)$, $x_t^r(4) = \dot{x}_t^r(3)$. Here $f(\cdot) : \mathbb{R}^4 \to \mathbb{R}^4$ are the system dynamics. v_t^r is the system process noise with the densities being ψ_v. The observer aircraft is an aircraft that has the capability of measuring the relative bearing and range information of

another aircraft. The measurement models of the aircraft is:

$$y_t^r = h(x_t^r) + u_t^r, \tag{2.5}$$

Here $y_t^r \in \mathbb{R}^Q$ is the target aircraft observation, and Q is the dimension of measurement variables. Here $h(\cdot) : \mathbb{R}^Q \rightarrow \mathbb{R}^Q$ is the measurement process. The process noise v_t^r and the measurement noise u_t^r are assumed to be mutually uncorrelated, with the densities of measurement noise being ψ_u.

Four measurement models were used in this thesis. The first measurement uncertainty model is based on bearing only information, the second measurement uncertainty model is based on both range and bearing information (radar observation), the third measurement uncertainty model is based on latitude and longitude information from automatic dependent surveillance-boardcast (ADS-B), and the forth measurement uncertainty model is based on range, bearing, latitude and longitude information (Radar + ADS-B). Here, range and bearing angle information are measured through a single sensor (radar). The range and bearing transformations are given by $r = \sqrt{x^2 + y^2}$, and $\theta = \arctan(y/x)$ respectively. Within these four models, the longitude and latitude information is obtained through ADS-B which are represented by x and y respectively. The sensor measurement noise w_k is assumed to follow a white Gaussian distribution with zero mean. The values in the covariance matrix represent the accuracy of the sensors, both nominal ADS-B noise standard deviation for latitude and longitude position measurements as well as nominal radar range and bearing errors are derived from Required Navigation Performance of 1 nautical miles (RNP-1). RNP is used as navigation specification that includes requirement for on-board performance monitoring and alerting.)

2.3 Filtering Techniques

Filtering techniques are needed in this work to estimate aircraft states from the observation. The filtering problem is a mathematical model for a number of filtering problems in signal processing. The general idea is to form an estimate for the true value of some system, given only some (potentially noisy) observations of that system. Here we will briefly introduce the particle filtering techniques and Kalman filtering techniques that are related to this thesis.

2.3.1 Particle Filtering

Let us consider the case of tracking N target aircraft. For this purpose, we allocate a set of M particles to each tracked target aircraft r. The states for the m^{th} particle that tracks target aircraft r is denoted by $x_k^{m,r}$. The particle filters first initialise all M particles based on the initial target aircraft state's probability density function (PDF). The particle filter then iterates the following four steps every time instant k [8]:

(i) Measurement update

(ii) Estimation

(iii) Resampling

(iv) Time update

2.3.1.1 Measurement Update

For particle number $m = 1, 2, ..., M$, find the weighting coefficient $w_{k|k}^{m,r}$:

$$w_{k|k}^{m,r} = \frac{1}{c_k} w_{k|k-1}^{m,r} p(y_k^r | x_k^{m,r}), \tag{2.6}$$

where c_k is the normalization weight given by:

$$c_k = \sum_{m=1}^{M} w_{k|k-1}^{m,r} p(y_k^r | x_k^{m,r}), \tag{2.7}$$

The weighting coefficient $w_{k|k}^{m,r}$ for m^{th} particle tracks target aircraft r at time instant at k.

The weighting coefficient for the m^{th} particle which tracks target aircraft r at time instant $k-1$ is denoted as $w_{k|k-1}^{m,r}$. The weighting coefficient is updated by the likelihood function $p(y_k^r | x_k^{m,r})$, which indicates the likelihood of observation y_k^r given the current state information for m^{th} particle.

2.3.1.2 Estimation

The filter density is approximated by:

$$\hat{p}(x^r_{[1,k]}|y^r_{[1,k]}) = \sum_{m=1}^{M} w^{m,r}_{k|k}\,\delta(x^r_{[1,k]} - x^{m,r}_{[1,k]}), \tag{2.8}$$

where the mean can be approximated by:

$$\hat{x}^r_{[1,k]} \approx \sum_{m=1}^{M} w^{m,r}_{k|k}\, x^{m,r}_{[1,k]}. \tag{2.9}$$

Here $x^{m,r}_{[1,k]}$ is the m^{th} particle trajectory from first sampling time instant to sampling time instant k, while $x^r_{[1,k]}$ represents target aircraft trajectory from first sampling time instant to sampling time instant k.

2.3.1.3 Resampling

At each time instant, M samples are chosen from the set $\{x^{m,r}_{[1,k]}\}^M_{m=1}$ where the probability of choosing replacement sample m is:

$$w^{m,r}_{k|k} = \frac{1}{M}. \tag{2.10}$$

2.3.1.4 Time Update

Particle filter predicts the future state according to the proposed distribution, or the state space model:

$$x^{m,r}_{k+1} \sim q(x^r_{k+1}|x^{m,r}_k, y_{k+1}), \tag{2.11}$$

and compensated by the importance weight:

$$w^{m,r}_{k+1|k} = w^{m,r}_{k|k}\frac{p(x^{m,r}_{k+1}|x^{m,r}_k)}{q(x^{m,r}_{k+1}|x^{m,r}_k, y^r_{k+1})}, \tag{2.12}$$

where $q(x^{m,r}_{k+1}|x^{m,r}_k, y^r_{k+1})$ is a proposed density function. This proposed distribution depends on the last states in the particle trajectory $x^{m,r}_{[1,k]}$, and also on the next measurement y^r_{k+1}. The simplest choice of the proposal is to use the dynamic model introduced in Section 2.1. Particle Filtering technique is later used in the risk ratio calculations to estimate probability of conflict.

By using particle filtering technique, the approach can be applied to more general cases than is possible using Kalman filter based concepts.

2.3.2 Kalman Filtering

A Kalman filter is also an useful tool for target tracking applications which is used in this thesis. Let n denote the number of elements in the state vector and m denote the number of observations in the measurement vector. Assume a target tracking filter with $n = 4$ states and $m = 2$ measurements. The filter is used to estimate from noisy measurements of the position and velocity of a maneuvering target. The tracking filter is based on the laws of motion. A discrete-time equation of target motion in Cartesian coordinates can be expressed by a state variable model given by:

$$\begin{aligned} \mathbf{x}(t+1) &= \Phi(\Delta t)\mathbf{x}(t) + \mathbf{w}(t) \\ \mathbf{y}(t) &= \mathbf{h}(\mathbf{x}(t)) + \mathbf{v}(t), \;\; t = 0, 1, \cdots \end{aligned} \tag{2.13}$$

where t is the normalized discrete time, Δt denotes the sampling, $\mathbf{x}(t)$ is a 4-dimensional state vector with position and velocity in each of the Cartesian coordinates axes x, y. Where Φ is a (4×4) matrix given by

$$\Phi = \begin{bmatrix} 1 & \Delta t & 0 & 0 \\ 0 & 1 & 0 & 0 \\ 0 & 0 & 1 & \Delta t \\ 0 & 0 & 0 & 1 \end{bmatrix} \tag{2.14}$$

The state vector $\mathbf{x}(t)$ is represented by

$$\mathbf{x}(t) = [x, \dot{x}, y, \dot{y}]^T \tag{2.15}$$

where T is a transpose operation. The noisy measurements of x and y are denoted by $\mathbf{y}(t)$.

$$\mathbf{y}(t) = [x, y]^T. \tag{2.16}$$

The vector $\mathbf{h}(\mathbf{x}(\mathbf{t}))$ is the transformation matrix defined by

$$\mathbf{h}(\mathbf{x}(\mathbf{t})) = \begin{bmatrix} 1 & 0 & 0 & 0 \\ 0 & 0 & 1 & 0 \end{bmatrix} \tag{2.17}$$

It is assumed that the state and measurement noise sequences $\{\mathbf{w}(t)\}$ and $\{\mathbf{v}(t)\}$ are zero mean gaussian random vector sequences with covariance matrices $Q(t)$ and $R(t)$ respectively.

The measurement errors in x and y (longitude and latitude) are assumed uncorrelated. Let σ_x^2, σ_y^2 denote the variance of the measurement noise in x and y respectively, the measurement noise covariance matrix $R(t)$ is given by

$$R(t) = diag[\sigma_x^2, \sigma_y^2]. \tag{2.18}$$

The filter consists of time update and measurement update equations summarized in the following.

2.3.2.1 Time Update

The time-update predicts the state and estimation error covariance matrix using the following equations:

$$\hat{\mathbf{x}}(t+1|t) = \Phi\hat{\mathbf{x}}(t|t) \tag{2.19}$$

$$P(t+1|t) = \Phi P(t|t)\Phi^T + Q(t) \tag{2.20}$$

where $\hat{\mathbf{x}}(t+1|t)$ denotes one-step state prediction at time $t+1$ based on the measurements at time t. The state estimate at time t denoted by $\hat{\mathbf{x}}(t|t)$ represents the estimate based on the measurements at time t. The state transition matrix Φ is defined in Equation (2.31) . The state estimation error covariance matrix is given by:

$$P(t|t) = E\{\hat{\mathbf{x}}(t|t)\hat{\mathbf{x}}^T(t|t)\}. \tag{2.21}$$

The state prediction covariance matrix is defined as:

$$P(t+1|t) = E\{\hat{\mathbf{x}}(t+1|t)\hat{\mathbf{x}}^T(t+1|t)\}. \tag{2.22}$$

The time update of the covariance matrix $P(t+1|t)$ accounts for modeling errors and disturbances by a suitable choice of $Q(t)$.

2.3.2.2 Measurement Update

The measurement update corrects the predicted state and error covariance using the measurement $\mathbf{y}(t)$ and the measurement noise covariance matrix $R(t)$ as follows: The prediction error known as *innovations* is denoted by $\mathbf{e}(t)$ and defined as

$$\mathbf{e}(t) = \mathbf{y}(t) - \mathbf{h}(\hat{\mathbf{x}}(t|t-1)) \tag{2.23}$$

The state estimate is given as

$$\hat{\mathbf{x}}(t|t) = \hat{\mathbf{x}}(t|t-1) + K(t)\mathbf{e}(t) \tag{2.24}$$

The covariance of the innovations is denoted by $R_e(t)$ and defined by

$$R_e(t) = HP(t|t-1)H^T + R(t) \tag{2.25}$$

The Kalman gain matrix $K(t)$ and the covariance matrix $P(t|t)$ are given by

$$K(t) = P(t|t-1)H^T R_e(t)^{-1} \tag{2.26}$$

$$P(t|t) = P(t|t-1) - K(t)HP(t|t-1) \tag{2.27}$$

The initial conditions to start the recursive computations are given by $\hat{\mathbf{x}}(0|0) = \mathbf{x}(0)$ and $P(0|0) = P(0)$, the *a priori* estimates. In practice, only the first few measurements are used to determine the initial conditions. Kalman Filtering technique is later used in the proposed automated separation management system. The proposed system utilizes inter-aircraft communication and bank of Kalman filters and is capable of resolving conflicts during periods of communication failure.

2.4 Filtering Techniques in Aircraft Conflict Problems

Target tracking using filtering techniques has being well studied in the literature. In this domain, filtering techniques has been used in solving aircraft conflict detection and/or resolution problems.

2.4.1 Kalman Filter Techniques in Conflict Detection Problem

Li *et al.* [9] proposed a conflict detection algorithm under constant velocity assumption. In their algorithm, a Kalman filter is used to project the flight trajectories of two aircraft into the future. According to the predicted flight trajectories, the projected distance between the two aircraft can be determined.

The probability of conflict is estimated on the basis of Monte Carlo simulations. One of the disadvantage of using a Kalman filter formulation for conflict detection is that the linear Gaussian distribution assumption required in the filter restricts usage of these techniques to specific class of problems with linear Gaussian distribution. For a more general case, the aircraft states could also includes both aircraft position and velocity as well as the position and velocity error. The situation is further complicated by the fact that the aircraft states measurements are often nonlinear. This implies that efficient filtering methods such as the Kalman filter cannot be used effectively for conflict detection without major modifications.

2.4.2 Particle Filter Techniques in Conflict Detection Problem

For a more general model, Zeng *et al.* [10] proposed an randomized approach for mid-range aircraft conflict detection based on the unscented particle filter. In their approach, the particle filter is used to estimate the instantaneous probability of conflict. The authors modelled radar measurement error as a combination of along track variance and cross track variance and results suggest that the probability of successfully detection increases and probability of false alarm decreases with the decreased measurement error variance. However in their approach, the measurement error model is limited to along track error and cross track error and realistic radar models which includes range and bearing accuracy was not been investigated explicitly.

Lymperopoulos *et al.* [11] proposed an advanced particle filtering algorithm that can efficiently cope with high dimensionality and non-linearity in the conflict detection problem. The performance of conflict detection is improved by reducing aircraft trajectories inaccuracies relate to wind forecast errors. In their algorithm, the wind forecast error is treated as a stochastic disturbance to the aircraft dynamics model and the observation model is based on measurements from ground radar. For simplicity reason, the measurement error is the set to a high variance of $80m$. From simulation, a significant increase in the successful alarms over the agnostic case were observed. However, there is a high rate of missed conflict detection. The author argued that the reason for low detection rate was due to a marginal conflict nature where conflict happens at the boundary of conflict zone. This marginal conflict problem can be resolved by increasing the margin of conflict radius. However, the method of increasing conflict margin comes with a cost which is the simultaneous increase in the rate of false alarms. Therefore there is trade-off between the successfully rate and false alarm rate. The performance of their algorithm can be further improved if an appropriate margin of conflict radius is selected. This marginal conflict problem has also being identified by Irvine [12], who proposed a method of estimating conflict probability. Irvine also proposed two different measurment error models, the first model only considers along-track errors, the second model includes the cross-track errors as well. Irvine then estimated the probability of conflict by using a cumulative probability distribution function (PDF). In both of his models, Irvine stated that the errors in position have a significant impact on the probability of conflict for marginal conflicts. This marginal conflict problem is a common problem across all models that have measurement/position uncertainty. Irvine's model has some drawbacks, he assumed that the position error are independently Gaussian distributed, however it may not be true in all situations.

Jansson *et al.* [13] proposed a probabilistic framework which can be used for analysing existing conflict detection and resolution algorithms. In this framework, risk for faulty intervention and consequence of different actions can be computed on-line based on statistical decision making and stochastic numerical integration. Their framework is based on Monte Carlo techniques; the framework can be used to deal with state estimate uncertainty. To deal with estimation uncertainty, the probability for each action is calculated. It is then possible to require a certain predefined confidence for each action. In their framework, particle filters were used to deal with non-linear and non-Gaussian models. However, the navigation, tracking and prediction models have not been discussed. This framework is limited when we examine the

impacts from different navigation models.

2.5 Mathematical Background of Separation Management

This section contains necessary mathematical background information on select separation management approaches.

2.5.1 Satisficing Approach

As discusses in Chapter 1, in order to understand the impact of uncertainty and risk ratio, it is important to consider evaluating existing separation management approaches. Satisficing game theory is a centralized multiagent approach to the resolution of aircraft conflict presented by Archibald *et al.* [14]. Collision is avoided by the joint actions of individual aircraft. There are two properties of aircraft involved in the deconfliction process, the Selectability and Rejectability of the particular heading option for that aircraft. At every time stamp, there are five directional options: ± 2.5 degrees, ± 5 degrees, 0 degrees. The direction is determined by utilizing these two properties. The calculation of Selectability is based on how direct the heading option is to the desired destination as well as the heading options that are conflicting with each other. The calculation of Rejectability P_{Ri} is based on the heading options that conflict with current headings of other aircraft. Rejectability $P_{Ri}(u_l)$ for heading (u_l) is calculated using the following equation.

$$P_{Ri}(u_l) \propto \sum_{X_k \in P_i} W_R(X_k(U_c), X_i(U_l)) \tag{2.28}$$

Where $\propto$ is the proportionality symbol. The weighting function W_R is defined by:

$$W_R(X_k(U_c), X_i(U_l)) = \begin{cases} 2\alpha, \text{ if } d_{min}(i,k) \leq R_c \\ \alpha, \text{ if } R_c \leq d_{min}(i,k) \leq R_{nm} \\ 0, \text{ otherwise} \end{cases} \tag{2.29}$$

Where $d_{min}(i,k)$ is the projected minimum separation distance between i^{th} and k^{th} aircraft.

R_c is the critical separation distance. R_{nm} is the near miss distance, and here α is defined as:

$$\alpha = \begin{cases} (1 + \frac{R_{nm} - d_{min}(i,j)}{R_{nm}})(\frac{1}{d(i,k)})^{\beta}, \text{ if } d(i,k) \leq 3R_{nm} \\ (\frac{1}{d(i,k)})^{\beta}, \text{ otherwise} \end{cases} \tag{2.30}$$

The parameter β is a variable that is experimentally tuned. As for the selectability calculation, a weight $w_s(u_l)$ is assigned as a function of $r(u_l)$ and the magnitude of $|u_{dir} - u_l|$. $r(u_l)$ is 1 when the heading option is closest to u_{dir} and 5 when the heading option furthest from u_{dir}.

$$w_s(u_l) = \begin{cases} 3, \ r(u_l) = 1 \\ 2, \ r(u_l) = 2 \\ 2, \ r(u_l) = 3, \ 2.5^\circ < |u_{dir} - u_l| \leq 5^\circ \\ 1.1, \ r(u_l) = 3, \ 5^\circ < |u_{dir} - u_l| \\ 1.1, \ r(u_l) = 4, \ |u_{dir} - u_l| \leq 5^\circ \\ 1, \ r(u_l) = 4, \ 5^\circ < |u_{dir} - u_l| \\ 1.1, \ r(u_l) = 5, \ |u_{dir} - u_l| \leq 5^\circ \\ 1, \ r(u_l) = 5, \ 5^\circ < |u_{dir} - u_l| \end{cases} \tag{2.31}$$

Here Equation 2.31 shows the weights for $w_s(u_l)$ under different conditions, the weights then normalized to form mass function $\sigma s_i(u_l^i)$.

$X_k \in P_i$, X_i calculates a matrix of weights for each of its parents:

$$W_{ik}(u_l^i, u_j^k) = W_s(X_i(u_l^i), X_k(u_j^k)), \ \ k = 0, 1, \cdots, |P_i| \tag{2.32}$$

Where

$$W_s(X_i(u_l^i), X_k(u_j^k)) = \begin{cases} 1, \ \text{ if } d_{min} > R_{nm} \\ 0, \ \text{ otherwise} \end{cases} \tag{2.33}$$

The column of the matrix of weights are then normalized such that

$$\sum_{u_i \in U} W_{ik}(u^i, u_j^k) = 1. \tag{2.34}$$

Then

$$\rho s_i | s_1, \cdots, s_{|P_i|}(u_l^i | \bar{u}^m) \propto \sum_{k=1}^{|P_i|} W_{ik}(u_l^i, (\bar{u}^m)_k), m = 1, \cdots, |U|^{|P_i|} \tag{2.35}$$

$$\begin{aligned} \rho s_i(u_l^i) = & \sum_{U^1 \in U} \sum_{U^2 \in U} \cdots \sum_{U^{P_i} \in U} \rho s_i | s_1, \cdots, s_{|P_i|}(u_l^i | u^1, \cdots, u^{|P_i|}) \\ & \cdot \hat{p} s_1(u^1) \cdot \hat{p} s_2(u^2) \cdots \hat{p} s_{P_i}(u^{P_i}). \end{aligned} \tag{2.36}$$

The selectability of that heading option can then be calculated as follows :

$$ps_i(u_l^i) = \lambda \sigma s_i(u_l^i) + (1 - \lambda) \rho s_i(u_l^i), \;\; \lambda \in [0, 1]. \tag{2.37}$$

Once the aircraft has determined its selectability and rejectability, it can identify the set of Satisficing options.

The fundamentally difference between satisficing approach and other conflict resolution approach is that it is not aiming to find a best solution. Instead, each aircraft determines the set of acceptable avoidance maneuvers by eliminating from the full set of options as many bad choices as possible based on safety and efficiency concern. The heading can then be chosen from remaining alternative according to different needs.

2.5.2 Decentralized Reactive Collision Avoidance Approach (DRCA)

The DRCA method developed by Lalish *et al.* [15] adopts the collision cone concept to perform conflict resolution. Conflict in this literature is defined as occurring when two vehicles that they are not currently in a collision, but with null control inputs (i.e. constant velocity); will at some future point in time enter a collision. Guaranteeing safety using DRCA is achieved in two steps: the DRCA method first resolve aircraft conflicts using initial deconfliction maneuvers, which

consists of hard turn left for aircraft involved in a conflict. And secondly the aircraft maintain their conflict free trajectories while changing over to their desired heading progressively.

The steps involves in DRCA as follows:

1. Define near side of the collision cone vector c

$$c = R(sgn(\beta)\alpha)\frac{r}{\|r\|}, \tag{2.38}$$

Where $sgn(x)$ is the sign function, taking on the value of 1 for $x \geq 0$ and -1 for $x < 0$.

2. Define the normal vector n from the collision cone to the relative velocity vector:

$$n = \begin{cases} \nu, \;\; c^T\nu \leq 0 \\ \\ R(\frac{\pi}{2})cc^TR(\frac{\pi}{2})^T\nu, \;\; c^T\nu > 0 \end{cases} \tag{2.39}$$

3. Define the following measures (valid only when not in conflict):

$$p_t = \frac{\|n\|^2}{s_i n^T g_i} \text{ and } p_a = \frac{\|n\|^2}{n^T h_i} \tag{2.40}$$

The algorithm running on the i^{th} vehicle simply computes the p_t and p_a to other vehicles and then finds the closest conflicts.

4. Find control input using the control function F: $u_t = F(p_t^+, p_t^-)$. where $p_t^+ = min\{p_t > 0, \varepsilon_t\}$, $p_t^- = -max\{p_t < 0, -\varepsilon_t\}$

The control function chosen is defined by the following order triples of the form (p^+, p^-, u):

$$\begin{cases} P_1 = (0, 0, 0) \\ \\ P_2 = (\varepsilon, 0, u_{max}) \\ \\ P_3 = (0, \varepsilon, u_{min}) \\ \\ P_4 = (\varepsilon, \varepsilon, u_d) \end{cases} \tag{2.41}$$

u_d must be saturated such that $u_{min} \leq u_d \leq u_{max}$.

The DRCA algorithm is generic and allows each vehicle to have different sizes, speed, actuation limitations, and gains. It can also be extended to three dimension method fairly easily. Further details on the DRCA method can be found in [15].

2.6 Summary

The mathematical framework introduced in this chapter provides the foundation for the separation management approaches and will be used in the following chapters. This mathematical framework includes models of aircraft dynamics, aircraft measurement process models, filtering techniques and mathematical background of separation management approaches.

Chapter 3

Review of Aircraft Conflict Modelling Tools

As mentioned briefly in Chapter 1, one of the primary essential abilities of any future air traffic separation management system is the ability to provide early conflict detection and resolution effectively and efficiently [16]. Here in this thesis, the risk of conflict is assumed to be a primary measurement to be used for early conflict detection. This chapter investigates related fields that could be used to better quantify the risk of conflict.

The specific areas that will be discussed in this chapter are: Section 3.1 defines some of the terminology and the concept of conflict risk and other related terms used throughout the subsequent chapters. Section 3.2 discusses different risk of conflict models. Section 3.3 describes methods for estimating the risk of conflict. Section 3.4 details the role of measurement uncertainty in conflict risk estimations. Section 3.5 provides a summary of the chapter.

3.1 Terminology and Definition

- **Critical separation distance**: In air traffic control, **critical separation distance** is the minimum distance that two aircraft are allowed to approach during normal operation. It is denoted as D_{cr}, normally defined by ICAO as 5 nmi [17].

- **Risk**: is the product of the probability or frequency of occurrence and the magnitude of consequences or severity of a hazardous event. Generally, risk cannot be determined directly, because the probability of the event is difficult to quantify.

- **Conflict**: The term **conflict** refers to an undesirable interaction event between two aircraft

where the separation distance is less than the **critical separation distance**. In this thesis, this situation is described by a **conflict indicator function** which is expressed as follows:

$$C(x_t^r, x_t^1) \triangleq \begin{cases} 1, & \text{if } D(x_t^r, x_t^1) \leq D_{cr} \\ 0, & \text{Otherwise,} \end{cases} \tag{3.1}$$

where $x_t^r \in \mathbb{R}^4$ is the target aircraft state, and $x_t^1 \in \mathbb{R}^4$ is the observer aircraft state. The distance between the target aircraft and the observer aircraft is denoted as $D(x_t^r, x_t^1)$.

- **Risk of Conflict**: is defined as the product of the probability of conflict and consequences of conflict event B_c. Let $P_r(C(x_t^r, x_t^1))$ denote the probability of the conflict event between two aircraft at time instant t. The risk of conflict R_t can be expressed as follows:

$$R_t(x_t^r, x_t^1) = B_c \times P_r(C(x_t^r, x_t^1)). \tag{3.2}$$

- **Estimated risk of conflict**: is defined as a product of consequences of the conflict event and the estimated probability of conflict (based on both existing measurement data and measurement model λ).

$$R_{\tau|t}(\lambda) = E[R_\tau(x_\tau^r, x_\tau^1)|y_{0,t}, \lambda] = B_c \times E[P_r(C(x_\tau^r, x_\tau^1))|y_{0,t}], \tag{3.3}$$

where: $E[R_\tau(x_\tau^r, x_\tau^1)|y_{0,t}, \lambda]$ is the expected value of R_τ at time instant τ, based on measurements up to time t using model λ.

$\tau = t + \ell$ and $\ell \in [0, T_p]$ represent the prediction length and T_p is the upper limit of the prediction length.

- **Conflict during horizon of interest** occurs where there is an undesirable interaction event between two aircraft where the minimum separation distance achieved during the interval of interest is less than the **critical separation distance**. In this thesis, this situation is described by the **interval conflict indicator** which is expressed as follows:

$$C^m_{t|T_p}(x^r, x^1) = \max_{\ell \in [0, T_p]} C(x^r_{t+\ell|t}, x^1_{t+\ell|t}). \tag{3.4}$$

where $x^r_{t+\ell|t}$ is the predicted target aircraft state at time $t + \ell$,and $x^1_{t+\ell|t}$ is the predicted

observer aircraft state at time $t + \ell$.

- **Future estimated risk of conflict** at time t is defined as the product of the maximum estimated probability of conflict during the prediction interval and consequences of the conflict event.

3.2 Models of Conflict Risk

Risk conflict models are used to improve the quantification of the risk of conflict [18]. In the literature, aircraft conflict risk models are proposed for different purposes. While some of the early risk models were designed to reduce required aircraft separation distance, thus increasing the capacity of airspace, recent risk models have emerged to mainly serve the purpose of detecting conflicts with moderate confidence.

3.2.1 Reich Conflict Risk Model and its Extensions

Early aircraft conflict risk models were mostly developed to assess risk due to a reduction of air traffic separation distance. The goal of these early models was to increase airspace capacity and thus cope with growing air transport demands while still maintaining a certain level of safety. The Reich model was developed by the UK Royal Aircraft Establishment in 1966 and has been used to estimate the collision risk for flights over the North Atlantic and specify appropriate separation standards [19]. The Reich model is based on the assumption that there are random deviations of aircraft positions and speeds from expected flight plans; this model represents aircraft with 3D boxes. The position errors of these 3D boxes are modelled as random variables with mean of zero and fixed standard deviations. Even though operationally sound, the Reich model needs to be extended for it to be used with more realistic uncertainty problems [20].

Since its inception in the mid 60s, many promising variants of the Reich model have been proposed [20] [21] [22], each with their own strengths and weaknesses. The Machol-Reich model for instance, was developed from the Reich model [20]. The Machol-Reich model incorporates realistic aircraft position uncertainties by using historical data about the lateral position errors for about 14000 flights over the North Atlantic. The Machol-Reich model enables prediction of collision risk with a moderate level of confidence. Although the Machol-Reich model has been proven to work well and doubled the capacity of the North Atlantic

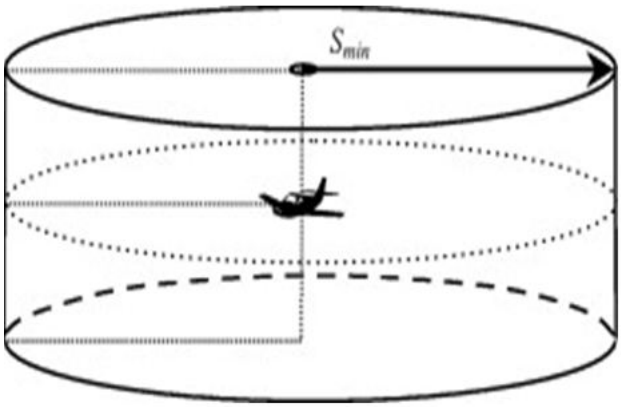

Figure 3.1: Aircraft representation in [2]

airspace [20], this model nevertheless requires a very large set of data to construct an accurate model in order to accurately estimate risk of conflict. There are often high costs involved in collecting the necessary amounts of data on three-dimensional aircraft positions to define the relevant statistical distributions. Additionally, the Machol-Reich model cannot be applied to the NextGen free flight concept where aircraft have the ability to choose their own flight plans [4].

During the mid 90s, the Generalized Reich model was proposed for the TOPAZ (Traffic Organization and Perturbation AnalyZer) accident risk assessment methodology [22]. The Generalized Reich model was based on hybrid-state Markov processes and quantifies risk using Monte Carlo simulations. The advantage of this model is the improved simulation efficiency. However, the complex nature of the Generalized Reich model used in TOPAZ means the model requires a high level of computational effort, and cannot be performed in a online manner if any of the aircraft in the scenario have changed their trajectories.

In 2010, a risk model based on Reich model was proposed by Yuling *et al.* [2]. In this risk model, variable separation distance between two aircraft is expressed as a function of time. This variable separation distance also takes the speed difference of two aircraft into consideration. Aircraft in the model is represented using a cylinder instead of the 3D-box representation in Reich model, where required minimum separation distance is denoted as S_{min}, see Figure 3.1. As with Reich's model [19], Gaussian distribution is selected for describing position error in sensor measurement and speed uncertainty. In addition, the distribution of position error and speed uncertainty are assumed to be independent. The key limitation of the risk model proposed in [2] is the scenario choice and only applies to a two-aircraft collision scenario where they are flying in a straight line path at the same nominal level on an identical track. Extended

applications to other more generic scenarios has not been established [2].

3.2.2 Conflict Risk Models Based on Historical Data

The US Department of Transportation extended the statistical probabilistic method of determining the collision risk from parallel straight-line flight paths to arbitrary flight paths in 1971 [23]. Of particular importance is that simultaneous curvilinear instrument approaches can be used to study the collision in parallel runways. Through multiple simulations of this extended model, it is concluded that collision risk increases dramatically with respect to both time between touchdowns and runway separation distance. The study claimed that if the standard separation for parallel runway is reduced by half, the collision risk will increase by a factor of 6000 [23]. This model allowed a more realistic calculation of collision risk by allowing more variations in flight conditions. However, the analysis of the error uncertainties distribution considers only the statistical combination of initial position and velocity uncertainties, pilot control uncertainties, and possible changes in flight path due to pilot or controller intervention. As a result, probability distributions that based on analytical convenience rather than accurate representations are employed, and therefore the usability of the model is limited when the environment change.

In [24], a prototype airborne collision alerting model for aircraft on approach to closely-spaced parallel runways based on collision probabilities was proposed by Carpenter *et al.* In terms of scope, this model is similar to Bellantoni's risk model presented in [23]. However, a different design methodology was used instead of the traditional alerting criteria (Where the alerting decision is based on the estimated probability of a collision to avoid large time delays and unacceptable false alert rates). In Carpenter's risk model [24], an alert will be issued when the probability of a collision exceeds an acceptable threshold value. A dynamic model is also developed that includes uncertainties in sensor measurement and in the intentions of the aircraft. In order to implement this collision alerting system in real time, probability contours were constructed through the use of Monte Carlo simulations over a range of aircraft positions, speeds, headings, and turn rate conditions. These contours were then stored in different look-up tables that can be accessed in real time for evaluation during numerical simulation of approaches. However, there are two limitations to this collision model: First, given that GPS and other navigation system are widely used and implemented, it will be necessary to incorporate data regarding aircraft tracking performance using different sensors (e.g. heading variability, lateral

deviation, etc.). Second, the impact of the collision model on the overall system must also be examined, so that trade-offs between collision models that incorporate different parameters can be compared.

Work in [25] demonstrated how the risk of collision can be estimated based on existing historical data. In this risk modelling approach, the collision risk is defined as the product of probability that a aircraft (on final approach during closely-spaced parallel landings) will "blunder" in a way that could endanger other aircraft, and the conditional probability that such a "blunder" will cause a collision. Unfortunately, Federal Aviation Administration was unable to estimate the conditional probability of a"blunder" that resulted in a collision with another aircraft because the probability of "blunders" was too small to produce enough data. However, this work provides an idea of how better estimation of collision risk can be achieved in the long run with more years of airport observations. One of the disadvantages of risk models based on historical data is that the scope of the model cannot be easily extended for applications in more generic situations.

In order to account for more generic conflict risk problems, a model for risk assessment is proposed by Willemain *et al.* [26]. Willemain improves barnett's approach [25] by removing three of the assumptions: directional restrictions at each altitude, level flight only, and all aircraft traveling at the same speed. The aircraft trajectories are generalized and numerical estimates are obtained for several measures of risk. In this risk model, different factors are considered for the problem: angles of entry and exit of the sector; altitudes at entry and exit of the sector; time of entry into the sector; and indicated airspeed. Conflict risk here is primarily assessed using two flight-wise measures: mean distance of closest approach to a given flight by other aircraft with which that aircraft shares the same sector; mean number of conflicts for a given flight. Three pairwise measures of risk were also developed, namely the percentage of pairs of flights sharing the sector, the percentage of pairs that share the sector and approach within five miles of each other (conflict situation), and the mean closest approach for pairs that share the sector. The resulting simulations provide quantitative relationships between the risk measures and demonstrates that risk of conflict under free flight is heavily dependent on the levels and combinations of several risk measures. It is suggested that time-average density would be a powerful measure of risk. However, Willemain's method relies on the fact that there is no uncertainty related to the generated trajectories. In real world exercises, uncertainty needs to be taken into account as one of the important factors that influences the risk of conflict.

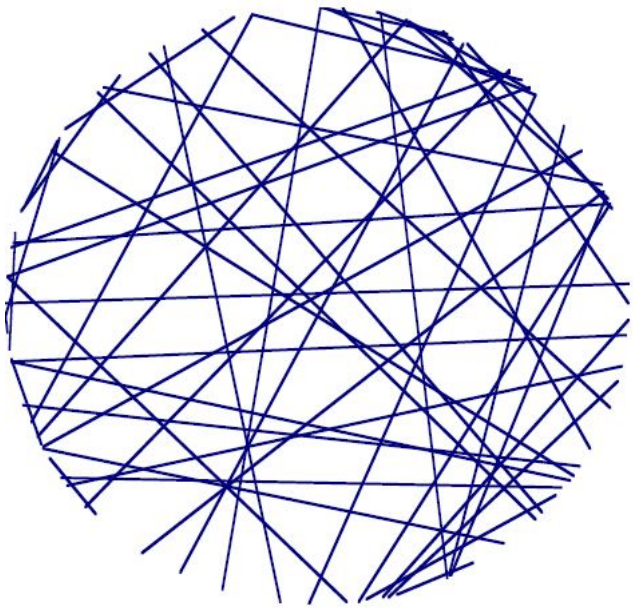

Figure 3.2: Figure shows the circular sector flight trajectory in Willemain's simulation

Improvement can also be made in terms of modelling fidelity.

Fulton categorized mid-air collision via concepts of collective risk and an individual risk [27]. Here collective risk is defined as fatalities per annum and individual risk is defined as the fraction of a population to die due to a specified accidental cause per annum. Fulton concluded that by associating each population group with an individual risk level, an assessment as to the acceptability of that risk can be formed. Fulton also stated that a predictive model and historic measurement are useful in developing these approaches to setting national policy and for long-term monitoring of accident and fatality rates. However, the predictive model has the limitation that in order to achieve appropriate risk level, one must manage an aircraft's exposure to a proximity event and minimize the probability that a collision will occur given that the proximity event occurs.

Brooker [28] discussed the quantification of the risk of mid-air collisions to commercial air transport aircraft receiving a Radar Advisory Service (RAS) in UK Class F/G airspace. RAS refers to the information about advice on action necessary to resolve potential conflicts and erosions of separation. They are provided by air traffic controllers (ATCs), based on a radar picture, of the bearing, distance and the flight level of other aircraft in the vicinity. The risk of mid-air collision in this context is defined as the proportion of fatal accidents per certain fixed flying hours and this risk is then estimated by means of causal chain analysis (CCA) sometimes

referred to as Probabilistic Risk Analysis (PRA) [28]. In causal chain analysis, in order to estimate the risk of mid-air collision, probabilities of the combinations of circumstances are multiplied together to calculate an overall risk. Through the use of CCA, Brooker provided a statistical method to quantify mid-air collision risk; however, the accuracy of this risk quantification method relies heavily on the statistical data available to use, and future risk on mid-air collision has not been addressed explicitly.

3.2.3 The MEBRA and Lindsten's Conflict Risk Model

Abbass *et al.* [29] proposed a risk assessment model called multi objective evolutionary-based risk assessment (MEBRA). Figure 3.3 shows the solution process in MEBRA model. Instead of estimating risk of conflict, the MEBRA model aims to assess risk due to conflict detection system failure in certain scenarios. MEBRA model performs searches on the problem space rather than on the solution space. By going through scenario representation, scenario generation, scenario evaluation and scenario mining, the MEBRA model offers a way of modelling and identifying the risk presented in complex systems. It is a quantitative framework which makes use of search capabilities of evolutionary computations. This risk model can be used to identify risky scenarios that 'break' the air traffic conflict detection system. Therefore MEBRA model is a good assessment tool for testing any air traffic conflict detection system. However, the main focus of this risk model is to represent air traffic scenarios. The MEBRA model lacks the ability to determine both current conflict risk and how future conflict risk evolves over time due to uncertainty in measurements.

Another conflict risk model was developed by Lindsten [30], this model is different from the majority of risk modelling methods found in literature (which commonly deal with instantaneous risk of conflict, i.e the risk of conflict at a certain time instant). One problem with instantaneous risk of conflict is how to interpret the result with respect to a predicted, not necessarily straight, trajectory. Note that simply integrating instantaneous probability over time does not yield an accurate risk estimate a function of the time interval (because the events representing instantaneous risk are dependent on consecutive time points). Rather than focusing on instantaneous risk, Lindsten's model estimates the risk of conflict using cumulated risk over time [30]. He claimed that accumulated risk can be used to overcome the disadvantage of instantaneous risk in situations where misleading information was presented choosing peaks or

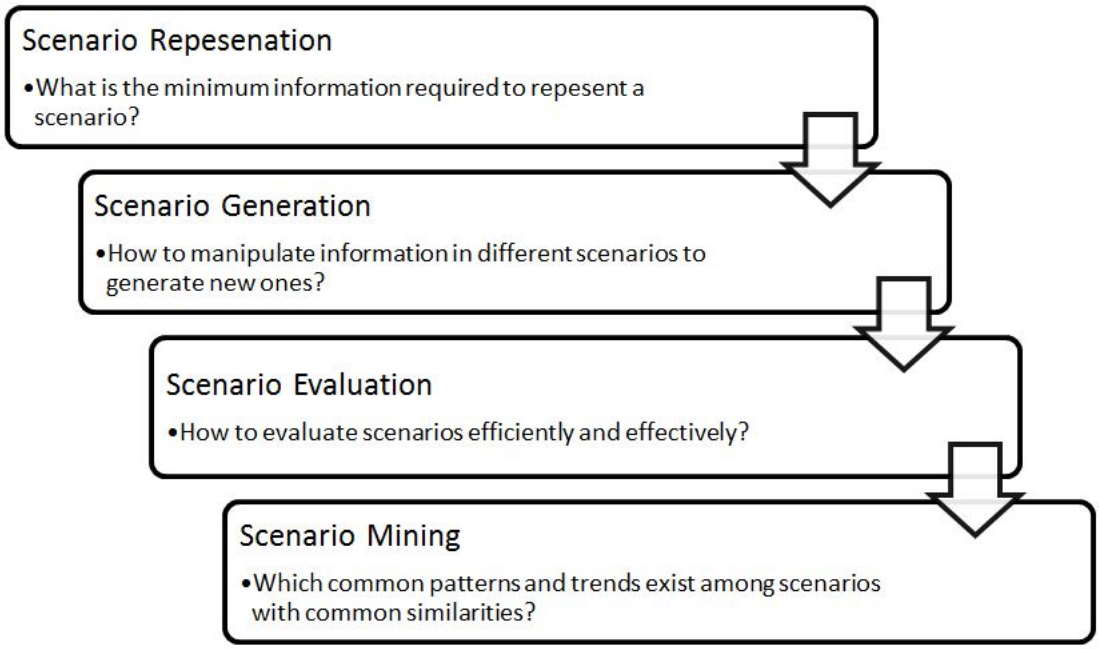

Figure 3.3: Figure shows the solution process in MEBRA model

means of the distribution. The accumulated risk assessment is based on the extended Kalman filter with angle-only measurements. Lindsten also evaluated the sensitivity of instantaneous risk and cumulated risk for different realistic conflict situations. Based on the results obtained using Monte Carlo methods, he concluded that the cumulated risk is more robust against state uncertainty instantaneous risk. As with other models, Lindsten's model has some drawbacks (for example, to accurately represent the conflict situation using cumulated risk, an appropriate critical time horizon must be chosen first). In addition, the lack of discussion on the critical time horizon narrows the scope of Lindsten's model [30]. Finally, in Lindsten's model, uncertainty is based on Gaussian normal distributions and different sources of uncertainty from non-linear measurement devices have not been separately addressed.

The following section will present the literature in the area of conflict risk estimation and related issues when there is measurement uncertainty.

3.3 Methods for Estimating the Risk of Conflict

Aircraft conflict probabilities, together with conflict cost, are the key components of conflict risk analysis [31]. Most researchers in the area of air traffic management have looked into

ways of determining or estimating conflict probabilities as part of the conflict detection and/or resolution problem [22, 24, 32–34]

One early aircraft collision probabilities estimation method was proposed by Hsu [35]. Hsu evaluated the aircraft collision probabilities at intersecting air routes over offshore and continental areas. Intersecting air routes imply that those routes arbitrarily cross one another at a particular point rather other than at a waypoint along a given route. In Hsu's modelling technique, a mixture of two double-double exponential (DDE) distributions were used to determine collision probabilities at intersection points along air routes. For reasons of simplicity, the aircraft collision problem was partitioned into two sub problems: One in the horizontal plane and one in the vertical plane. The horizontal plane sub problem is applicable to aircraft flying at the same altitude on level flight routes and the flight routes are valid if the respective components of position error are independent of each other. The independent binomial variables were approximated by Poisson random variables. Hsu was able to determine the targeted collision probabilities using approximated Poisson distributions. However, in real life scenarios, the assumption on independent position error is not valid when disturbances such as wind perturbations are present.

Several models have been proposed to account for uncertainty associated with conflict probability (such as wind perturbations). Prandini *et al.* [36] proposed a conflict probability model for two mid-range aircraft encounter problem that takes wind contribution into consideration. The mid-range model is meant to provide centralized conflict information to the ATC. In this model, the resultant deviation from the nominal trajectory is modelled as the sum of different independent random perturbations acting together. The tracking errors in Prandini's model are described by using four parameters: zero-mean Gaussian random variable; variance of the along-track error which grows quadratically with time; variance of the horizontal cross-track error which grows quadratically with the travelled distance until the error reaches a fixed value and, finally, the variance of the vertical cross-track error which remains constant. By using the stochastic ODE model presented in [36], the criticality measure which is the maximum value of the probability of conflict over a finite horizon of length (i.e. the time horizon =20 min) can be determined. Prandini *et al.* [36] also proposed a model for computing the probability of conflict for short-range two aircraft encounters. Different from the mid-range model, the short-range model on the other hand provides decentralized advisories to the pilot. The proposed

short-range model is based on an approximation of the mid-term prediction model; the short-range model represents the motion of aircraft as a deterministic motion plus a Brownian motion perturbation. In contrast to the variance of along-track and cross-track error in mid-range models, the variance of error in short-range models grow linearly with time. By doing so, the model allows for very fast computations while still approximating the conflict probabilities. One major limitation of both models is that they ignore errors in the radar and other sensor measurements which are a normal part of the uncertainty in aircraft trajectories.

Another way to account for uncertainty is by utilizing Markov chain approximations. Hu *et al.* [37] improved the model from their previous work in [38] and [39] where independence perturbation assumptions were used. They addressed wind perturbation in their conflict probability model [37], where the aircraft future position is predicted based on a stochastic model that incorporates the information on the aircraft plan, and takes into account the presence of wind as the main source of uncertainty on the aircraft motion. The wind is modelled as a three dimensional field with spatially correlated random perturbations. Based on the predicted position of aircraft, the probability of conflict can then be estimated using an iterative algorithm which is based on the Markov chain approximation method. In Hu's conflict probability model, the state space is formed by gridding the region of airspace with a fixed grid size. The Markov chain, with a proper choice of transition probabilities, guarantees to converge weakly to the solution of the approximated stochastic system as the grid size approaches zero. However with a decrease in grid size, the Markov chain approximation will potentially become computationally expensive and not feasible for real time processes.

Based on [36] and [37], Al-Basman combined a Multi-level (ML) method with Markov chain approximation to improve the conflict probability estimation performance of his algorithm [3]. ML methods have been widely and successfully used to solve partial differential equations, the approximation method proposed by Al-Basman consisted of a Fine-Level Markov Chain (FLMC) and a Coarse-Level Markov Chain (CLMC). The FLMC is used in a smaller subset 'S' of the open domain 'U' where accurate estimates of probability of conflict are performed. CLMC is used in the open domain 'U'. Figure 3.4 shows the relationship between FLMC and CLMC. The use of the two-level method increases the speed of the algorithm since the common grid points of the CLMC and the FLMC are updated more frequently. Therefore, this two-level Markov chains approximation method achieved a better solution speed compared with the traditional one-level Markov chain method. On the other hand, Al-Basman uses a

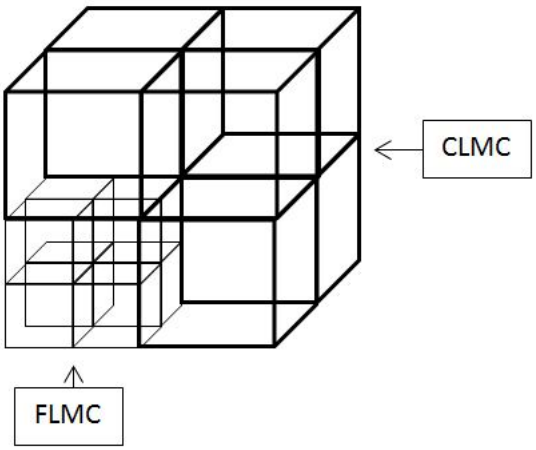

Figure 3.4: Figure shows the relationship between FLMC and CLMC in Al-Basman combined Multi-level (ML) method [3]

linear dynamics representation of aircraft and a Guassian uncertainty model. Thus, complex factors such as sensor choice and sensor errors cannot be modelled.

3.4 Measurement Uncertainty in Conflict Risk Estimations

In the area of conflict risk estimation, many researchers have claimed that measurement uncertainty from different sensors impacts on the estimated risk of conflict [40, 41].

3.4.1 Measurement Uncertainty using Gaussian Distribution Representation

Prandini *et al.* [40] proposed a conflict risk estimation model that can be used in conflict detection systems to provide ATC with assistance. In this model, radar measurements are represented using simple additive white noise and aircraft movement is represented using stochastic differential equations. The position estimates from radar measurement are available every few seconds (typically 12 seconds) where the measurement noise is described as a sequence of independent identically distributed (i.i.d.) Gaussian random variables with zero-mean and a fixed noise covariance. The Prandini's model makes extensive use of randomized algorithms for estimating integrals and carrying out optimisations. The advantage of using these implemented randomized techniques is that they tend to be computationally more efficient and provide analytical bounds on the accuracy of the approximation involved.

However, there are two assumptions required in the Prandini's model. Firstly, the flight plan of each aircraft is known and the flight plan is described in terms of a sequence of way points. Secondly, Prandini *et al.* assumes that measurement noise is independent of all the other random variables involved in the conflict probability model. However, the tracking noise is partially due to the wind perturbations, which may be strongly correlated between the two aircraft, especially near the conflict point where the aircraft are close to each other. In addition, the limitation of using Gaussian variables restricts the usage of this conflict probability model cases where there are limited sensor observation choices.

Temizer *et al.* [6] recognized the importance of measurement uncertainty in the process of conflict risk estimation. In Temizer's model, Temizer applied Markov Decision Process (MDP) and Partially Observable Markov Decision Process (POMDP) solution methods to the problem of collision avoidance where the sensor has positional uncertainty or limited field-of-view constraints. Temizer estimated the risk of conflict based on different sensor choices (TCAS Sensor, Radar Sensor, EO/IR Sensor). In this work, risk ratio was used as a metric to determine the performance of different sensors (Here,the risk ratio associated with a particular sensor is defined as the probability that an encounter will lead to a near mid-air-collision (NMAC) using the sensors divided by the probability that an encounter leads to an NMAC without the sensor). Note that, better performance is indicated by a smaller risk ratio. Temizer's model model performed well under two assumptions, (1) The sensor measurements are modelled based on Gaussian distribution. This Gaussian distribution assumption restricts the model's use to only few selected sensors. (2) It is assumed that the sensor error standard deviation is fixed. As a result, the model cannot be easily extended for applications in more generic situations where sensors have different levels of accuracy.

Chen *et al.* [42] proposed an probabilistic algorithm for multi-aircraft conflict detection . Within Chen's probabilistic algorithm, uncertainties in the aircraft position are represented using Gaussian distribution with zero-mean and fixed value variance. The probabilities of conflict are estimated by using integrals over the conflict zone and the maximum value of probabilities is chosen as a metric for detection of conflict. Chen's algorithm is suitable for piecewise flight plans. However, as pointed out by Chen *et al.*, the accuracy of the algorithm relies heavily on the accuracy of the measurement models. Therefore, it is important to investigate how measurement accuracy impacts on the probability of conflict.

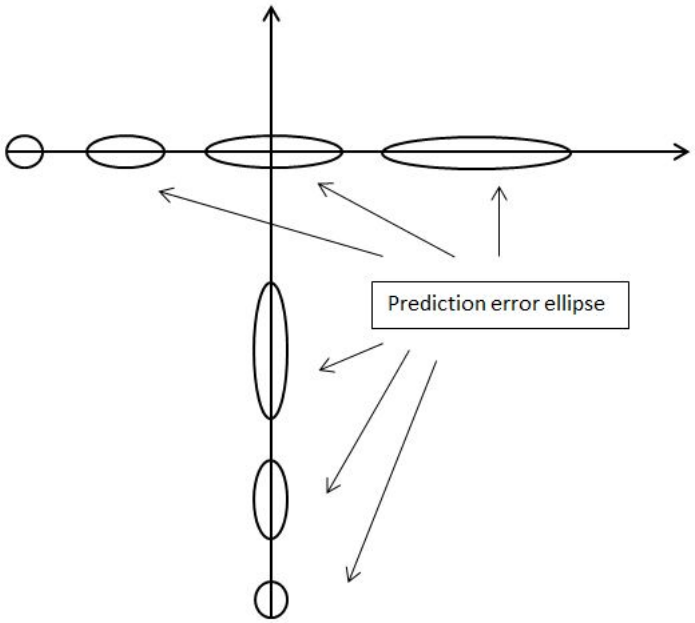

Figure 3.5: Encounter geometry in the horizontal plane: prediction error ellipse grows with respect to predicted time

Paielli *et al.* [33] proposed a conflict probability estimation method given a pair of predicted trajectories and their levels of uncertainty as illustrated in Figure 3.5. In Paielli's work, the trajectory prediction errors are modelled as normally distributed, and the two error covariances for an aircraft pair are combined into a single, equivalent covariance of the relative position. A coordinate transformation is then used to derive an analytical solution of predicted trajectories uncertainties. Later in 1999, Paielli *et al.* introduced a different method called conflict probability estimation (CPE) which can be applied in non-level flight [43]. In this later work, the uncertainty in aircraft trajectory prediction is modelled as an extension of the earlier uncertainty model. Now, the combined error ellipsoid is calculated and assigned to one of the aircraft, referred to as the stochastic aircraft, while the other aircraft is regarded as having no positional uncertainty. Then the total conflict probability is equal to the portion of probability mass within the extended conflict zone, where the extended conflict zone is defined as the volume swept by the conflict zone (a vertical cylinder) during an aircraft encounter event. Paielli *et al.* introduced a number of the modelling assumptions that are not valid in general and fail to properly model prediction errors. Hence, unfortunately, Paielli's estimation method needs to be modified and further developed in order to account for a different prediction error model.

3.4.2 Other Measurement Uncertainty Representations

Yang *et al.* [44] proposed a prototype alerting system in 1997 which was based on probabilistic analysis through modelling of aircraft sensor and trajectory uncertainties. Yang's model assumed that data-link between aircraft is available and that information can be exchanged to resolve any potential conflict. The probability of conflict was estimated using Monte Carlo simulations. In this model, a System Operating Characteristic (SOC) curve is presented by plotting the probability of success alert against the probability of unnecessary alert (Figure 4.3 shows an example of a SOC curve). The most effective avoidance options can then be determined from the shape of their SOC curves. In regards to uncertainty, Yang *et al.* specified the uncertainty model parameter according to different distributions, e.g. Lateral position error was modelled as Gaussian distribution with standard deviation of 50 meters. These uncertainty model parameter have been pre-set and then used to determine the probability of conflict through Monte Carlo simulations. A major limitation of Yang's model is that a significant amount of pre-processing power was required. In addition, Yang's model applies only to the specific probabilistic parameter used in the Monte Carlo runs. If a change in Yang's model is required (e.g., to examine the effect of varying sensor accuracy or different sensor combinations), then the Monte Carlo simulations must be rerun using different parameter settings in the model. A real-time model that incorporates the probability of conflict would be valuable in terms of improving the model's flexibility.

Chryssanthacopoulos *et al.* [45] also addressed the importance of accommodating state uncertainty within probability models. The authors presented a computationally efficient probability model for accounting for state uncertainty based on dynamic programming. The problem of collision avoidance using TCAS sensor was first introduced as a POMDP and solved approximately. In Chryssanthacopoulos's work, the belief state was computed using Kalman filters, and the state-action utilities were then computed by solving the underlying MDP using dynamic programming. Then the probability of conflict can be estimated by Monte Carlo simulations. Through the use of Monte Carlo simulations for realistic encounter scenarios, Chryssanthacopoulos et al. demonstrated that properly handling state uncertainty rather than simply using point estimates which can cut the estimated probability of conflict by half without increasing the alert rate. This reduction in the probability of conflict significantly improves

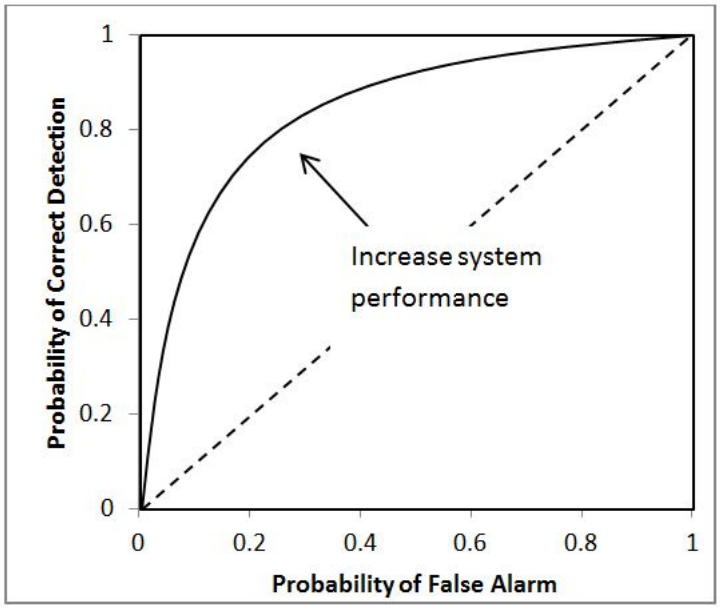

Figure 3.6: An example of a System Operating Characteristic (SOC) curve

the robustness and reduces sensor error effects on the collision avoidance model. Chryssanthacopoulos also showed that using point estimates leads to severely degraded performance when sensor noise is increased, compared to the graceful degradation that occurs when full distributions are used. Therefore, Chryssanthacopoulos's risk model becomes more important in situations where noisy sensors such as passive radar or electro-optical/infrared (EO/IR) were used. However, Chryssanthacopoulos *et al.*'s model introduced a number of assumptions: firstly, the model considered only the Gaussian posterior distribution on sensor position and velocity errors. Secondly, range error was modelled as a zero-mean Gaussian with 50 ft standard deviation. Lastly, the bearing error was modelled as a zero-mean Gaussian with 10 degree standard deviation. This fixed-accuracy assumption limits the application of Chryssanthacopoulos's model. More importantly, other distributions should also be considered in order to include more sensor choices in this model.

3.4.3 Sensor Accuracy and Sensor Choices in Measurement Uncertainty

Measurement uncertainty models should reflect both sensor accuracy and sensor choices. Sensor accuracy is an important factor that contributes to aircraft position uncertainty, but not all prediction models address measurement uncertainty. Models that do account for measurement uncertainty are generally in the form of Gaussian distribution errors and are presented in terms

of along-track error and cross-track errors. Although this uncertainty presentation helps to analytically estimate the probability of conflict, this uncertainty model cannot be used to investigate the impact of varying different components of sensor accuracy (e.g. radar range, radar bearing, radar elevation).

There is some literature that tries to address the sensor accuracy problem. For example, Chen *et al.* [42] identified the issue of sensor accuracy in their multi-aircraft conflict detection algorithm. Yang *et al.* [44] and Carpenter *et al.* [24] attempted to address sensor accuracy in relation to the probability of conflict; However, the Gaussian distribution model limited the scope of the model. Chryssanthacopoulos [45] also demonstrated that properly handling state uncertainty can reduce the estimated probability of conflict and improve the robustness of conflict models to sensor errors. Although sensor accuracy plays an important role in position uncertainty, the sensor accuracy requirement has never been motivated from a risk of conflict perspective. By understanding the sensor accuracy requirement, industry manufacturers can use the sensor requirement as a reference to choose sensors with appropriate levels of accuracy. This in turn can save expenditure on excessively accurate but expensive sensors for aircraft avionics systems.

Sensor choices can also impact on estimated risk of conflict. For example, in a paper by Temizer *et al.* [46], Partially Observable Markov Decision Process models (POMDP) was used in determining the differences in risk between radar sensor, TCAS sensor and EO/IR sensor.The authors estimated the risk of conflicts based on different sensor options. However, conflict risk benefits brought about by combining different sensor systems have not been examined in the literature. Such examples include a combination of existing radar with growing implemented ADS-B. Currently, ADS-B has 3 protocols: 1090Mhz extended squitter (selected as the initial link for European airspace), VDL Mode 4 (Very High Speed Data link), and UAT (Universal Access Time). Globally the ADS-B data link is 1090 ES, UAT and VDL-4 will be used on regional basis. UAT met more of the performance-related link evaluation criteria addressed by the TLAT than either of the other two candidates in the future high-density Los Angeles Basin 2020 scenario. Therefore, different use of ADS-B protocols would affect the performance of different risk models [47].

Tools such as risk ratio can then be used as an excellent candidature metric to evaluate the conflict risk benefits brought about by using different sensor combinations [46].

Most existing measurement models use Gaussian distribution in either their sensor error model or aircraft position uncertainty model. However, Campos [48] [49] claimed that his exponential parametric model is more appropriate than Gaussian distribution models. Therefore non-linear filters such as particle filters are needed, so that more complicated situations can be modelled.

3.5 Summary

A number of conflict risk models and risk estimation methods were presented in this chapter. The detailed estimation methods form the basis of evaluating risk of conflict later in Chapter 5. Furthermore, some literature has been identified that discusses the relations between measurement uncertainty and estimated risk of conflict. Chapter 4 will present a comprehensive literature review related to separation management system approaches. The approaches include both centralized and decentralized approaches.

Chapter 4

Review of Separation Management Approaches

This chapter presents an overview of separation management approaches used for air traffic management. Some of the concepts form the basis of the augmented separation management systems proposed in later chapters. Throughout this chapter, the following definitions will be used:

- Automated Aircraft Separation Management: An automated decision making approach for controlling the movement of aircrafts through a defined airspace to ensure suitable separation is maintained.
- Collision Avoidance Manoeuvre: Proactively manoeuvre to prevent collision with another aircraft.
- Centralized Separation Management: A separation management approach where one central decision location makes decisions for all aircraft.
- Decentralized Separation Management: A separation management approach where individual aircraft make their own individual decision about how to achieve separation based on their on-board information.

Here the term "conflict" refers to an undesirable interaction event between two aircraft where the separation distance is less than the critical separation distance. (normally defined by ICAO as 5 nmi) [31]. There are many ways to categorize separation management approaches. In a journal paper by Kuchar and Yang [31], the authors describe a framework in which 68 previously published methods for separation management system are categorized. Critical factors in their taxonomy included:

- Method of dynamic state propagation and its related conflict detection threshold (nominal, worst-case, or probabilistic)
- Resolution methods (prescribed, optimized, force-field, or manual)
- Maneuvering options (speed change, lateral, vertical, or combined)
- Ability to manage multiple aircraft

Most of the current separation management system literature has assumed that a separation management system can be designed using one of two approaches: decentralized or centralized approaches [50].

4.1 Decentralized Separation Management Approaches

This section briefly describe a number of the key decentralized separation management approaches, namely: non-cooperative game theory, myopic decentralized approach, look-ahead decentralized approach, Auto Air Collision Avoidance System, model predictive control method, Kripke approach, and Decentralized Reactive Collision Avoidance for multivehicle system (DRCA).

4.1.1 Non-cooperative Game Theory

A game theory approach attempts to mathematically capture behavior in situations in which an individual's success in making choices depends on the choices of others. While initially developed to analyse competitions in which one individual does better at another's expense, the game theory approach has been expanded to different areas such as resolution strategy for non-cooperative conflicts between non-UAV aircraft. In a paper presented by Tomlin *et al.* [5] in 1997, a technique for UAV conflict resolution using game theory was proposed. Tomlin suggested that the safest possible strategy for each aircraft was to fly a trajectory which guaranteed the minimum allowable separation while considering the worst action that could be taken by the other aircraft. Later in 1998, Tomlin *et al.* [51] improved their algorithm by incorporating calculations of corresponding safe set of control inputs, providing a methodology for their Multiagent Hybrid System. One feature in their algorithm is partitioning the alert zone

into safe and unsafe regions based on the aircraft's maneuver capability. This is an important feature as the partition maximizes the number of options available for potential manoeuvres while not sacrificing the safety requirement. However, due to the the assumption of known exact states of every other aircraft, this algorithm cannot be fully utilised when dealing with uncertainties.

4.1.2 Myopic Decentralized approach

There are two decentralized air traffic separation approaches presented by Krozel *et al.* [50]. The myopic decentralized approach is one of them; the approach is a user-oriented strategy which emphasizes the efficiency of individual aircraft. A conflict is "detected" if a conflict is predicted to occur with a time to closet approach value of less than 8 minutes. If an aircraft detects conflicts with more than one aircraft within the 8-minute window, the myopic separation approach resolves them in a sequential pair-wise fashion. Only the most immediate conflict will be resolved. The myopic decentralized strategy determines the most efficient resolution, and executes the maneuver that requires the least amount of heading change. The myopic decentralized strategy is a classic decentralized approach; however, it lacks the conflict resolution ability in scenarios like formation flight.

4.1.3 Look-ahead Decentralized Approach

Similar to the myopic decentralized approach, the look-ahead decentralized strategy is the second approach presented by Krozel [50]. It first determines the more efficient maneuver (front side/back side), then it checks if this maneuver would create a new conflict with time to closest approach value less than that of original conflict. If no such conflict is found, it executes the more efficient maneuver which yields the same solution as the myopic approach. However if a new conflict is detected, it checks the other (back side/front side) solution to see if a conflict-free path is available. If so, it executes that solution. If not, this strategy searches for conflict-free paths, starting from the more efficient solution with heading change increments of 5 degrees, until a conflict-free path is found. Figure 4.1 shows the main difference between the myopic decentralized approach and the look-ahead decentralized approach in a situation where a domino effect will happen. The look-ahead decentralized method has addressed the main disadvantage of the decentralized approach. The look-ahead decentralized method has the

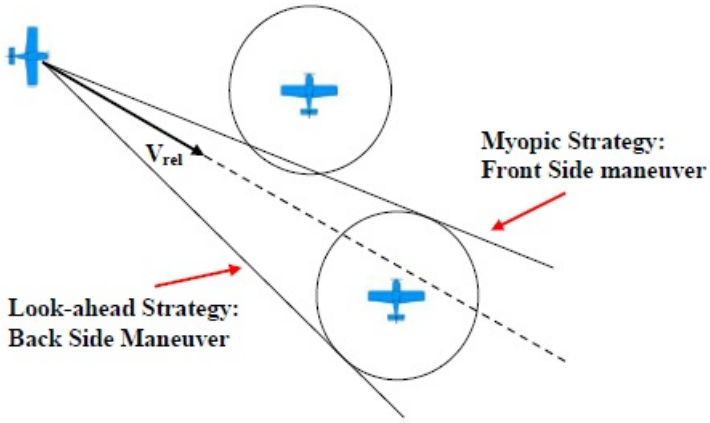

Figure 4.1: Figure shows the comparison of two decentralized approaches.

flexibility to trade off some efficiency in return for some overall stability, enabling it to mitigate the domino effect which is a potential limitation of the decentralized approach. However, the look-ahead decentralized method still lacks the ability to resolve conflicts that involve multiple domino effects (where the resolution of one conflicting manoeuvre can cause conflict with another aircraft).

4.1.4 Auto Air Collision Avoidance System

The increasing rate of mid-air collision incidents has lead to the development of Automatic Air Collision Avoidance System (Auto ACAS). The algorithm for this system was first proposed by Ikeda *et al.* in 2001 [52]. It uses optimal coordinated escape maneuvers to avoid mid-air collision. There are two advantages when compared with other separation management approaches. First of all, when it is activated, the system will take control of the aircraft at the last possible moment to avoid a collision then return control to the pilot as soon as the aircraft begins separating. By doing this, it will reduce the interference with the pilot's ability to perform the mission. Secondly, the algorithm is designed to operate safely despite failures such as GPS or data link dropout. The system has demonstrated successful performance in both simulations and flight tests with F16 aircraft in 2003 [53].

The Auto ACAS uses a different approach from the existing separation management techniques, and is intended to complement other systems rather than replace them. It was designed such that it will perform separation maneuvers at the last second if other separation systems fail to do so. The algorithm used by Auto ACAS is relatively simple. Each aircraft equipped with

Auto ACAS calculates three possible manoeuvre to escape the potential collision, then shares the information with other nearby aircraft, and then the Auto ACAS select the best manoeuvre which maximizes the minimum separation distance.

While the simulation presented by Ikeda *et al.* [52] shows promising results, the impact of low communication rates was not been addressed in the paper. Furthermore, there is still a need for future development of the algorithm in order to provide protection for aircraft/UAV not equipped with Auto ACAS.

4.1.5 Model Predictive Control Method

Model Predictive Control (MPC), also known as receding horizon control, is an advanced method of process control that has been used in the process industries since the 1980s. MPC relies on a dynamic model of the process under control, most often these models are linear empirical models obtained by system identification. These models are sometimes used to predict the behavior of dependent variables (i.e. outputs) of a non-UAV system with respect to changes in the process independent variables (i.e. inputs). Recently, this methodology was used to deal with UAV formulation tracking and separation issues.

In some of the early work published in the field of MPC, Dunbar *et al.* [54, 55] demonstrated that the desired UAV formation is not necessarily a unique state for each vehicle in the formation. Simulation results presented by Dunbar *et al.* [54] demonstrated the ability of the MPC algorithm to guarantee stabilization and constrain performance in preventing collisions. A similar approach was also developed by Tamas Keviczky *et al.* [56]. The authors implemented a decentralized receding horizon control for high level control and coordination of UAV teams and their research was focused on minimization of error between UAV relative distances. By doing this, the formation can allow collision avoidance requirements to be easily included as additional constraints between each pair of UAVs. The major advantage of this approach compared to later discussed centralized approaches is that the computational effort remain feasible when facing an increasing number of UAVs in formation. Their simulation presented in research paper [56] demonstrated impressive performance in different scenarios. However a number of limitations and assumptions are identified, such as omitting wind gusts and UAV flying dynamics. Such omissions will result in potential errors in realistic environments where UAVs are very sensitive to wind gusts and its dynamics.

In a recent publications on this topic (2008), Lavaei *et al.* [57] presented a MPC technique for decentralized control of aircraft with reduced communication requirements. Lavaei's technique can minimise the information exchange, thus establish communication links using lower rate. Lavaei's technique can potentially be used to help solving communication issues such as low communication rates and communication failure. On the other hand, this technique can also potentially have a negative impact on the output performance in the presence of uncertainties. Therefore, trade-offs between communication cost and robust performance will need to be further investigated.

4.1.6 Kripke Approach

The Kripke approach is a formal semantics for non-classical logic systems created in the late 1950s and early 1960s by Saul Kripke. Kripke models have been adopted as the standard type of models for modal and related non-classical logics. Tsourdos *et al.* [58] uses Kripke models with temporal logic statements and their automatic verification of the model to handle different kinds of uncertainty and dynamics in co-operating multiple UAVs. The main advantage of this decentralized approach is its ability to represent real world uncertainty using a formal, yet intuitive model in the form of a directed graph. Although these models are relatively simple, they are sufficiently expressive to capture those aspects of dynamic and discrete event behaviors that are most important for reasoning about reactive systems. However, the performance of such algorithms has not been addressed explicitly.

4.1.7 Decentralized Reactive Collision Avoidance for Multivehicle system

The DRCA method developed by Lalish and Morgansen adopts the collision cone concept to perform conflict resolution [15]. The guarantee of safety is achieved in two steps: Firstly, the DRCA method resolves aircraft conflicts using initial deconfliction maneuvers, which consist of "hard turn left" for aircraft involved in a conflict. Secondly, the aircraft change over to their desired directions progressively after conflict is resolved. The DRCA algorithm allows each vehicle to have different size, speed, actuation limitations, and gains. It can also be extended to a three dimension method fairly easily [15]. However, the major disadvantage of this method is the inability to guarantee a successful conflict resolution from the initial deconfliction maneuvers in the DRCA algorithm. Furthermore, due to the nature of the algorithm, the DRCA method

does not deal with non-cooperative aircraft which also reduces the usability of the algorithm.

4.1.8 Other Techniques

Other techniques for decentralized separation management have also been identified: self organizational approach [59]; modified potential algorithm [60]; the geometric optimization approach [61] and KB3D algorithm and its extension [62].

4.2 Centralized Separation Management Approaches

One major disadvantage of decentralized separation management techniques is that they suffer from the "domino effect" where the resolution of one conflicting manoeuvre can cause conflict with another aircraft. This can be overcome, however, by using a centralized separation management approach. The following sections introduce seven centralized separation management approaches: Brute-force algorithm, genetic algorithm, primal-dual quadratic programming, semidefinite programming, mixed integer programming, grid-based approach, satisficing approach and delay based ranking separation algorithm.

4.2.1 Brute-Force Algorithm

In computer science, brute-force or exhaustive search approaches provide general problem-solving techniques, which involve systematically enumerating all possible candidates for the solution and checking whether each candidate satisfies the problem's statement. Dejong, in his master thesis [63], discussed the usage of brute force in separation management. This method is guaranteed optimal for considering the smallest possible situation. This approach may be quite satisfactory for a small number of aircraft, but may exceed the bounded time requirements for a large number, therefore brute-force algorithms are rarely used in separation management due to their inability to handle large numbers of candidates.

4.2.2 Genetic Algorithm

A genetic algorithm (GA) is a search technique used in computing to find exact global or approximate solutions to optimization and search problems. Genetic algorithms are a particular

class of evolutionary algorithms that use techniques inspired by evolutionary biology. The GA optimization process involves four steps: generating the population of problem solutions as gene strings (initially random); evaluating these solutions; selecting the solutions that should survive to the next generation; and combining the survivors into new solutions. GA algorithms have previously been used to solve en-route aircraft conflict automatically. For example, Durand *et al.* [64] (1996) proposed a separation management approach based on the genetic algorithm that took aircraft speed uncertainties into account. Because of uncertainties, the aircraft manoeuvres must be started as late as possible with respect to the aircraft constraints to avoid generating new conflicts with any other aircraft. The major disadvantage is that genetic algorithms are slow and computationally expensive. The manoeuvres considered in algorithm presented by Durand *et al.* are limited to only the 2D plane.

4.2.3 Semidefinite Programming

Semidefinite programming (SDP) is a subfield of convex optimization concerned with the optimization of a linear objective function over the intersection of the cone of positive semidefinite matrices with an affine space. Many practical problems in operations research and combinatorial optimization can be modelled or approximated as semidefinite programming problems.

An example of using semidefinite programming in designing separation management is presented by Frazzoli *et al.* [65] published in 1999, where the authors formulate the conflict resolution problem as a non-convex, quadratically constrained quadratic program. It was developed on the basis of previously discussed primal dual quadratic programming. Like all other optimization problems, constraints need to be defined first; in this case, constraints of the following three types have been considered: collision avoidance constraints (based on exact location of the aircraft pair); manoeuvring constraints (based on max/min speed); cost function (chosen to minimize the speed deviations from the desired speed).

The optimization then is solved via semidefinite programming combined with a randomization scheme. The research paper which shows simulations involves two crossing aircraft strings suggest that the algorithm has a very good ability in handling multiple aircraft [65]. The advantage of using such an semidefinite programming approach is that it will always generate straight, conflict-free trajectories over a time horizon longer than necessary and generate segmented trajectories only through updates from individual preferences while other approaches

generate trajectories with little or no guarantees about what happens if the waypoints are missed. However, further investigation of this method is needed to evaluate if it can account for communication issues such as low communication rates and communication failure.

4.2.4 Mixed Integer Programming

In mathematics, linear programming problems determine ways of achieving the best outcomes given some requirements represented as linear equations. If only some of the unknown variables are required to be integers, while others are real numbers, then the problem becomes a mixed integer programming (MIP) problem which is a special case of linear programming.

Pallottino *et al.* [66] designed a system in which the way-points were given to avoid all possible conflicts while minimizing the total flight time. The system consists of two main parts: firstly, building conflict avoidance constraints for both velocity change and heading angle deviation and secondly formulating the constraint as mixed-integer linear constraints suitable for a standard optimization software such as CPLEX [67]. Simulation testing results presented by Pallottino *et al.* [66] showed that their system can handle situations where 15 aircraft cross the origin at the same time. It was highlighted that few assumptions such as fixed altitude and known exact position and velocity were made in the research paper to idealize the environment. In Christodoulou *et al.*'s paper [68], a more complex model was created to manage the conflict resolution. A combination of the velocity and heading angle control were used to resolve the conflict with the use of the optimization software GAMS [69]. However, measurement issues were not addressed.

4.2.5 Grid-Based Approach

The Conflict Grid method is a separation management designing technique based on the use of a 4-dimensional space grid (three spatial dimensions and time) to represent airspace for computationally efficient strategic air traffic conflict detection method. The idea was to store aircraft trajectories in 4-D grid space and set the value of the grid cell to 1. The benefit of such an approach is that the region of bad weather and special-use airspace can easily be incorporated into the conflict grid by denoting the grid as inaccessible. In the research paper [70], Jardin et al extended the grid method to the stochastic conflict grid method, which stores the probability that at least one active constraint exists in any given grid cell rather than using 1 or 0. The

advantage of using such an approach is that it addresses the uncertainty issue of the aircraft trajectory. The downside is that it increases the computational effort of the algorithm which becomes a key issue when facing increased numbers of aircraft.

4.2.6 Satisficing Approach

Satisficing game theory is a centralized multiagent approach to the resolution of aircraft conflict presented by Archibald [14]. Collisions are avoided by the joint actions of individual aircraft. The aircraft actions are determined from two properties, namely, the *Selectability* and *Rejectability* of the particular heading option for that aircraft. At every time stamp, there are five directional options: ± 2.5 degree, ± 5 degree, 0 degree. The direction of aircraft is determined by utilizing these two properties. The calculation of *Selectability* is based on how direct the heading option is to the desired destination as well as the heading options that are in conflict with each other. The *Rejectability* calculation is based on the heading options that conflict with current headings of other aircraft. The fundamentally difference between the satisficing approach and other conflict resolution approaches is that the satisficing approach does not aim to find a "best" solution. Instead, each aircraft determines a set of acceptable avoidance maneuvers by eliminating from the full set of options as many bad choices as possible based on safety and efficiency concerns. The heading can then be chosen from the remaining alternatives according to different needs. The downside of this approach is the increasing computational effort when facing increased numbers of aircraft.

4.2.7 Delay based Ranking Separation Algorithm

The *delay based ranking separation algorithm* proposed by Qian Hui in 2008 is a centralized approach [71]. It is similar to the Satisficing approach discussed above, in the sense of ordering the priority of a limited list of possible heading changes. The rank of each aircraft is based on their flight hours and their delay. After the rank of each aircraft is determined, their individual heading change can then be selected from 5 different heading change options, 0 degree, ± 2.5 degree, ± 5 degree, in order of preference. The basic principle of selection is based on conflict detection; however, the aircraft only needs to consider the conflicts involving the higher rank ones. Therefore, the order of determining heading change is based on their rank. If all five heading change options for a particular aircraft will all result in a conflict, the higher rank

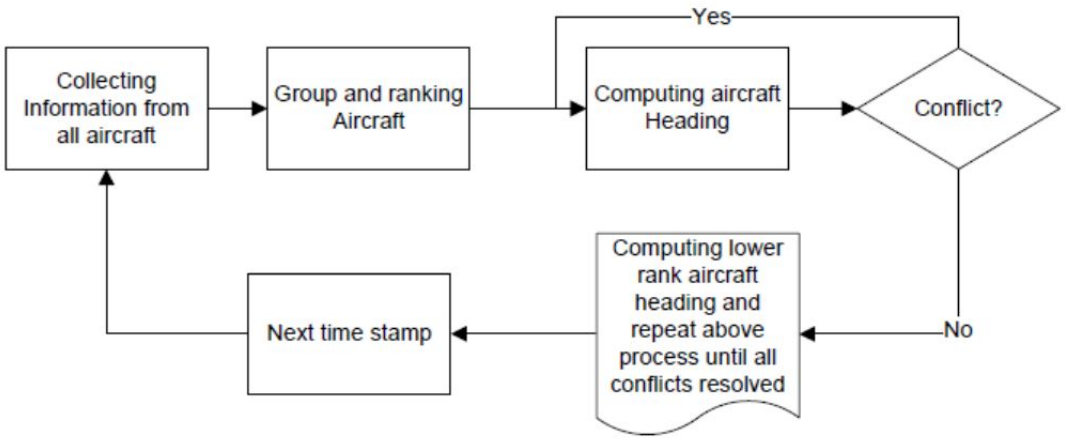

Figure 4.2: Process of Delay based Ranking Separation Algorithm

aircraft will need to select its heading change again. This process goes on until all aircraft have successfully selected their own heading change. The drawback of this approach is the excessive computational effort required when the aircraft numbers increase.

4.2.8 Other Techniques

Some other techniques for centralized separation management include: cost graphs method [72]; multi-party algorithm collision avoidance (MPCA) approach [73] and cooperative geometric optimization algorithm [61].

4.3 Separation Management Approaches in NextGen and SESAR

NextGen and SESAR have been compared in a recent study [74], Operational performance for the methods proposed by NextGen and SESAR are continuously evaluated and compared by the Performance Review Commission, a joint effort between the FAA and EUROCONTROL. The U.S. Government Accountability Office (GAO) has also recommended to improve the information exchange between NextGen and SESAR to improve the interoperability of the two projects [75].

Although the basic concept is fundamentally the same, SESAR, being a more decentralized model, calls for the establishment of a Reference Model for data normalization and standardization. While NextGen, envisioning a more centralized approach describing not only

data but the provision of ”information services” in a networked environment [74]. In order to achieve a high level of safety in both concepts, separation management must be considered. Such as the en-route Decision Support Tools that is being deployed to support NextGen separation(URET/ERAM) [76] and separation management capabilities for SESAR, which is developed under the FASTI project [77]. Both concepts call for systems to make use of centralized and decentralized services, delivered in a network enabled environment. Therefore, both NextGen and SESAR will have to deal with identical problems in terms of communications issues.

4.4 Summary

This chapter presented a comprehensive literature review related to separation management system approaches. A number of state-of-the-art separation management approaches were discussed. Figure 4.3 shows an overview of separation management approaches. Furthermore, some literature was identified as the basis for the new proposed separation system. The specific approaches used in this study will be tested and compared in Chapter 6 (as identified in Figure 4.3). Chapter 5 will discuss the Risk-Ratio concepts in relation to measurement uncertainty and separation management systems.

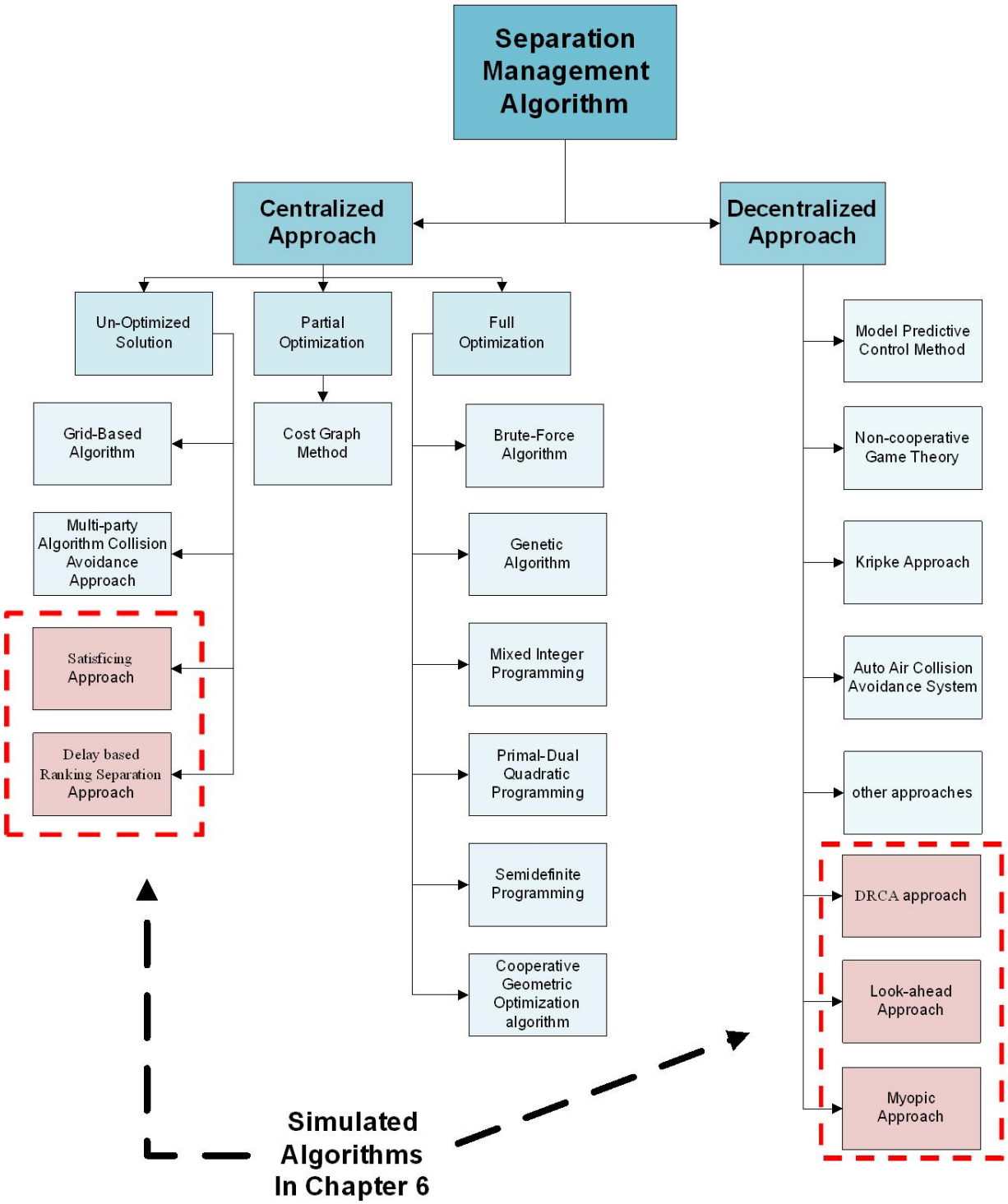

Figure 4.3: Knowledge map of literature review for separation management approaches

Chapter 5

Measurement Uncertainty and Separation Management System: Risk-Ratio Concepts

---

One of the primary desired abilities of any future air traffic separation management system is the ability to provide early conflict detection and resolution effectively and efficiently. This chapter considers the risk of conflict as a primary measurement to be used for early conflict detection. When estimating the risk of conflict, sensor measurement uncertainty cannot be neglected. This chapter proposes a novel approach to assessing the impact of different measurement uncertainty models on the estimated risk of conflict. The measurement uncertainty model can be used to represent different sensor accuracy and sensor choices. The chapter is organized as follows: Section 5.1 describes the past work conducted in the area of conflict risk and risk estimation. Section 5.2 formulates the conflict estimation and risk-ratio concepts using a dynamic state space model. Section 5.3 describes the particle filter implementation for the risk-ratio estimation problem. Section 5.4 provides a simulation study that compares the impact of different sensor choices on the estimated risk-ratio. Section 5.5 concludes the chapter.

5.1 Past Work

As discussed in Chapter 1 and 4, the aim of any separation management systems is to predict if a conflict is going to occur, and communicate any detected conflicts to a human operator to assist in the resolution of the conflict situation [31]. To successfully detect a conflict, the traffic environment must be first monitored, then appropriate state information must be collected and disseminated using sensors and appropriate communication equipment. The collected state

information provides an estimate of the current traffic situation. An aircraft dynamic model is also needed to project any state knowledge into the future so that it is possible to predict whether a conflict will occur at some future time epoch. Such a prediction can be solely based on collected state information or may be based on additional information, such as flight plans or knowledge of sensor accuracy. However, there is generally some uncertainty in the values of the collected states due to sensor errors or limited update rate [31].

Risk of conflict is defined as the product of the probability and consequences of the conflict event [18]. Generally, risk of conflict cannot be determined directly, because the probability of the conflict event is difficult to quantify. There has been some research on improved quantification of the risk of conflict over the past decade; however, research on the estimated risk of conflict has often focused on different aspects and from different perspectives [18]. Young, for example, describes risk concept using measurement of new technologies' readiness level (TRLs) [78]. Young's risk concept has been used to assess the maturity of new technologies as a means of evaluating their readiness for incorporation in new aircraft systems. Rather than quantifying the estimated risk itself, Young focuses on presenting a framework which captures the risk characterisation. Research in this area has usually approached the conflict risk estimation problem using a probabilistic calculation method [18]. Most probabilistic calculation methods do not require any additional information. As a result, the error in estimation tends to grow quadratically with time [18]. However, some previous research has addressed the importance of using additional information in estimating conflict risk [79]. One example of using additional information to estimate the risk of conflict is to incorporate aircraft intent information. By using additional intent information, unnecessary uncertainties in conflict risk estimation can be reduced [79]. However, in the NextGen concept, aircraft intent information could dynamically change over time. Thus a key limitation of this approach is that the quality of estimated risk of conflict information depends on the accuracy of the intent information.

5.2 Problem Formulation and Definition of Assessment Criteria

5.2.1 Risk of Conflict Estimation

This chapter classifies aircraft into two basic types: observer aircraft and target aircraft which were detailed in Chapter 2. The distance between the target aircraft and an observer aircraft

$D(x_t^r, x_t^1)$ can be written as:

$$D(x_t^r, x_t^1) = \sqrt{(x_t^r(1) - x_t^1(1))^2 + (x_t^r(3) - x_t^1(3))^2}, \tag{5.1}$$

The estimated risk of conflict is based on the knowledge of the current state and any additional information that may be available.

The conflict between a target aircraft and an observer aircraft is defined by an indicator function $C(\cdot, \cdot)$ which indicates whether a conflict exists between the two aircraft:

$$C(x_t^r, x_t^1) \triangleq \begin{cases} 1, & \text{if } D(x_t^r, x_t^1) \leq D_{cr} \\ 0, & \text{Otherwise,} \end{cases} \tag{5.2}$$

where $C(\cdot, \cdot)$ is a function of the states x_t^r and x_t^1, and D_{cr} is defined as the critical separation distance.

We will let $P_r(C(x_t^r, x_t^1))$ denote the probability of the conflict event at time instant t. Now risk of conflict R_t can be defined based on this conflict probability, as the product of conflict event cost B_c and the probability of the conflict event as follows:

$$R_t(x_t^r, x_t^1) = B_c \times P_r(C(x_t^r, x_t^1)). \tag{5.3}$$

To allow us to consider the impact of different models on estimated risk of conflict, λ is introduced to denote the model under consideration. The estimated risk of conflict based on observed information can be expressed as:

$$R_{\tau|t}(\lambda) = E[R_\tau(x_\tau^r, x_\tau^1)|y_{0,t}, \lambda], \tag{5.4}$$

where $E[R_\tau(x_\tau^r, x_\tau^1)|y_{0,t}, \lambda]$ is the expected value of R_τ at time instant τ, based on measurements up to time t using model λ. Here $\tau = t + \ell$ and $\ell \in [0, T_p]$ represents the prediction length, and T_p is the upper limit of the prediction length. Whilst $R_{\tau|t}(\lambda)$ is estimated risk of conflict at time instant τ, it is also important to estimate the risk of conflict during the next period of time. To describe the worst conflict situation during the period $[t, t + T_p]$, we define the future estimated risk of conflict as the maximum estimated risk of conflict that occurs during

the period $[t, t+T_p]$ which is indicated by superscript m, this future estimated risk of conflict can be expressed as:

$$R^m_{t|T_p}(\lambda) = \max_{\ell \in [0,T_p]} R_{t+\ell|t}(\lambda), \tag{5.5}$$

5.2.2 The Risk-Ratio Concept

Risk-ratio is a relative measure of the safety benefit brought about in a given environment by changes in the procedure or equipment [80]. For air traffic separation management systems, safety is measured in terms of the estimated risk of conflict [81]. When we want to evaluate the utility of a model λ, it may be useful to quantify its performance by a nominal model (λ°) using the concept of risk-ratio. For these reasons, the risk-ratio on interval $[t, t+T_p]$ will be defined as:

$$F_{t|T_p}(\lambda, \lambda^\circ) = \frac{R^m_{t|T_p}(\lambda)}{R^m_{t|T_p}(\lambda^\circ)}, \tag{5.6}$$

where $R^m_{t|T_p}(\lambda)$, defined by equation (5.5), is the future estimated risk of conflict using model under test.

5.3 Calculation of Risk-Ratio using Particle Filters

In order to compute the estimated risk of conflict, the probability of conflict needs to be estimated first. In general, it is difficult to evaluate $Pr(C(\cdot,\cdot))$ analytically [43]. A particle filter approach can be used to numerically estimate $Pr(C(\cdot,\cdot))$. Particle filter is an approximate non-linear filter for discrete time nonlinear state-space models, relating a hidden state x_k to the observation y_k [82]. By using particle filter algorithms, the approach can be applied to more general cases than is possible using Kalman filter based concepts.

5.3.1 Particle Filter Algorithm

Let us consider tracking N target aircraft. For this purpose, we allocate a set of M particles to each tracked target aircraft r. The states for m^{th} particle that tracks target aircraft r are denoted by $x^{m,r}_k$. The particle filters first initialise all M particles based on the initial target aircraft state's probability density function (PDF). The particle filter then iterates four steps every time instant k [8].

5.3.2 Conflict Risk Estimation

Particle filters can be used to estimate the states of the aircraft and predict future state information based on current and past observation. State predictions after p time samples can be evaluated with the reapplication of the time update algorithm in equation (2.11) p times [8]. From the particle filter output ($x_{k+1}^{m,r}$ and $w_{k+1|k}^{m,r}$), by predicting into the future p time samples, the probability of conflict between the r^{th} target aircraft and an observer aircraft $P_r(C(x_\tau^r, x_\tau^1))$ can be estimated by summing up the product of individual particle's weight $w_{k+p|k}^{m,r}$ and its corresponding particle's indicator function $C(x_{k+p}^{m,r}, x_{k+p}^1)$ which can be calculated using equation (5.2).

For computational reasons, discrete time analysis of concepts previously defined in continuous time are introduced. We let P_r denote the probability of the conflict event, and be written as:

$$P_r(\bar{C}(x_{k+p}^r, x_{k+p}^1)) = E[P_r(C(x_\tau^r, x_\tau^1))], \tag{5.7}$$

where $\bar{C}(x_{k+p}^r, x_{k+p}^1)$ is the mean of the indicator value for conflict between target aircraft r and the observer aircraft (1). Sampling time instant k in equation (5.7) is the discrete representation of continuous time t in equation (2.4) to (5.6). Prediction time p in equation (5.7) is the discrete representation of prediction time l in continuous time that appeared in equation (5.5).

The probability of the conflict event can also be expressed as:

$$P_r(\bar{C}(x_{k+p}^r, x_{k+p}^1)) = \frac{\sum_{m=1}^{M} w_{k+p|k}^{m,r} \times C(x_{k+p}^{m,r}, x_{k+p}^1)}{\sum_{m=1}^{M} w_{k+m|k}^{m,r}}, \tag{5.8}$$

where k is the current time sample, and $w_{k+p|k}^{m,r}$ represents the predicted conditional weighting for the m^{th} particle with prediction length p for target aircraft $r(m = 1, 2, ...M)$. In equation (5.8), the indicator function $C(x_{k+p}^{m,r}, x_{k+p}^1)$ gives an indication whether this particular particle is in conflict with observer aircraft after p time samples.

The mean value of estimated risk of conflict at prediction time p from current time instant k can then be re-expressed as :

$$\bar{R}_{k+p|k} = \frac{\sum_{m=1}^{M} w_{k+p|k}^{m,r} \times C(x_{k+p}^{m,r}, x_{k+p}^1)}{\sum_{m=1}^{M} w_{k+p|k}^{m,r}} \times B_c, \tag{5.9}$$

where $\bar{R}_{k+p|k}$ is the mean value of the estimated risk of conflict at p time interval from current time instant k and B_c is the cost of conflict event. The discrete representation of risk-ratio on interval $[t, t+T_p]$ is given by:

$$F_{k|T_p}(\lambda, \lambda^\circ) = E[F_{t|T_p}(\lambda, \lambda^\circ)], \tag{5.10}$$

where T_p is the upper limit of the prediction length under consideration.

5.4 Simulation Study and Results

5.4.1 Simulation Implementation

The particle filters were implemented in the MATLAB®simulation environment using ReBEL version 0.2.7. ReBEL is a MATLAB® toolkit of functions and scripts, designed to facilitate sequential Bayesian estimation in general state space models [83]. The software consolidates research on new methods for recursive Bayesian estimation and Kalman filtering.

5.4.2 Simulation Setup

In the following simulations, we consider different cases of one maneuvering target aircraft observed by other nearby aircraft. The sensor under consideration is located on the observer aircraft. The target aircraft dynamics are modeled in Cartesian coordinates as $x_k = Hx_{k-1} + Gv_{k-1}$ where the states of the target are position and velocity in each of the two Cartesian coordinates (x and y). Thus x_k is a vector of dimension 4. The system matrices H and G are defined as:

$$H = \begin{bmatrix} 1 & T & 0 & 0 \\ 0 & 1 & 0 & 0 \\ 0 & 0 & 1 & T \\ 0 & 0 & 0 & 1 \end{bmatrix}, G = \begin{bmatrix} T^2/2 & 0 \\ T & 0 \\ 0 & T^2/2 \\ 0 & T \end{bmatrix}, \tag{5.11}$$

where T is the sampling period. The standard deviation of the process noise is 0.1.

First, an evaluation for estimated risk of conflict in a single head-on collision case is conducted, then, it followed by two other simulations. In the first simulation, state estimation for the target was performed using a particle filter with four different measurement uncertainty models which were introduced in Chapter 2. All simulations involve a critical separation distance of $500m$. In the simulation, the target tracking algorithms were initialized near the actual target states.

Four different scenarios were performed in the first simulation (Simulation 1). In each of the scenarios, the observer aircraft travels from west to east and the target aircraft travels from east with different bearing angles as indicated in Figure 5.1. The major difference between these four scenarios is the minimum separation distance achieved between the observer aircraft and target aircraft. Case I, II and III represent conflict cases, while Case IV represents a non-conflict case. In all four cases, the target aircraft starts at a location approximately $2000m$ away from the observer. The velocity of the observer aircraft and target aircraft are both 100 knots ($51.4m/s$) [84]. All four different measurement uncertainty models were implemented and applied to the scenarios to compare the impact of different sensor choices on future estimated risk of conflict.

In the second simulation (Simulation 2), we examined two different scenarios representing a conflict case and a non-conflict case (as shown in Figure 5.2) and compared the impact of varying range or bearing accuracy on the future estimated risk of conflict using the risk-ratio concepts. The target aircraft started at a location approximately $1500m$ away from the observer aircraft. The observer aircraft had a bearing angle of 45 degrees for the conflict case and 30 degrees for the non-conflict case. The target aircraft traveled from south to north, the velocity of the observer aircraft and target aircraft were both set to $100knots$ ($51.4m/s$).

5.4.3 Simulation Results

5.4.3.1 Particle Filter Risk Prediction

In order to establish the relationship between time-to-conflict and quality of estimated risk of conflict, we evaluated the estimated risk of conflict $\bar{R}_{k+p|k}$, as defined by equation (5.9), for a simple head-on collision case. Figure 5.3 shows that the estimated risk of conflict $\bar{R}_{k+p|k}$ decreases as the prediction interval p increases. This occurs because the certainty in estimated risk of conflict increases as range decreases. However, the aircraft could declare a conflict

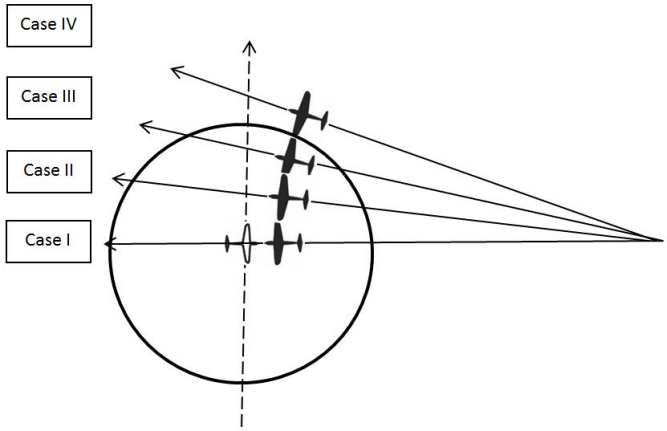

Figure 5.1: Head on Conflicts: Figure shows trajectories for four different scenarios respectively (Simulation 1). Each black aircraft represents the target aircraft in a different scenario labeled Case I, Case II, Case III and Case IV. The white aircraft represents the observer aircraft which is the same in each scenario. The circle represent the critical separation distance for the observer aircraft at one particular time instant. The minimum separation distance achieved in these four scenarios are $46m$, $234m$, $488m$ and $547m$ respectively, Case I, Case II and Case III represent conflict cases and Case IV represents a non-conflict case.

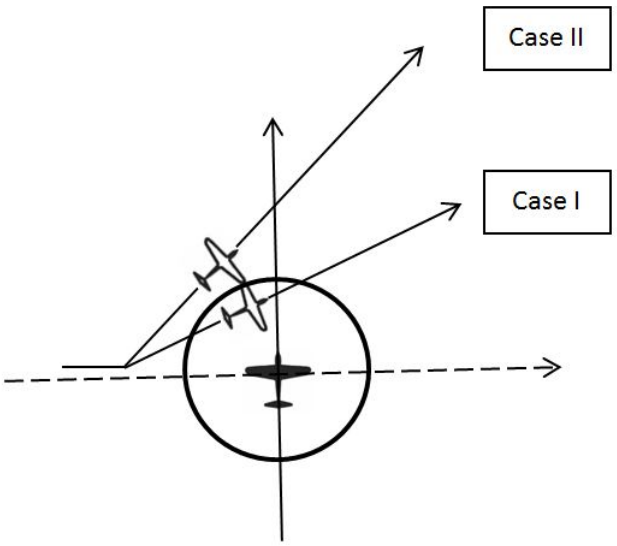

Figure 5.2: Crossing Conflict: Figure shows the trajectories for two different scenarios (Simulation 2), the black aircraft represents the target aircraft which is the same in each scenario. The white aircraft represents the observer aircraft in two scenarios Case I and Case II. The circle represent the critical separation distance for the target aircraft at one particular time instant.

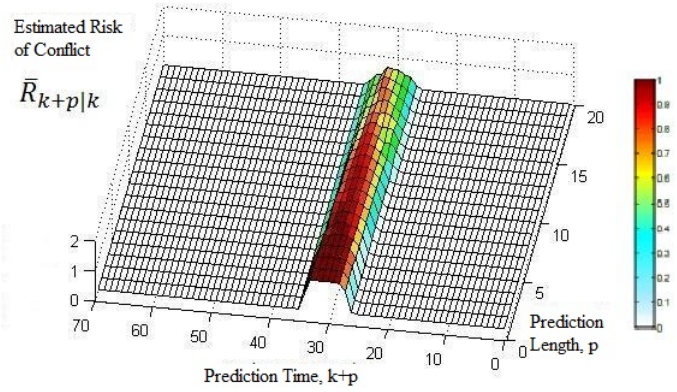

Figure 5.3: Estimated risk of conflict at time instant k, prediction time p. Color bar red indicates a higher value of risk while blue indicates a lower value of risk.

Table 5.1: Table of future estimated risk of conflict $\bar{R}^m_{10|20}$ and risk-ratio $\bar{F}_{10|20}(\lambda, \lambda^\circ)$ with four different measurement uncertainty models in conflict case.

		Sensor Choices			
	Case	Bearing only (λ°)	Radar	ADS-B	ADS-B + Radar
Future Estimated risk-of-conflict $\bar{R}^m_{10\|20}$	I	0.53 ± 0.01	0.76 ± 0.01	0.65 ± 0.02	0.86 ± 0.01
	II	0.45 ± 0.01	0.70 ± 0.02	0.60 ± 0.02	0.75 ± 0.02
	III	0.32 ± 0.01	0.50 ± 0.02	0.50 ± 0.02	0.49 ± 0.03
Risk Ratio $\bar{F}_{10\|20}(\lambda, \lambda^\circ)$	I	1	1.444 ± 0.004	1.226 ± 0.005	1.625 ± 0.004
	II	1	1.555 ± 0.008	1.323 ± 0.008	1.659 ± 0.009
	III	1	1.576 ± 0.038	1.591 ± 0.038	1.541 ± 0.038

earlier; with lower confidence, if earlier declaration is required to ensure that there is sufficient time to execute a suitable avoidance maneuver. Therefore, there is a trade-off between time-to-conflict and accuracy of estimated risk of conflict. In order to get an accurate estimate risk of conflict value (with sufficient time to resolve the conflict), we need to understand how different measurement uncertainty models impact on estimated risk of conflict. The relationship between measurement uncertainty models and estimated risk of conflict is further explored in the following subsection.

5.4.3.2 Risk-Ratio Comparison for Sensor Choices

In the first simulation, risk-ratio concepts are used to assess the impact of sensor choice on the future estimated risk-of-conflict. In this study, sensor accuracy is set to RNP-1 (which

Table 5.2: Table of future estimated risk-of-conflict $\bar{R}^m_{10|20}$ and risk-ratio $\bar{F}_{10|20}(\lambda, \lambda^\circ)$ with four different measurement uncertainty models in non-conflict case

		Sensor Choices			
	Case	Bearing only (λ°)	Radar	ADS-B	ADS-B + Radar
$\bar{R}^m_{10\|20}$	IV	0.086 ± 0.014	0.067 ± 0.010	0.073 ± 0.015	0.035 ± 0.006
$\bar{F}_{10\|20}(\lambda, \lambda^\circ)$	IV	1	0.779 ± 0.002	0.849 ± 0.004	0.407 ± 0.001

corresponding to a standard deviation of $944.92m$ for latitude, longitude, range measurements and $0.492rad$ for bearing angle measurements). The future estimated risk-of-conflict $R^m_{t|T_p}$ is computed at $t = 10$ seconds using a maximum prediction length of $T_p = 20$ seconds. Table 5.1 provides the results for the future estimated risk-of-conflict $\bar{R}^m_{t|T_p}$ and risk ratios $\bar{F}_{t|T_p}(\lambda, \lambda^\circ)$, as defined in equation (5.10), for the four measurement uncertainty models in conflict cases. Case I to Case III are conflict cases in which the maximum value for conflict indicator function from $10th$ to $30th$ time instant is equal to 1 (this is what conflict means). Bearing-only sensor model is considered to be the the nominal model for the risk-ratio comparison study. Similarly, Table 5.2 provides the results for the future estimated risk-of-conflict $\bar{R}^m_{t|T_p}$ and risk ratios $\bar{F}_{t|T_p}(\lambda, \lambda^\circ)$ for four measurement uncertainty models in the non-conflict case. The value for conflict indicator function during $10th$ to $30th$ time instant for the non-conflict case is 0 (this is what non-conflict means).

For all conflict cases, a risk-ratio higher than 1 indicates better risk estimates than the nominal model. A risk-ratio lower than 1 suggests that the model selected does not represent the situation as accurately as the nominal model. For the non-conflict case, a risk-ratio lower than 1 indicates better risk estimation than under the nominal model. In this situation, cases when the risk-ratio is higher than 1 suggests that the model selected does not represent the situation as accurately as the nominal model.

From Table 5.1, we observed that the bearing-only sensor model performed slightly worse than the other 3 sensor models, whilst ADS-B, radar and ADS-B + Radar model achieved similar performance. Furthermore, for the same sensor choice and sensor accuracy, conflict geometry also effects the ability to accurately estimate the future risk-of-conflict. In conflict cases when the minimum separation distance achieved is close to the critical separation distance, the estimation accuracy for future risk-of-conflict is reduced. This reduction in performance is

Table 5.3: Table of future estimated risk-of-conflict $\bar{R}^m_{5|20}$ and risk-ratio $\bar{F}_{5|20}(\lambda, \lambda^\circ)$ with varying bearing parameter A in a non-conflict case

A	0.01	0.1	1 (λ°)	10	100
$\bar{R}^m_{5\|20}$	0	0.000 ± 0.000	0.003 ± 0.001	0.083 ± 0.014	0.222 ± 0.032
$\bar{F}_{5\|20}(\lambda, \lambda^\circ)$	0	0.039 ± 0.002	1	24.301 ± 0.080	64.563 ± 0.200

Table 5.4: Table of future estimated risk-of-conflict $\bar{R}^m_{5|20}$ and risk-ratio $\bar{F}_{5|20}(\lambda, \lambda^\circ)$ with varying range parameter B in a non-conflict case

B	0.01	0.1	1 (λ°)	10	100
$\bar{R}^m_{5\|20}$	0	0.002 ± 0.001	0.004 ± 0.001	0.016 ± 0.003	0.084 ± 0.012
$\bar{F}_{5\|20}(\lambda, \lambda^\circ)$	0	0.419 ± 0.003	1	3.605 ± 0.016	18.73 ± 0.079

evident when comparing future estimated risk-of-conflict in different conflict cases.

5.4.3.3 Risk-Ratio Comparison for Sensor Accuracy

In the second simulation, risk-ratio concepts are used to assess the impact of sensor accuracy on the future estimated risk-of-conflict. Nominal sensor accuracy of RNP-1 is used in these simulations. In this simulation, conflict occurs when the minimum distance achieved between observer and target aircraft is less than $500m$. The future estimated risk-of-conflict $R^m_{t|T_p}$ is computed at $t = 5$ second with a maximum prediction length of $T_p = 20$ seconds. Here we define A and B as the bearing and range accuracy modification factors respectively (e.g. $A = 10$ is equivalent to a bearing accuracy of RNP-10). By choosing different values for A and B, we can model the impact of different radar bearing and range observation accuracies. The future estimated risk-of-conflict $\bar{R}^m_{t|T_p}$ and risk-ratio $\bar{F}_{t|T_p}(\lambda, \lambda^\circ)$ compared with the nominal model is shown in Table 5.3 while the parameter A varies from 0.01 to 100 and parameter B is fixed to 1. Table 5.4 compares the future estimated risk-of-conflict $\bar{R}^m_{t|T_p}$ and risk-ratio $\bar{F}_{t|T_p}(\lambda, \lambda^\circ)$ when varying parameter B from 0.01 to 100 ($A = 1$).

For the non-conflict case in Tables 5.3 and 5.4, a risk-ratio lower than 1 indicates improved quality of future estimated risk-of-conflict when compared to the performance achieved under the nominal model. In cases when the risk-ratio is higher than 1 indicates a lower quality of estimated risk-of-conflict compared to the performance achieved under the nominal model. When either parameter A or B are decreased, as seen in Table 5.3 and Table 5.4, resulted a

Table 5.5: Table of future estimated risk-of-conflict $\bar{R}^m_{5|20}$, and risk-ratio $\bar{F}_{5|20}(\lambda, \lambda^\circ)$ with varying parameter A in a conflict case

A	0.01	0.1	1 (λ°)	10	100
$\bar{R}^m_{5\|20}$	0.850 ± 0.032	0.742 ± 0.036	0.536 ± 0.028	0.432 ± 0.017	0.469 ± 0.013
$\bar{F}_{5\|20}(\lambda, \lambda^\circ)$	1.586 ± 0.001	1.386 ± 0.001	1	0.807 ± 0.001	0.876 ± 0.001

Table 5.6: Table of future estimated risk-of-conflict $\bar{R}^m_{5|20}$ and risk-ratio $\bar{F}_{5|20}(\lambda, \lambda^\circ)$ with varying parameter B in a conflict case

B	0.01	0.1	1 (λ°)	10	100
$\bar{R}^m_{5\|20}$	0.843 ± 0.024	0.639 ± 0.031	0.536 ± 0.028	0.399 ± 0.015	0.482 ± 0.011
$\bar{F}_{5\|20}(\lambda, \lambda^\circ)$	1.573 ± 0.001	1.192 ± 0.001	1	0.744 ± 0.001	0.899 ± 0.001

better future estimated risk-of-conflict value. Tables 5.3 and 5.4 also demonstrate that a false alarm could possibly be produced if excessive measurement noise was present in the Figure 5.2 simulation 2 (e.g. a large A or B value).

When comparing the radar accuracy impact on the future estimated risk-of-conflict and risk-ratio in a conflict case, the minimum separation distance achieved during the simulation is $459m$. Table 5.5 compares the future estimated risk-of-conflict and risk-ratio when varying the A factor from 0.01 to 100 ($B = 1$). Table 5.6 shows the future estimated risk-of-conflict $\bar{R}^m_{5|20}$ and risk-ratio $\bar{F}_{5|20}(\lambda, \lambda^\circ)$ for a varying B factor from 0.01 to 100 in a conflict case ($A = 1$). In conflict cases, a risk-ratio higher than 1 indicates improved future estimated risk-of-conflict when compared to performance achieved under the nominal model. A risk-ratio lower than 1 indicates that the model selected does not represent the situation as accurately as the nominal model.

Table 5.3-5.6 also show a marginal decrease in the error between future estimated risk-of-conflict and the corresponding conflict indicator function in cases where a greater sensor accuracy is used. For example, for a measurement uncertainty model in which sensor accuracy is equal to RNP-0.1, the quality of future estimated risk-of-conflict is only marginal lower than that obtained in model where sensor accuracy is equal to RNP-0.01. This observation implies that sensors do not need to be excessively accurate in order to obtain a good quality future estimated risk-of-conflict. It is also evident from Table 5.3-5.6 that within the same sensor

choice, higher sensor accuracy corresponds to a more accurate future estimated risk-of-conflict.

5.4.4 Discussion of Results

The results from our simulations can be interpreted in the following three ways.

Firstly, in terms of prediction horizon, the results of the simulation study suggest that sensor accuracy affects the length over which reliable prediction is possible. In other words, with higher sensor accuracy, we can predict relatively further ahead in time.

Secondly, in terms of sensor choices, the radar observation model performs slightly better in assessing the future estimated risk-of-conflict compared with the bearing-only sensor model, as is expected because the radar observation model provides additional range information. The risk-ratio analysis also shows that the radar model, ADS-B model and ADS-B+radar model have similar performance in assessing the future estimated risk-of-conflict. The risk-ratio analysis implies that the separation management system does not significantly benefit from additional sensor measurements (if the additional sensors have similar accuracy, at the same data rate). However, the aircraft separation management system can benefit from ADS-B's high update rates compared to the radar measurements. This risk-ratio approach helps to quantify the risk-of-conflict benefits brought about by combining different sensor systems.

Thirdly, in terms of sensor accuracy, our simulation results show that estimation is improved as sensor accuracy increases. The improved estimation characteristics are illustrated through larger risk-ratios in conflict cases and smaller risk-ratios in non-conflict cases. However, the simulation study also suggests that sensors do not need to be excessively accurate in order to obtain reasonably accurate estimations of the risk-of-conflict. Furthermore, the study also indicates that conflict geometry impacts accurate risk-of-conflict estimation, especially at the boundary of the conflict zone.

5.5 Conclusion

In this chapter,a new risk-ratio based approach for assessing the impact of sensor accuracy and sensor choice on the ability to accurately predict conflicts was proposed. The proposed risk-ratio based approach was implemented using particle filter estimation and prediction techniques.

Use of particle filters allows consideration of more complex aviation scenarios that include non-linear characteristics of measurement devices. Next, in Chapter 6, additional insights into the uncertain environment problem will bring forth by a comparison of separation performance behavior of several popular algorithms in an uncertain communication environment.

Chapter 6

Communication Uncertainty and Separation Management System: Five Approaches Compared

---

As noted in chapter 1, new air traffic automated separation management concepts are constantly under investigation. Yet most of the automated separation management algorithms proposed over the last few decades have assumed either perfect communication or exact knowledge of all aircraft locations. In realistic environments, these idealized assumptions are not valid and any communication failure can potentially lead to disastrous outcomes. This is a brief simulation study chapter that examines the separation performance behavior of several popular algorithms in an uncertain communication environment. The chapter is organized as follows: Section 6.1 describes the past work conducted in the area of separation management systems. Section 6.2 compares the separation performance behavior of several popular algorithms during periods of information loss. Section 6.3 describes the simulation study conducted. Section 6.4 draws some conclusions.

6.1 Past Work

In recent years, air traffic management systems have faced increasing levels of air traffic demands [85]. Current solutions to congestion problems have included building more facilities, hiring more controllers and expanding existing Air Traffic Control technologies. These patchwork solutions have been only marginally effective, at a huge cost. There is increasing motivation to improve the efficiency of the air traffic management process by investigating the use of automation technologies [86]. In this regard, there has been some notable work in

the area of next generation air traffic management; two examples of these programs are the SESAR project in Europe and the NextGen project in the US. These two projects are different in scope, but they share a common understanding of a possible future air traffic management capability, which would include automation functions that assist the decision making of air traffic controllers. However if these automated concepts are to be adopted then the safe guards that are present in current operational procedures will no longer be sufficient. This chapter is specifically focused on the (automated) separation management system which has the task of maintaining safe separation distances between aircraft and, in the event of a potential conflict arising, this system also has the task of resolving conflicts in a safe manner. However if a communication failure event occurs, there is a possibility that a given separation management system might incorrectly handle the information available, and that these incorrect actions might lead into a mid-air collision.

6.2 Existing Separation Management Algorithms

There is a need to develop an automated separation management approach that has robust behavior with respect to the communication issues that arise in the uncertain communication environments. For this purpose, we present a simulation study that investigates the performance of several separation management approaches during communication failure. Whilst the complete loss of a central communication network would clearly cause total failure of centralized separation management, our simulation study also suggests that loss of communication with just one aircraft may significantly reduce the performance of both centralized and decentralized separation management algorithms. The study also suggests that the degree of performance degradation depends on the nature of the air traffic scenario.

In the study presented in this chapter, two centralized separation management and three decentralized separation management approaches are examined and compared. Details of each these algorithms can be found in Chapter 4. The following algorithms are examined:

1. Centralized separation management approaches

    (a) Satisficing Approach [14]

    (b) Delay Ranking Approach [71]

2. Decentralized separation management approaches

   (a) Decentralized Reactive Collision Avoidance Approach [15]

   (b) Myopic Decentralized Approach [50]

   (c) Look-ahead Decentralized Approach [50]

6.3 Simulation Study

Five of the selected separation management algorithms were simulated, the evaluation was carried out using the following implementation choices.

6.3.1 Dynamics

The dynamics of each aircraft was represented using the simplified 3DOF kinematics model presented in Chapter 2, Section 2.1. The control inputs u_i are restricted to $u_{i,min} \leq u_i \leq u_{i,max}$. where $u_{i,min}$ and $u_{i,max}$ represents the minimum and maximum turning rate of the aircraft.

6.3.2 Traffic pattern Scenarios (Four Aircraft)

Figure 6.1, 6.2 and 6.3 show the three scenario types were examined this study: the cross passing scenario, the choke point scenario and the 4 vehicle mixed benchmark scenario. All aircraft used are simulated to have constant speed $s_i = 100m/s$ (which corresponds to 360km/hour and is roughly representative of a GA Class aircraft). Control limits $u_{i,min}$ and $u_{i,max}$ were assumed to be -5 degree/second and $+5$ degree/second, respectively (see [71] for justification).

6.3.3 Performance Metrics

Algorithms are compared on the basis of minimum separation distance. Other metrics such as traffic complexity metric and route planning efficiency are meaningful but minimum separation distance describes the most important algorithm characteristic.

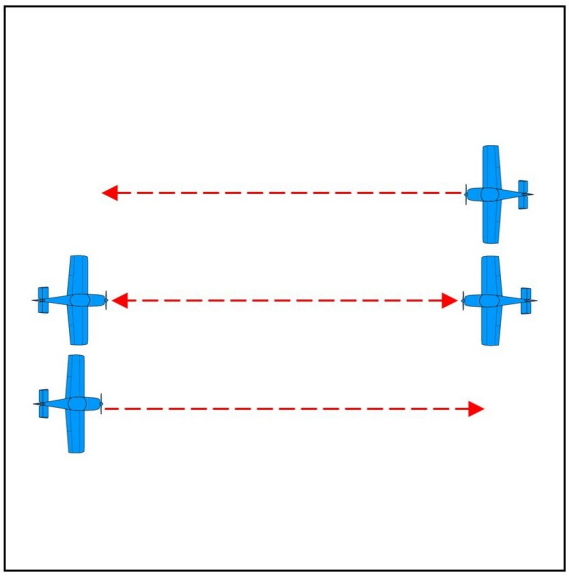

Figure 6.1: The Cross Passing Scenario

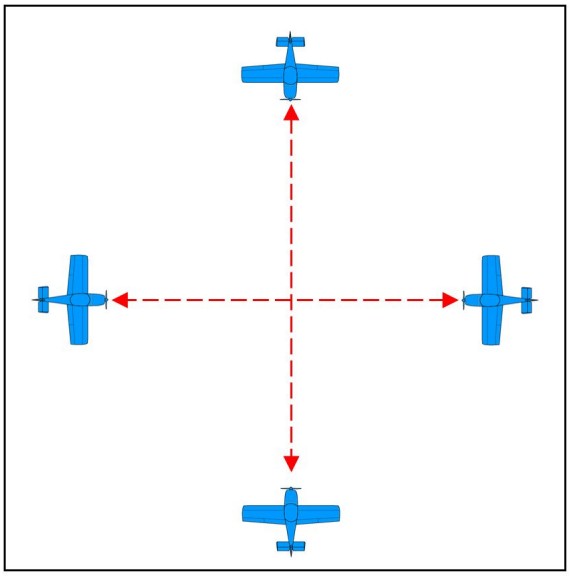

Figure 6.2: The Choke Point Scenario

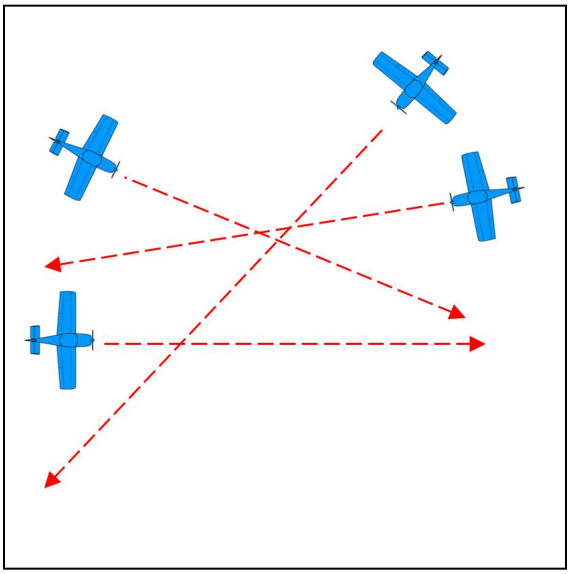

Figure 6.3: 4 Vehicle Mixed Benchmark Scenario

6.3.4 Simulation Results

This section describes the results of the simulation study in which the performance of the five algorithms in a situation when a communication failure related to one of the aircraft has occurred are compared. The data update rate of 2Hz was used in both simulations and the desired separation distance was set to 400m.

6.3.4.1 Centralized Separation Management

In this part of the simulation study, two centralized approaches are compared: satisficing approach and delay ranking approach. Each of these separation algorithms was examined in the three traffic pattern scenarios described in earlier. For each traffic pattern scenario, the algorithms were examined in two information situations: perfect information situation, and in the presence of a single uncooperative aircraft. An uncooperative aircraft is defined as an aircraft that does not follow the separation instructions issued by the central controller (perhaps this instruction was not received due to equipment failure on the aircraft). Table 6.1 shows the separation distances achieved by the centralized separation management algorithms. Note that both algorithms managed separation correctly when full information was available.

The impact of having a single uncooperative aircraft in these traffic patterns is evaluated next. Table 6.2 shows the effective reduction in minimum separation distance caused by the

Table 6.1: Performance of Centralized Separation Management Approaches (minimum separation distance) in Perfect Information Situation

Performance (minimum separation distance)	Choke Point	Cross Passing	Four Vehicle Mixed Benchmark
Satisficing	$456.4m$	$413.1m$	$453.1m$
Delay Based	$436.3m$	$434.1m$	$434.1m$

Table 6.2: Centralized Separation Management: the **reduction** in separation distance due to an uncooperative aircraft, a positive value means worse performance

Performance Degradation (Compared to Table 6.1)	Choke Point	Cross Passing	Four Vehicle Mixed Benchmark
Satisficing	$247.6m$	$133.6m$	$130.0m$
Delay Based	$159.3m$	$35.0m$	$27.0m$

single uncooperative aircraft (that is, minimum separation distance in the prefect information case minus the minimum separation distance achieved in the presence of a single uncooperative aircraft).

6.3.4.2 Decentralized Separation Management

The DRCA approach, the myopic approach and the look-ahead (LA) approach are compared. Each of these separation algorithms was examined in the three traffic pattern scenarios described in section 6.3.2. For each traffic pattern scenario, the algorithms were examined in two information situations: perfect information, and in the presence of an uncooperative aircraft. An uncooperative aircraft here is defined as an aircraft that cannot perform decentralized separation management (perhaps on-board sensors are not functioning correctly) Such an aircraft is assumed to maintain straight flight. Table 6.3 shows the separation distances achieved by the decentralized separation management algorithms when all four aircraft all fully operational. Both the Myoptic and Look-ahead approaches failed in the cross passing pattern (even when all aircraft at fully operational). We next evaluated the impact of having a single uncooperative aircraft in these traffic patterns. Table 6.4 shows the effective reduction in minimum separation distance caused by the single uncooperative aircraft (that is, minimum separation distance in the prefect information case minus the minimum separation distance achieved in the presence of a single uncooperative aircraft). Two cases in which the separation distance increased actually

Table 6.3: Performance of Decentralized Separation Management approaches (minimum separation distance) in Perfect Information Situation

Performance (minimum separation distance)	Choke Point	Cross Passing	Four Vehicle Mixed Benchmark
DRCA	$399.6m$	$423.6m$	$401.4m$
Myopic	$399.8m$	$26.5m$	$398.6m$
LA	$398.5m$	$33.5m$	$400.4m$

Table 6.4: Decentralized Separation Management: the **reduction** in separation distance due to an uncooperative aircraft, a positive value means worse performance

Performance Degradation (Compared to Table 6.3)	Choke Point	Cross Passing	Four Vehicle Mixed Benchmark
DRCA	$131.9m$	$23.0m$	$0.7m$
Myopic	$1.3m$	$-72.2m$	$231.3m$
LA	$0.0m$	$-65.2m$	$15.5m$

corresponded to the case when separation failed in the fully operational case.

6.3.5 Summary of Simulation Study

The results given in the Table 6.1 and 6.2 suggest that centralized separation approaches tend to have a degraded performance if there is communication loss in one of the aircraft in the airspace. The main reason for this degraded performance is that these approaches assume perfect communication. It would expected that performance to be even worse if additional aircraft have communication problems. Table 6.3 and 6.4 highlight that some traffic patterns are difficult for decentralized approaches (even for fully operational aircraft); however, there is some suggestion that decentralized approaches may be slightly less sensitive to communication failure.

6.4 Summary

This chapter compared the impact of communication loss on several existing automated separation management approaches. Our studies showed that these algorithms all exhibit significantly degraded performance when communication failure occurs, centralized separation approaches

tend to have worse degraded performance compared with decentralized approaches, it suggests that decentralized approaches may be slightly less sensitive to communication failure. However some traffic patterns are difficult for decentralized approaches. Performance would expected to be even worse for both centralized and decentralized approaches if additional aircraft have communication problems. This chapter provides foundation to the new automated separation management concepts that will be proposed in chapter 7.

Chapter 7

Communication Uncertainty and Separation Management System: Proposed Safety Augmented System and Flight Test Results

---

Future air traffic management concepts often involve the proposal of automated separation management algorithms that replace human air traffic controllers. This chapter proposes a new type of automated separation management algorithm (based on the satisficing approach [14]) that utilizes inter-aircraft communication and a track file manager (or bank of Kalman filters) and is capable of resolving conflicts during periods of communication failure. The proposed separation management algorithm is tested in a range of flight scenarios involving periods of communication failure, in both simulation and flight test (flight tests were conducted as part of the Smart Skies project [87] [1]). The chapter is organized as follows: Section 7.1 describes the background knowledge. Section 7.2 proposes a new type of automated separation management algorithm. Section 7.3 presents a simulation study. Section 7.4 describes two flight tests. Section 7.5 provides flight testing results for the proposed new type of automated separation management systems. Section 7.6 draws some conclusions.

7.1 Background

Air traffic management has faced significant traffic growth over the past decade. Future ATM systems will need to handle this growth in increased demand, while at the same time, maintain

[1] A three-year, multi-award winning international project that researched and developed new technologies.

or even improve the level of safety [87]. In these future ATM systems, communication links are vital components because they allow for information sharing, situation awareness and air traffic separation management commands to be issued. Previously, it has been observed that in order to enhance the safety, efficiency and capacity, next generation air traffic management algorithms will need to be robust against communication issues [84, 88]. In Chapter 6, we examined the benefits of switching between centralized and decentralized separation management algorithms. In this chapter we will examine the benefits of using inter-aircraft communication. There are two main ways to maintain situation awareness during the event of communication failure. In the first type of approach, using the prediction capabilities of filters, an on-board air-traffic picture can be maintained using a track file manager that predicts future air-traffic location information on the basis of previously received aircraft location information. However, the key drawback of this approach is that the error in predicted aircraft position tends to grow as time elapses following the communication failure event. In the second type of approach, new information is used to update air traffic picture (information that can be gaining through additional on-board sensors or via information shared over inter-aircraft communication links). One example of this second type of approach is the additional information that is provided by the automatic dependent surveillance-broadcast (ADS-B) system; ADS-B is a cooperative surveillance technique for air traffic control in which an ADS-B-equipped aircraft determines its own position using a global navigation satellite system and periodically broadcasts this position and other relevant information to potential ground stations and other aircraft with ADS-B-in equipment. In alternative situations, extra or new air traffic information might be requested via inter-platform communication (link2000+, a European pioneer air traffic management); other possible resources of traffic information includes on-board Radar or EO sensors. The range of possible communication systems currently available suggests that in the near future it may be routine to request critical information from nearby aircraft through suitable peer-to-peer communication links, and that this new information will be used in support of air traffic separation during any periods of failure in the centralized communication network. In this chapter we propose the use of a safety augmentation system containing a decentralized separation management system involving a track file manager, an on-board conflict detection system, and a separation manager based on a modified satisficing approach. The proposed system will provide separation support during a period of central communication network failure (by switching to a safe decentralized mode of operation that offers separation protection

through the use of inter-aircraft communication).

Safety in air traffic operations is generally understood to involve the five layers of safety processes and systems that are shown earlier in Figure 1.1 [89]. These five layers provide multiple levels of collision protection and, as such, each of these layers would have to fail in order for a mid-air collision to occur. This layered approach starts in Layer 1 which contains the basic procedures and structure of airspace management (aspects such as predefined operational altitudes and predefined flight routes) that provides the basic framework for air-traffic operation. In the 2nd and 3rd layers a centrally located air traffic management system (human operators and ground-based radar systems) performs aircraft traffic separation management. Layers 4 and 5 related to emergency safety systems that are beyond the scope of this study. This research is specifically focused on (automated) separation management (in the 2nd and 3rd layers) which is the task of maintaining safe separation distances between aircraft and, in the event of a potential conflict arising, this system also has the task of resolving conflicts in a safe manner. However if a communication failure event occurs (such as the failure of receiver or transmitter hardware or a failure of the ground based radar system), then there is a possibility that a centralized ATM system might incorrectly handle the information available, and that this incorrect response might lead into a mid-air collision. For these reasons, we will examine the separation management problem in an environment involving possible periods of communication failure. That is, the systems we investigated must operate in two environments:

- A normal operating environment; and
- A communication failure operating environment.

In a normal operating environment, the central information network is assume to be presented and functional in the sense that it allows separation commands to be transmitted to all air traffic. For our purposes here, we will assume that air-traffic picture used for centralized separation management is perfect; that is all aircraft information is known by the centralized separation manager. We will also assume that ideal communication with aircraft occurs which means neither delay/loss packets nor noise is introduced into the problem.

In a communication failure operating environment, the central information network is assumed to have lost connection with all aircraft; in this case, we assume all aircraft operate without any situation awareness information being provided by the central ATM system. We

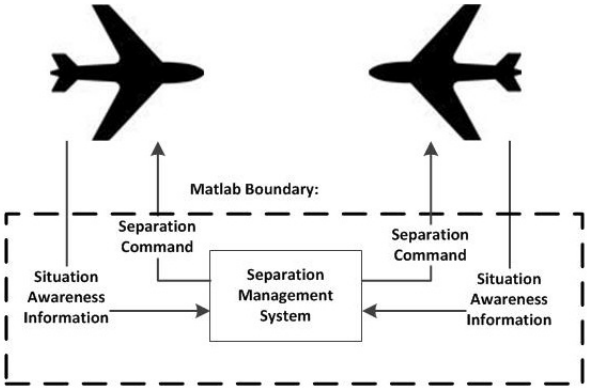

Figure 7.1: Automated separation management system overview

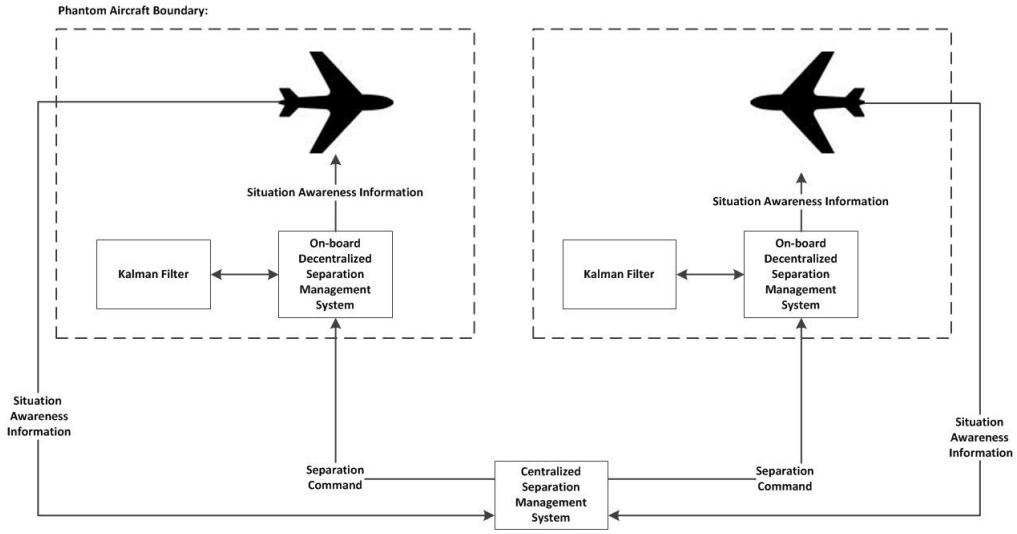

Figure 7.2: The automated separation management system architecture with phantom aircraft boundary

will assume that inter-aircraft communication exists.

7.2 Proposed separation management system

An overview of the separation management system is provided in Figure 7.1. Figures 7.2 and 7.3 both represent the automated separation management system architecture, but with different perspectives. Figure 7.2 outlines the phantom aircraft boundary and Figure 7.3 shows the realization of the system architecture by identifying the Matlab boundary.

The proposed on-board decentralized separation management system involves: a) track

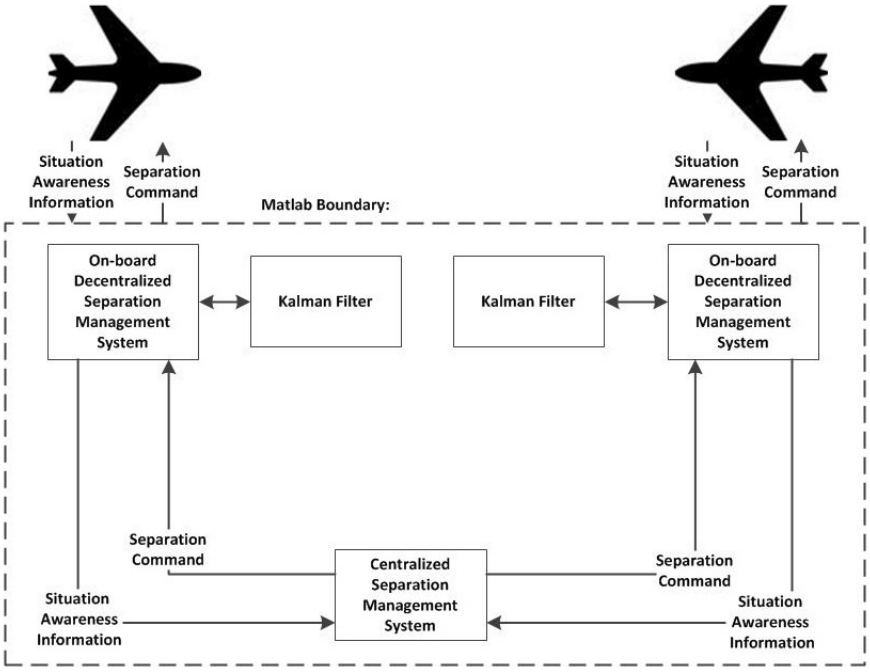

Figure 7.3: The automated separation management system architecture with Matlab boundary

file manager; b) request/response system; c) a conflict detection system; and d) a separation manager as shown in Figure 7.4. We now separately describe each of the components:

7.2.1 Track file manager

The track file manager involves a bank of Kalman filters and also includes algorithms that perform data association, track initialization and track termination processing. At the core of the track file manager there is one Kalman filter for each aircraft in the airspace. The state of each Kalman filter describes the position and velocity vector of the aircraft. The track file manager operates in both normal and failure environments. In particular, the track file manager operates during the normal communication environment so that a current picture of air-traffic is available if the centralized communication network ever fails.

7.2.2 Request/response system

This module of the system manages communication with central air traffic manager and inter-aircraft communication. For inter-aircraft communication purposes, the communication protocol contains a request message (that requests a position update from nearby aircraft) and

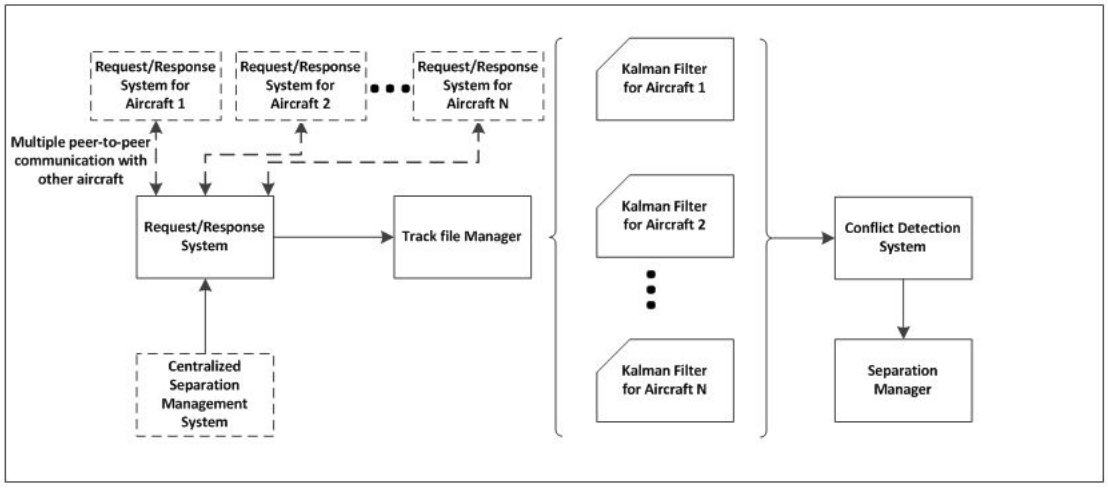

Figure 7.4: On-board Decision System contains 4 main modules: a request/response system to manage communication with central ATM or manage inter-aircraft communication, a track file manager to maintain local situational awareness, a conflict detection system, and a decentralized separation manager to determine suitable separation actions, when required.

response message. This system operates in both normal and failure environments.

7.2.3 Conflict detection system

The function of this module is to evaluate the air-traffic map, as described by the Kalman filter bank; to determine if a potential conflict exists between this aircraft and any other aircraft in the region. This system operates only in the failure environment.

7.2.4 Separation manager

The function of the separation management module is to determine suitable separation commands to resolve any conflicts identified by the on-board conflict detection system. In this research, the satisficing game theory (Described in Chapter 6) is the centralized multi-agent approach used to resolve aircraft conflicts (but other separation algorithms might also be considered). This system operates only in the failure environment.

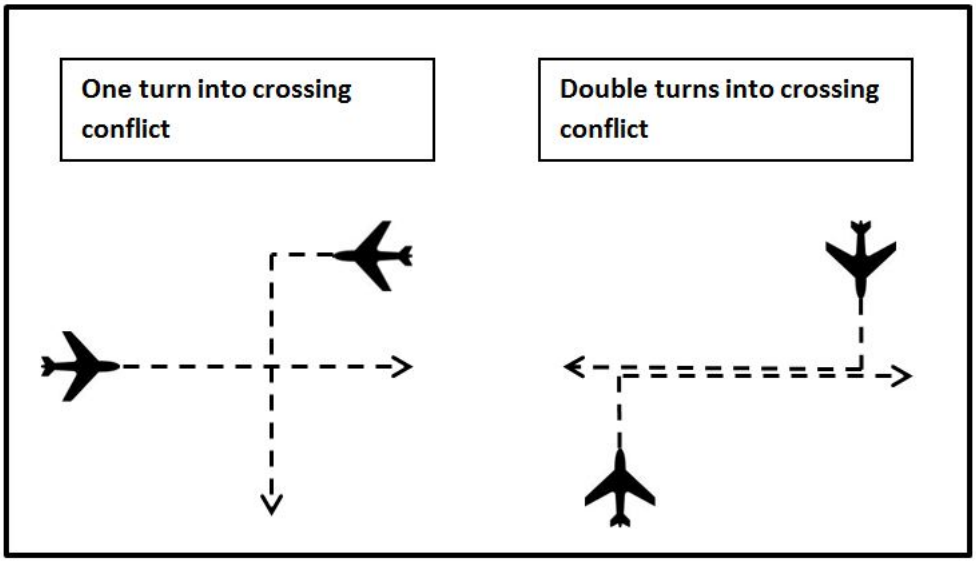

Figure 7.5: Simulation Scenarios. These two scenarios represent the two simplest scenarios under which a two-aircraft conflict can arise during communication failure.

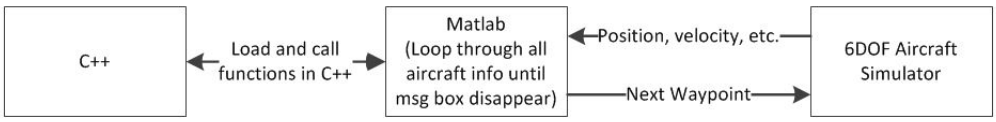

Figure 7.6: Programming Interface

7.3 Simulation Study

We simulated the separation management system discussed above to evaluate its performance in different scenarios. The dynamics of each simulated aircraft were represented using sophisticated six degree of freedom (6DOF) C172 aircraft simulator developed in the University of Sheffield [90]. All aircraft have a constant speed of 100 knots. Evaluation of the separation management system will be based on the minimum separation distance achieved during the simulation. Figure 7.5 shows the two scenario types that were examined in this study: one turn into crossing conflict, and double turns into crossing conflict. These two encounters are the topological equivalent to a range of encounters between two-aircraft (involving different approach angles). The angle of approach in the encounter does not significantly impact the issues considered in this chapter. Other realistic scenarios such as choke point, landing and departing from airport should also be considered in the further study.

Figure 7.6 shows the programming interface between C++, Matlab and 6DOF C172 aircraft

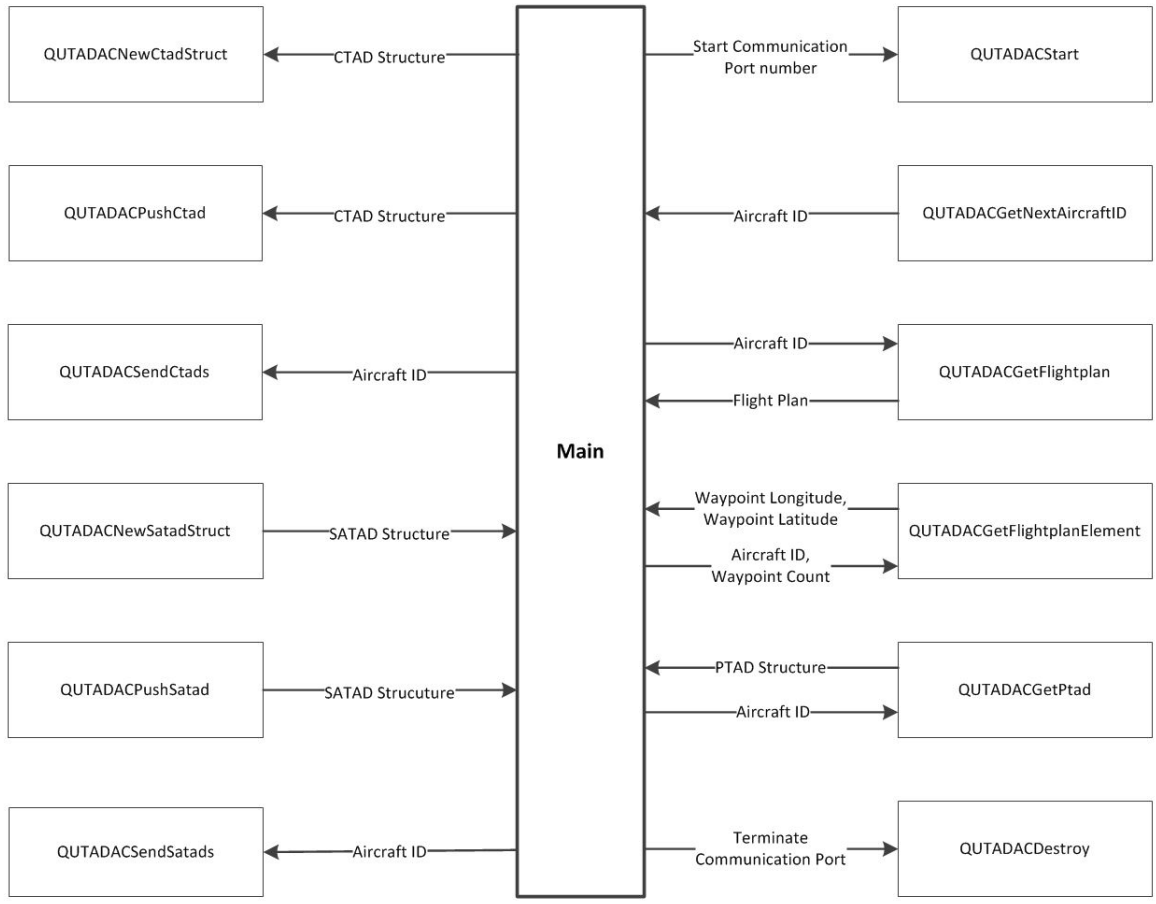

Figure 7.7: The basic function diagram for the separation system, refer to Appendix A for details.

simulator and Figure 7.7 shows the basic function diagram for the separation system.

In Figure 7.7, the term *PTAD* refers to predicted position information. *CTAD* refers to command information. *SATAD* refers to situational awareness information. *Position3D* refers to a structure contains GPS location information. *Flight Plan* refers to flight plan information of a particular aircraft. Table A.1, A.2, A.3, A.4 and A.5 in the appendix list the structure element of *PTAD*, *CTAD*, *SATAD*, *Position3D* and *Flight Plan* respectively.

7.3.1 Simulation results

For each of the traffic pattern scenario, algorithms were examined in the two operational modes: normal operating environment and failure operating environment. In each operational mode, for each traffic scenario, we compared a pure centralized approach with the new proposed

Table 7.1: Normal Operating Environment Performance (Separation distance achieved)

Case for Normal Operating Environment	**One Turn**	**One Turn Case 2**	**Double Turn**	**Double Turn Case 2**
Pure centralized	$2632m$	$2144m$	$1752m$	$1832m$
Pure decentralized	$4551m$	$4423m$	$3383m$	$3462m$

Table 7.2: Failure Operating Environment Performance (Separation distance achieved)

Case for Failure Operating Environment	**One Turn**	**One Turn Case 2**	**Double Turn**	**Double Turn Case 2**
Without inter-aircraft communication	$2777m$	$3017m$	$42m$	$58m$
With inter-aircraft communication	$3683m$	$3815m$	$3453m$	$3312m$

system both with and without access to inter-aircraft communication. In these simulations, all aircraft are assumed to have initial communication with central information network, and it was assumed that central information network failure occurs just before the aircraft turns commence. During the failure period, all aircraft traffic information is propagated in track file managers on-board each aircraft. This on-board air-traffic picture is used for conflict detection. When inter-aircraft communication is available, any information communicated to an aircraft is used in its on-board track file managers, and hence impacts on conflict detections and separation management commands that this aircraft generates. Table 7.1 shows the separation distance achieved (during normal communication network operation) by the original centralized separation management and a pure decentralized separation management approach. Table 7.2 shows the separation distances achieved (during communication network failure) by the new proposed approach with/without inter-aircraft communication (separation is deemed to have been maintained if separation distance is kept greater than $1500m$)

The results given in Table 7.1 show that the decentralized separation management system achieved separation distances significantly larger than required minimum separation distances, corresponding to large heading deviations from original trajectory (these large deviations are undesirable). These large deviations suggest that a pure decentralized approach is not desirable.

The results given in Table 7.2 suggest that, in two-aircraft scenario, the aircraft will be able to resolve potential conflicts even during a communication network failure with the help of

Table 7.3: Flight Test Setups common to both Flight test 1 and 2

Aircraft	Cessna 172R
Aircraft Communication Equipment	Next-G Modem
Communication Requirement	Internet through UMTS HSDPA Network using 850MHz band
Software Requirement	Mixed modules in both C++ and Matlab (Version 7.5) with instrument toolbox Sheffield 6DOF Aircraft Simulator
Location	Burrandowan near Kingaroy Airport (GPS Location: -26.5808333, 151.8411111)
Computer Specification	CPU:AMD Athlon 64 3200+ 2GHz Memory: 512MB Hard Drive: 80GB Operating System: Microsoft Windows XP

decentralized separation management on the basis of propagated traffic information (without the need for new information), as long as only one aircraft changes their course after network failure. However if both aircraft change their course during the period of communication blackout then it is possible for conflict to occur if no additional information is obtained from inter-aircraft communication. However, successful separation could be achieved in the double turn case (even during communication failure) if additional information was provided by inter-aircraft communication.

7.4 Flight Tests Setup

Two rounds of flight tests were conducted. The primary purpose of our initial flight tests was to provide preliminary verification of our new architecture, while the purpose for our second flight tests were to provide verification of our new proposed safety augmentation separation system. The actual flight test will take place at Burrandowan Homestead with manned aircraft (AC) flights originating and terminating from the Kingaroy Airport approximately 100 miles west of Brisbane, Australia. The separation management system, running from ARCAA research centre, will track and perform separation management for real and simulated aircraft flying over Burrandowan area. The following tables detail the basic setups for both flight tests.

Table 7.4: First Flight Test Details

Date	Wednesday 16th Nov 2009
Start Time	8:30AM
Duration	2 hours and 15 minutes
Wind Condition (Pilot Estimation)	2000 feet 110° /15 knots

Table 7.5: Second Flight Tests Details

Date	Thursday 27th May 2010
Start Time	9:00AM
Duration	4 hours
Wind Condition (Pilot Estimation)	3500ft 115° /15knots

7.5 Flight Tests

7.5.1 Flight Test: Verification of Experiment

The architecture was designed to provide a common environment for the development of candidate next generation separation management concepts (Only Satisficing approach was implemented in this work) The flight test architecture is shown Figure 7.8. This development environment allows both high fidelity simulation testing (6DOF dynamic models) and flight testing of proposed algorithms, and includes:

- Several computers hosting parts of the system (remote hosting is possible),
- Specialized communication layers to manage air-traffic communication (both software protocol interfaces and hardware), Communication occurs over 3.5G telephone data networks (or satellite networks).
- Specialized automated separation management approaches (based on satisficing approach, but conforming to interfacing requirements) ,
- Specialized 6DOF simulation models for virtual aircraft (conforming to interfacing requirements),
- **[Optional]** a Cessna 172R aircraft (equipped with specialized avionics such as high-grade IMUs and various data connections).

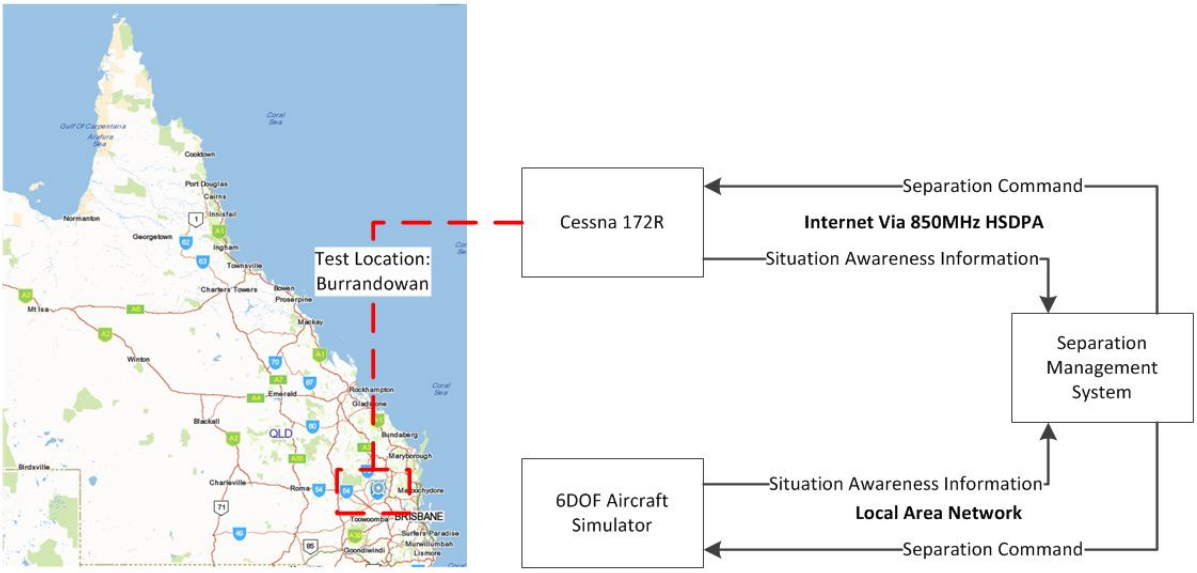

Figure 7.8: Overall System Architecture: Flight tests were conducted in Burrandowan area (near Brisbane).[Left side image credit: Google Maps] Central communication network was provided by mobile data network. This network connected the separation manager (in Brisbane) with aircraft in the flight test area. Simulated aircraft developed by the University of Sheffield were also involved in the flight test.

Note that the communication layer and other aspects of this architecture were developed as part of the Smart Skies Project.

The Sheffield 6DOF Simulator has few assumptions and limitations. Firstly, the simulator sustains a 50Hz update rate at all times. The simulator can be modified to run at higher frame rates, however higher frame rates are dependent on the processor speed. Secondly, the flight is a simplified model where the simulator linearised about one specific operating point. Furthermore, the flight control laws in the Sheffield simulator are implemented in the primary flight computer. This limits the implementation of different flight control laws. An alternative approach is to develop the flight control laws in Matlab in a dedicated PC under Linux or Windows, where packets are transmitted to the Matlab application once per frame; the corresponding control surface positions are computed by the Matlab computer and transmitted to the primary flight computer. This alternative approach enables different control laws to be implemented in the simulator without any specific re-programming of the simulator.

The primary advantage of the developed architecture is that it allows us to first perform rapid algorithm developments in a friendly simulation environment. Once verified in simulation, we can then easily transition to actual flight testing (because our architecture will work with

Table 7.6: A comparison study of simulation and real flight behavior, ✓means satisfactory separation was achieved in that test case; ✗means that the minimum required separation distance was not maintained; In the last row, ✓/✗denotes whether similar behavior was seen in both the simulation and the flight tests

Case	22.5°	45°	67.5°	90°	112.5°	135°	157.5°	180°
Simulation	✗	✓	✓	✓	✓	✓	✓	✓
Flight Test	✓	✓	✓	✗	✓	✓	✓	✓
Similar	✗	✗	✓	✗	✗	✓	✗	✓

both simulated hardware and real hardware). The primary purpose of our initial flight tests was to provide preliminary verification of our new architecture. A secondary purpose was to evaluate how well our simulation models (primarily our 6DOF) match the real interactions that occur during real conflict resolution. We stress that these tests did not aim to investigate the impact of communication loss, and hence these first tests involved only simple conflicts involving two aircraft approaching at a variety of different angles (from 22.5 degrees to 180 degrees in increments of 22.5 degrees). One aircraft was our specially equipped Cessna 172R aircraft. The other aircraft was a computer simulation of an aircraft (that mimicked all the required interfaces, the aerodynamic behavior and the response to separation instructions).

Table 7.6 shows a comparison, for different approach angles, between pure simulation tests and flight tests involving one real aircraft (with real communication links) and one simulated aircraft. In this table, in the 2nd and 3rd rows, a tick means satisfactory separation was achieved in that test case; a cross means that the minimum required separation distance was not maintained. In the last row, the tick/cross denotes whether similar behavior was seen in both the simulation and the flight tests.

To highlight some of the features present in real flight tests we will now describe some of the data collected in the 67.5 degree approach angle case (other approach angles exhibited similar features). Figure 7.9 shows the trajectories followed by the aircraft during this scenario. The solid red trajectory corresponds to the real aircraft and the dash blue trajectory corresponds to the simulated aircraft. We highlight that in this scenario both aircraft received commands to change heading for the purposes of avoiding the potential collision identified; the solid red aircraft is instructed to turn right so that it passes ahead of the dash blue aircraft (which is also instructed to turn right so that it passes behind the solid red aircraft). Once the

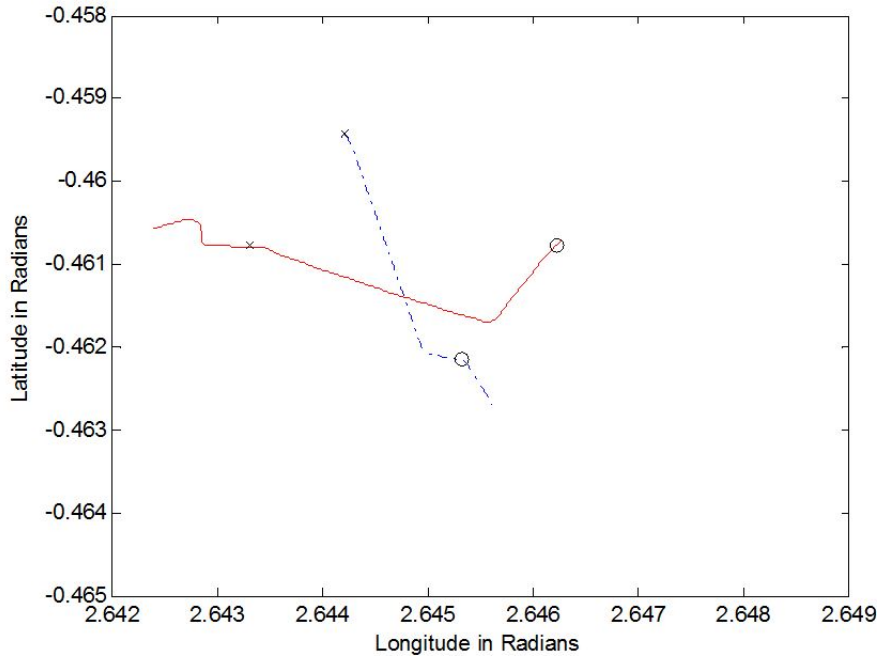

Figure 7.9: The resolved trajectories in the 67.5 degree scenario (real flight test). The real aircraft is denoted in solid red (starting from the left end of its shown trajectory) and the simulated aircraft is denoted in dash blue (starting from the top end of its shown trajectory). Initial points of the aircraft are denoted with x and destination waypoints of the aircraft are denoted with o. At the very left, some of the solid red (real) aircraft's trajectory prior to the experiment is shown (and should be ignored).

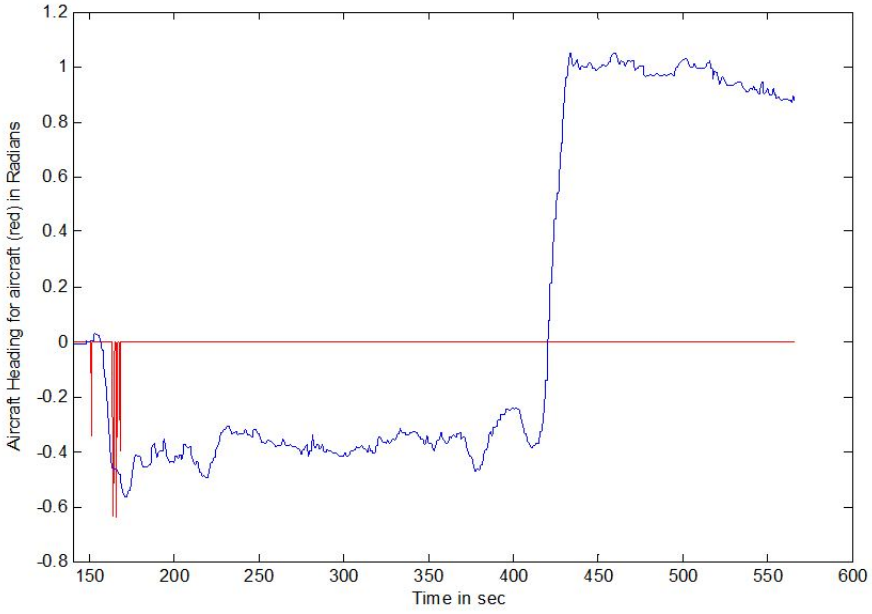

Figure 7.10: The real (red) aircraft heading commands are shown in red. The aircraft actual heading is shown in blue

potential conflict has been resolved, both aircraft head towards their original way-points. In Figure 7.10 we show the commands issued and response behavior of the real (red) aircraft. In this figure, the red tick marks correspond to time instants in which the centralized separation manager issues a heading instruction to the real aircraft (the size of the tick corresponds to the value of the heading instruction). These instructions are issued between $150s$ and $175s$. The aircraft's actual heading is denoted by the blue line. In the shown scenario, the separation instruction is issued several times, and adjusted, until the algorithm is happy that the aircraft is on a conflict-free trajectory (in an approximate sense, this corresponds to aircraft's heading matching the heading instruction). The aircraft starts returning to its initial way-point at a time of approximately 425 seconds. We highlight that during simulation of the 67.5 degree approach case, a minimum separation distance of $1612.42m$ was achieved (the flight delay caused was 30 seconds). However, during the actual flight test, a minimum separation distance obtained was $2573.92m$ (the flight delay caused was 53 seconds). We highlight that the separation manager used a similar separation strategy in both the simulation and flight test. Hence, whilst both tests satisfy the desired separation distance of $1500m$ and used roughly a similar separation strategy, significantly different performance numbers were seen in the two cases. In summary, this initial flight test program illustrated the feasibility and provided preliminary validation of our new architecture for testing new automated separation management concepts. However, this initial test also highlights that simulation environments only provide a crude approximation of flight behavior during conflict and avoidance.

7.5.2 Flight Test of Proposed System

The proposed separation management system was also examined in flight tests. Table 7.7 shows the test results obtained through flight test which involved one real aircraft and one simulated aircraft. Note that the flight test cases marked with "X" were not performed due to the technical issues.

The normal operation results given in Table 7.7 show that the decentralized separation management system achieved separation distances significantly larger than required minimum separation distances ($1500m$), corresponding to large heading deviations from original trajectory (these large deviations are undesirable). These large deviations suggest that a pure decentralized approach is not desirable.

Table 7.7: Flight Test Separation Management Performance (Separation distance achieved), note that the flight test cases marked with ✗were not performed due to the technical issues.

Case	One Turn	One Turn Case 2	Double Turn	Double Turn Case 2
Normal: Pure Centralized	$2574m$	$2419m$	$1531m$	$1916m$
Normal: Pure Decentralized	$3715m$	$3470m$	$3764m$	$3613m$
Failure Mode: Without inter-aircraft communication	✗	✗	✗	✗
Failure Mode: With inter-aircraft communication	✗	✗	✗	$2640m$

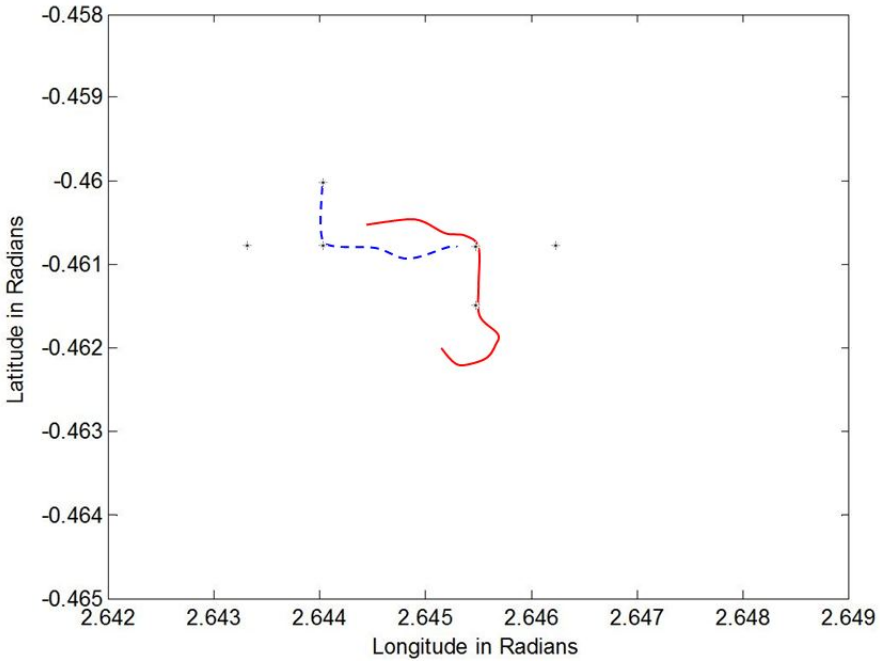

Figure 7.11: The resolved flight test trajectories in the double turn into crossing conflict scenario (Real flight test). The real aircraft is denoted in red (starting from the lower right of its shown trajectory) and the simulated aircraft is denoted in blue (starting from the top left of its shown trajectory). At lower right, some of the red (real) aircraft's trajectory prior to the experiment is shown (and should be ignored)

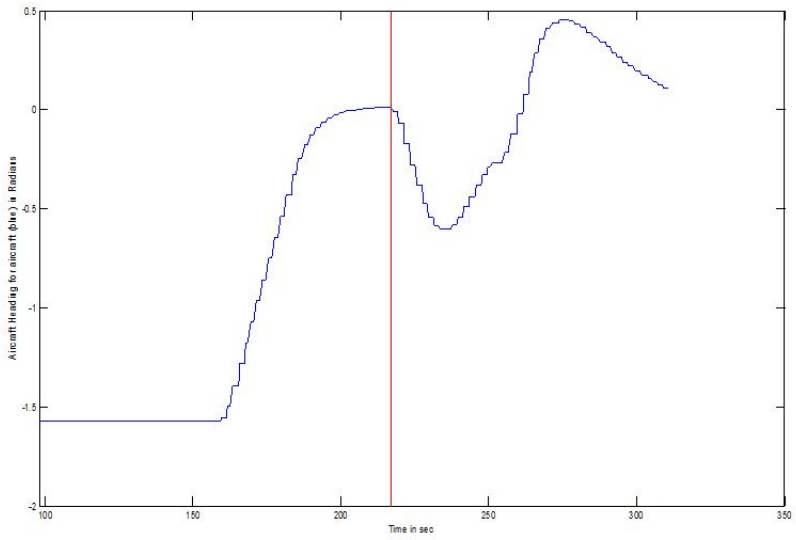

Figure 7.12: The 6DOF aircraft actual heading is shown in blue, the vertical line denotes the time that a conflict was detected, separation instruction were issued to the aircraft that cause the aircraft to turn to a heading of -0.6 Rad.

The double turn case for failure mode with inter-aircraft communication in Table 7.7 suggests that, successful separation could be achieved (even during communication failure) if additional information was provided by inter-aircraft communication.

We will now describe some of the data collected for double turn case in a failure environment operation, with access to inter-aircraft communication. Figure 7.11 shows the trajectories followed by the aircraft during this scenario. The red trajectory corresponds to the real aircraft and the blue trajectory corresponds to the simulated aircraft. We highlight that in this scenario the central information network failed just before aircraft commenced their turns; therefore neither aircraft was aware of the potential conflict until they were able to update their local air traffic map using information received via inter-aircraft communication. In this situation with inter-aircraft communication, the conflict is detected and resolved once the traffic map has been updated in both of the decentralized separation management systems on each aircraft. Once the potential conflict has been resolved, both aircraft return to flight towards their original waypoints. Figure 7.12 shows the trigged message from decentralized separation management and response behavior of the 6DOF aircraft (the blue line), the red line corresponds to the time instant in the conflict has been detected and the decentralized separation management starts issuing separation instructions to the real aircraft. The instructions were issued at 217 seconds into the flight test. 20 seconds after the trigged message, the aircraft achieves it separation

instruction designed to avoid the detected collision. We highlight that during the flight test, a minimum separation distance of $2640m$ was achieved and we highlight that there is no significant difference between the performance of the simulation tests and the flight tests. In summary, this flight test provided a preliminary validation of the new automated separation management concepts. Since there is no significant different performance observed between simulation and flight test, no further flight tests related to this experiment were conducted.

7.6 Summary

In this chapter, a new safety augmentation system is proposed. The new system uses a decentralized separation management system that involves a track file manager, an on-board conflict detection system, and a separation manager based on a modified satisficing approach. Simulation and flight tests showed that with the help of inter-aircraft communication, the proposed separation management system was able to resolve potential conflict during a period of central communication failure.

Chapter 8

Conclusion

The development, investigation and analysis of new automated separation management concepts are the major outcomes of this research. This final chapter summarizes the results presented in this thesis in terms of following two main research questions identified in the introduction chapter.

Question 1: How does the information about measurement uncertainty (i.e. sensor accuracy and choices) impact the quality of our estimates of the risk of mid-air collision?

The first research question was resolved by utilizing risk ratio concept in our conflict risk estimation. Our study demonstrated the value of modelling measurement uncertainty in the conflict risk estimation problem and presented techniques providing a means of assessing sensor requirements to achieve desired conflict detection performance.

Question 2: Can inter-aircraft communication be used to improve separation management system performance during communication uncertainty environment (e.g. communication failure)?

The second research question was resolved in two steps. Firstly, comparison of separation performance behavior of several popular algorithm in an uncertain communication environment was conducted. This comparison was done through simulation studies. These simulation studies suggested that communication failure can cause the performance of these separation management algorithms to degrade significantly. Secondly, a new type of automated separation management algorithm that utilizes inter-aircraft communication and a track file manager (or bank of Kalman filters) is proposed. The proposed separation management algorithm is tested in a range of flight scenarios involving during periods of communication failure, in both simulation and flight test (flight tests were conducted as part of the Smart Skies project). The intention of

the conducted flight tests was to investigate the benefits of using inter-aircraft communication to provide an extra layer of safety protection in support air traffic management during periods of failure of the communication network.

8.1 Summary of Contributions

In this thesis, we first investigated the impact of measurement uncertainty on the estimated risk of conflict. Then we compared the separation performance of several algorithms in uncertain communication environment. Finally, we proposed an inter-aircraft communication and a track file manager based automated separation management algorithm and demonstrated its ability in resolving conflicts during a period of central communication failure. A brief summary of the key contributions and outputs from the research is provided below:

Key contributions:

- Characterized the separation performance in communication failure situations for both centralized and decentralized separation management approaches.
- Established performance comparisons for impact of communication loss on several existing automated separation management approaches.
- Identified suitable sensor accuracy requirement from risk of conflict modelling.
- Illustrated the risk of conflict benefits from combining ADS-B and radar measurements.
- Explained the influence of measurement choices and accuracy on estimated risk of conflict.

Research Outputs:

- Proposed a new safety augmentation system using a decentralised separation management system that involves a track file manager, an on-board conflict detection system, and a separation manager based on a modified satisficing approach.
- Proposed a methodology that considers generic distribution in measurement uncertainty/-position error model.

- Proposed a new risk-ratio based approach for assessing the impact of sensor accuracy and sensor choice on the ability to accurately predict conflicts.

8.2 Future Work

We have identified some possible areas for further consideration and future research:

- In this thesis, we have mainly dealt with the uncertainty from measurements and communication loss, other classes of uncertainty such as uncertainty from communication delay is also an interesting area for future research.
- We have shown the impact on estimated risk of conflict from different types of sensor information, further development of conflict detection that uses the risk ratio concept can be conducted to possibly improves the performance of separation managements. The more accurate the estimated risk of conflict, the more likely an ideal conflict detection system can be designed. (no false alarms and no missed detections).
- We can combine the risk ratio concept based conflict detection with the proposed new safety augmentation system. We anticipate a better conflict detection performance in the separation management system, however, the exact relationship between the conflict detection and overall separation performance is yet not known. Characterizing this relationship can help determine the optimal implementation of sensor accuracy in particular scenarios.

Appendix A

Appendix

A.1 Simulation Function Detail Description

Function Name: QUTADACStart

Function Input: Port, Type, Option

Function Output: Nil

Function Description: This function is used to start up the server, and define a port number for communication. The server will automatically stop on disconnect.

Function Name: QUTADACGetNextAircraftID

Function Input: Nil

Function Output: Aircraft id

Function Description: This function is used to get vaild next aircraft ID from the system. It output the aircraft ID for separation management to access its information.

Function Name: QUTADACGetFlightplan

Function Input: Aircraft id

Function Output: Flight plan

Function Description: This function uses aircraft ID to access the aircraft flight plan. It get a flight plan tad from the system for that particle aircraft.

Function Name: QUTADACGetFlightplanElement

Function Input: Aircraft id, Waypoint count

Function Output: position3d structure

Function Description: This function uses aircraft ID and the current count of waypoint, It will output the position information for that particle requested waypoint, the position information is in postion3d structure.

Function Name: QUTADACGetPtad

Function Input: Aircraft id

Function Output: PTAD structure

Function Description: This function uses aircraft ID to access the information about PTAD, it get a predicted position tad from the system.

Function Name: QUTADACNewCtadStruct

Function Input: Nil

Function Output: CTAD structure

Function Description: This function construct a CTAD, and return a new command tad structure.

Function Name: QUTADACPushCtad

Function Input: Nil

Function Output: CTAD structure

Function Description: This function push a command tad into the stack.

Function Name: QUTADACSendCtads

Function Input: Aircraft id

Function Output: Nil

Function Description: This function send off queued command Tads for aircraft to execute.

Function Name: QUTADACNewSatadStruct

Function Input: Nil

Function Output: SATAD structure

Function Description: This function returns a new situational awareness tad structure.

Function Name: QUTADACPushSatad

Function Input: Nil

Function Output: SATAD structure

Function Description: This function push a situational awareness tad into the stack.

Function Name: QUTADACSendSatads

Function Input: Aircraft id

Function Output: Nil

Function Description: This function send off queued situational awareness tads.

Function Name: QUTADACSendSatads

Function Input: Aircraft id

Function Output: Nil

Function Description: This function send off queued situational awareness tads.

Function Name: QUTADACDestroy

Function Input: Nil

Function Output: Nil

Function Description: This function Stop the running server and destroy flight management data.

A.2 Structure Descriptions

PTAD refers to predicted position information. The structure elements are listed in table A.1. CTAD refers to command information. The structure element is listed in table A.2. SATAD refers to situational awareness information. The structure elements are listed in table A.3. Position3D refers to a structure contains GPS location information. The structure elements are listed in table A.4. Flight Plan refers to flight plan information of a particular aircraft. The structure elements are listed in table A.5.

Table A.1: PTAD Structure

Structure element	**Data type**
Aircraft ID	32-bits integers
Prediction time stamp	64-bits integers
Expected Latency	32-bits floating points
Behaviour	8-bits characters
Current Waypoint	8-bits characters
Position3D	Structure
Confidence predicted	8 bits characters
Confidence current	8 bits characters
Height type	8 bits characters
Ground speed	32-bits floating points
Heading	32-bits floating points
Roll	32-bits floating points
Pitch	32-bits floating points
Check sum	32-bits integers
Valid	Boolean

Table A.2: CTAD Structure

Structure element	**Data type**
Aircraft ID	32-bits integers
Position3D	Structure
Arrival time	64-bits integers

Table A.3: SATAD Structure

Structure element	**Data type**
Aircraft ID	32-bits integers
Aircraft Type	16-bits integers
Time stamp	64-bits integers
Position3D	Structure
Heading	64-bits double floating points
Ground speed	32-bits floating points
Uncertainty	32-bits floating points

Table A.4: Position3D Structure

Structure element	**Data type**
Latitude	64-bits double floating points
Longitude	64-bits double floating points
Altitude	32-bits floating points

Table A.5: Flight plan Structure

Structure element	**Data type**
Aircraft ID	32-bits integers
Flight ID	32-bits integers
flight Rules	8-bits characters
Pob	8-bits characters
Equipment	16-bits integers
Ground speed	32-bits floating points
Waypoint count	32-bits unsigned integers
Check sum	32-bits integers
Valid	Boolean

References

[1] C. Manning and M. Hanson, "Criterion measures of air traffic controller job performance: The current state of affairs," *Staffing the ATM System- The selection of air traffic controllers*, pp. 45–57, 2002.

[2] Q. Yuling and H. Songchen, "A method to calculate the collision risk on air-route," in *Management and Service Science (MASS), 2010 International Conference on*. IEEE, 2010, pp. 1–4.

[3] M. Al-Basman and J. Hu, "Probability of conflict analysis of 3d aircraft flight based on two-level markov chain approximation approach," in *Networking, Sensing and Control (ICNSC), 2010 International Conference on*. IEEE, 2010, pp. 608–613.

[4] T. Prevot, E. Palmer, N. Smith, and T. Callantine, "Future air traffic management: A perspective on distributed automation," in *Proceedings of the 8th European Conference on Cognitive Science Approaches to Process Control*, 2001.

[5] C. Tomlin, G. Pappas, and S. Sastry, "Noncooperative conflict resolution [air traffic management]," in *Decision and Control, 1997., Proceedings of the 36th IEEE Conference on*, vol. 2. IEEE, 1997, pp. 1816–1821.

[6] S. Temizer, M. Kochenderfer, L. Kaelbling, T. Lozano-Pérez, and J. Kuchar, "Collision avoidance for unmanned aircraft using markov decision processes," 2010.

[7] E. Duke, R. Antoniewicz, and K. Krambeer, "Derivation and definition of a linear aircraft model," in *NASA Reference Publication 1207*, 1988.

[8] F. Gustafsson, F. Gunnarsson, N. Bergman, U. Forssell, J. Jansson, R. Karlsson, and P. Nordlund, "Particle filters for positioning, navigation, and tracking," *Signal Processing, IEEE Transactions on*, vol. 50, no. 2, pp. 425–437, 2002.

[9] B. LI and Z. WU, "Flight conflict detection based on flight path prediction," *Microprocessors*, 2011.

[10] Y. Zeng, J. Zhou, and Y. Wu, "A randomized approach for mid-range aircraft conflict detection based on the unscented particle filter," in *Computational Intelligence and Security, 2006 International Conference on*, vol. 2. IEEE, 2006, pp. 1659–1664.

[11] I. Lymperopoulos, G. Chaloulos, and J. Lygeros, "An advanced particle filtering algorithm for improving conflict detection in air traffic control," in *4th International Conference on Research in Air Transportation (ICRAT)*, 2010.

[12] R. Irvine, "A geometrical approach to conflict probability estimation." *Air Traffic Control Quarterly*, vol. 10, no. 2, pp. 85–113, 2002.

[13] J. Jansson and F. Gustafsson, "A framework and automotive application of collision avoidance decision making," *Automatica*, vol. 44, no. 9, pp. 2347–2351, 2008.

[14] J. Archibald, J. Hill, N. Jepsen, W. Stirling, and R. Frost, "A satisficing approach to aircraft conflict resolution," *Systems, Man, and Cybernetics, Part C: Applications and Reviews, IEEE Transactions on*, vol. 38, no. 4, pp. 510–521, 2008.

[15] E. Lalish and K. Morgansen, "Decentralized reactive collision avoidance for multivehicle systems," in *Decision and Control, 2008. CDC 2008. 47th IEEE Conference on*. IEEE, 2008, pp. 1218–1224.

[16] M. Ballin, D. Wing, M. Hughes, and S. Conway, "Airborne separation assurance and traffic management: Research of concepts and technology," in *Proc. of the AIAA Guidance, Navigation, and Control Conference and Exhibit, Portland, USA*. Citeseer, 1999.

[17] G. Bakker, H. Kremer, and H. Blom, "Geometric and probabilistic approaches towards conflict prediction," in *Proceedings of 3rd USA/Europe Air Traffic Management R&D Seminar, Italy*, 2000.

[18] F. Netjasov and M. Janic, "A review of research on risk and safety modelling in civil aviation," *Journal of Air Transport Management*, vol. 14, no. 4, p. 213, 2008.

[19] P. Reich, "Separation standards, i," *J. Instit. Navigation*, vol. 19, pp. 88–98, 1966.

[20] R. Machol, "An aircraft collision model," *Management Science*, pp. 1089–1101, 1975.

[21] ——, "Thirty years of modeling midair collisions," *Interfaces*, pp. 151–172, 1995.

[22] G. Bakker and H. Blom, "Air traffic collision risk modeling," in *Decision and Control, 1993. CDC 1993. 32nd IEEE Conference on*. IEEE, 1993.

[23] J. Bellantoni, "The calculation of aircraft collision probabilities," DTIC Document, Tech. Rep., 1971.

[24] B. Carpenter and J. Kuchar, "Probability-based collision alerting logic for closely-spaced parallel approach," in *Proceedings of the AIAA 35th Aerospace Sciences Meeting and Exhibit, AIAA*, 1997, pp. 97–0222.

[25] A. Barnett, "A" parallel approach" path to estimating collision risk during simultaneous landings," *Management science*, pp. 382–394, 1999.

[26] T. Willemain, "Factors influencing blind conflict risk in en route sectors under free-flight conditions," *Transportation science*, vol. 37, no. 4, pp. 457–470, 2003.

[27] N. Fulton, M. Westcott, and S. Emery, "Decision support for risk assessment of mid-air collisions via population-based measures," *Transportation Research Part A: Policy and Practice*, vol. 43, no. 2, pp. 150–169, 2009.

[28] P. Brooker, "The risk of mid-air collision to commercial air transport aircraft receiving a radar advisory service in class f/g airspace," *Journal of Navigation*, vol. 56, no. 2, pp. 277–289, 2003.

[29] H. Abbass, S. Alam, and A. Bender, "Mebra: multiobjective evolutionary-based risk assessment," *IEEE Computational Intelligence Magazine*, vol. 3, no. 4, pp. 29–36, 2009.

[30] F. Lindsten, P. Nordlund, and F. Gustafsson, "Conflict detection metrics for aircraft sense and avoid systems," in *7th IFAC Symposium on Fault Detection, Supervision and Safety of Technical Processes*, 2009.

[31] J. Kuchar and L. Yang, "A review of conflict detection and resolution modeling methods," *Intelligent Transportation Systems, IEEE Transactions on*, vol. 1, no. 4, pp. 179–189, 2000.

[32] G. Heuvelink and H. Blom, "An alternative method to solve a variational inequality applied to an air traffic control example," *Analysis and optimization of systems*, pp. 617–628, 1988.

[33] R. Paielli and H. Erzberger, "Conflict probability estimation for free flight," *Journal of Guidance, Control and Dynamics*, vol. 20, no. 3, pp. 588–596, 1997.

[34] P. WILLIAMS, "Aircraft collision avoidance using statistical decision theory," *Sensors and sensor systems for guidance and navigation II*, 1992.

[35] D. Hsu, "The evaluation of aircraft collision probabilities at intersecting air routes," *Journal of navigation*, vol. 34, no. 01, pp. 78–102, 1981.

[36] M. Prandini, J. Hu, J. Lygeros, and S. Sastry, "A probabilistic approach to aircraft conflict detection," *Intelligent Transportation Systems, IEEE Transactions on*, vol. 1, no. 4, pp. 199–220, 2000.

[37] J. Hu, M. Prandini, and S. Sastry, "Probabilistic safety analysis in three dimensional aircraft flight," in *Decision and Control, 2003. Proceedings. 42nd IEEE Conference on*, vol. 5. IEEE, 2003, pp. 5335–5340.

[38] J. Hu, J. Lygeros, M. Prandini, and S. Sastry, "Aircraft conflict prediction and resolution using brownian motion," in *Decision and Control, 1999. Proceedings of the 38th IEEE Conference on*, vol. 3. IEEE, 1999, pp. 2438–2443.

[39] J. Lygeros and M. Prandini, "Aircraft and weather models for probabilistic collision avoidance in air traffic control," in *Decision and Control, 2002, Proceedings of the 41st IEEE Conference on*, vol. 3. IEEE, 2002, pp. 2427–2432.

[40] M. Prandini, J. Lygeros, A. Nilim, and S. Sastry, "A probabilistic framework for aircraft con ict detection,"," in *AIAA Guidance, Navigation and Control*, 1999.

[41] M. Prandini and O. Watkins, "Probabilistic aircraft conflict detection," *HYBRIDGE, IST-2001*, vol. 32460, 2005.

[42] X. Chen, W. Song, and H. Yang, "Algorithm of multi-aircraft mid-term conflict detection with multi-waypoints," *Computer Engineering and Design*, vol. 31, no. 12, 2010.

[43] R. Paielli and H. Erzberger, "Conflict probability estimation generalized to non-level flight," *Air Traffic Control Quarterly*, vol. 7, no. 3, pp. 195–222, 1999.

[44] L. Yang, J. Kuchar, U. S. N. Aeronautics, and S. Administration, "Prototype conflict alerting system for free flight," *Journal of Guidance, Control, and Dynamics*, vol. 20, no. 4, pp. 768–773, 1997.

[45] J. Chryssanthacopoulos and M. Kochenderfer, "Accounting for state uncertainty in collision avoidance," *Journal of guidance, control, and dynamics*, vol. 34, no. 4, pp. 951–960, 2011.

[46] L. Kaelbling, M. Kochenderfer, S. Temizer, T. Lozano-Perez, J. Kuchar *et al.*, "Collision avoidance for unmanned aircraft using markov decision processes," 2010.

[47] E. A. Lester, "Benefits and incentives for ads-b equipage in the national airspace system," Ph.D. dissertation, Massachusetts Institute of Technology, 2007.

[48] L. Campos and J. Marques, "On the calculation of collision probabilities as an assurance of safe separation between aircraft," *ICAS 2002*, 2002.

[49] ——, "On safety metrics related to aircraft separation," *Journal of Navigation*, vol. 55, no. 1, pp. 39–63, 2002.

[50] J. Krozel, M. Peters, K. Bilimoria, C. Lee, and J. Mitchell, "System performance characteristics of centralized and decentralized air traffic separation strategies," in *Fourth USA/Europe Air Traffic Management Research and Development Seminar*, 2001.

[51] C. Tomlin, G. Pappas, and S. Sastry, "Conflict resolution for air traffic management: A study in multiagent hybrid systems," *Automatic Control, IEEE Transactions on*, vol. 43, no. 4, pp. 509–521, 1998.

[52] Y. Ikeda, B. Nguyen, A. Barfield, B. Sundqvist, and S. Jones, "Automatic air collision avoidance system," in *SICE 2002. Proceedings of the 41st SICE Annual Conference*, vol. 1. IEEE, 2002, pp. 630–635.

[53] B. Sundqvist and S. AB, "Auto-acas-robust nuisance-free collision avoidance," in *Decision and Control, 2005 and 2005 European Control Conference. CDC-ECC'05. 44th IEEE Conference on*. IEEE, 2005, pp. 3961–3963.

[54] W. Dunbar and R. Murray, "Model predictive control of coordinated multi-vehicle formations," in *Decision and Control, 2002, Proceedings of the 41st IEEE Conference on*, vol. 4. IEEE, 2002, pp. 4631–4636.

[55] ——, "Receding horizon control of multi-vehicle formations: A distributed implementation," in *Decision and Control, 2004. CDC. 43rd IEEE Conference on*, vol. 2. IEEE, 2004, pp. 1995–2002.

[56] T. Keviczky, F. Borrelli, K. Fregene, D. Godbole, and G. Balas, "Decentralized receding horizon control and coordination of autonomous vehicle formations," *Control Systems Technology, IEEE Transactions on*, vol. 16, no. 1, pp. 19–33, 2008.

[57] J. Lavaei, A. Momeni, and A. Aghdam, "A model predictive decentralized control scheme with reduced communication requirement for spacecraft formation," *Control Systems Technology, IEEE Transactions on*, vol. 16, no. 2, pp. 268–278, 2008.

[58] A. Tsourdos, R. Zbikowski, and B. White, "Cooperative control strategies for swarm of unmanned aerial vehicles under motion uncertainty," in *Autonomous Systems, 2007 Institution of Engineering and Technology Conference on*. IET, 2007, pp. 1–5.

[59] M. Eby, "A self-organizational approach for resolving air traffic conflicts," *The Lincoln Laboratory Journal*, vol. 7, no. 2, pp. 239–254, 1994.

[60] J. Hoekstra, R. Ruigrok, R. van Gent, J. Visser, B. Gijsbers, M. Clari, W. Heesbeen, B. Hilburn, J. Groeneweg, and F. Bussink, "Overview of nlr free flight project 1997-1999," vol. 2, no. 12, p. 1, 2000.

[61] K. Bilimoria, "A geometric optimization approach to aircraft conflict resolution," in *Aiaa guidance, navigation, and control conference and exhibit*, 2000.

[62] G. Dowek, "Tactical conflict detection and resolution in a 3-d airspace," DTIC Document, Tech. Rep., 2001.

[63] P. DeJong, "Coalition formation in multi-agent uav systems," Ph.D. dissertation, University of Central Florida Orlando, Florida, 2005.

[64] N. Durand, J. Alliot, and J. Noailles, "Automatic aircraft conflict resolution using genetic algorithms," in *Proceedings of the 1996 ACM symposium on Applied Computing*. ACM, 1996, pp. 289–298.

[65] E. Frazzoli, Z. Mao, J. Oh, and E. Feron, "Resolution of conflicts involving many aircraft via semidefinite programming," 1999.

[66] L. Pallottino, E. Feron, and A. Bicchi, "Conflict resolution problems for air traffic management systems solved with mixed integer programming," *Intelligent Transportation Systems, IEEE Transactions on*, vol. 3, no. 1, pp. 3–11, 2002.

[67] C. INC, "Using the cplex callable library," 1994.

[68] M. Christodoulou and C. Costoulakis, "Nonlinear mixed integer programming for aircraft collision avoidance in free flight," in *Electrotechnical Conference, 2004. MELECON 2004. Proceedings of the 12th IEEE Mediterranean*, vol. 1. IEEE, 2004, pp. 327–330.

[69] R. Rosenthal and A. Brooke, *GAMS: a user's guide*. GAMS Development Corporation, 2007.

[70] M. Jardin, "Grid-based strategic air traffic conflict detection," in *2005 AIAA Guidance, Navigation, and Control Conference and Exhibit; San Francisco, CA*. American Institute of Aeronautics and Astronautics, 1801 Alexander Bell Drive, Suite 500, Reston, VA, 20191-4344, USA,, 2005, pp. 1–11.

[71] Q. Hui, "Research on the algorithm for flight-conflict avoidance in the centralized approach [j]," *Ship Electronic Engineering*, vol. 5, 2008.

[72] R. Saber, W. Dunbar, and R. Murray, "Cooperative control of multi-vehicle systems using cost graphs and optimization," in *American Control Conference, 2003. Proceedings of the 2003*, vol. 3. IEEE, 2003, pp. 2217–2222.

[73] J. Samek, D. Sislak, P. Volf, and M. Pechoucek, "Multi-party collision avoidance among unmanned aerial vehicles," in *Intelligent Agent Technology, 2007. IAT'07. IEEE/WIC/ACM International Conference on*. IEEE, 2007, pp. 403–406.

[74] E. Ulfbratt and J. McConville, "Comparison of the sesar and nextgen-concepts of operations," *NCOIC Aviation IPT*, 2008.

[75] U. S. G. A. Office, "Collaborative efforts with european union generally mirror effective practices, but near-term challenges could delay implementation," *GAO-12-48 Report*, 2011.

[76] H. Ryan, G. Chandler, C. Santiago, M. Paglione, and S. Liu, "Evaluation of en route automation trajectory generation and strategic alert processing: Analysis of eram

performance," *Dept. of Transportation/Federal Aviation Administration, TC-TN08/10*, 2008.

[77] B. Petricel and C. Costelloe, "First atc support tools implementation (fasti) operational concept," Technical report, EUROCONTROL, Tech. Rep., 2007.

[78] T. Young, "Aircraft design innovation: creating an environment for creativity," *Proceedings of the Institution of Mechanical Engineers, Part G: Journal of Aerospace Engineering*, vol. 221, no. 2, pp. 165–174, 2007.

[79] I. Hwang and C. Seah, "Intent-based probabilistic conflict detection for the next generation air transportation system," *Proceedings of the IEEE*, vol. 96, no. 12, pp. 2040–2059, 2008.

[80] M. Shirakawa, Y. Sumiya, and S. Ozeki, "A numerical evaluation method of the revised acas algorithms using a smoothed spline interpolation," in *Aerospace Conference Proceedings, 2000 IEEE*, vol. 1. IEEE, 2000, pp. 539–545.

[81] J. Kuchar, J. Andrews, A. Drumm, T. Hall, V. Heinz, S. Thompson, and J. Welch, "A safety analysis process for the traffic alert and collision avoidance system (tcas) and see-and-avoid systems on remotely piloted vehicles," in *AIAA 3rd" Unmanned Unlimited" Technical Conference, Workshop and Exhibit, September 20-23 2004, Chicago, Illinois*, 2004.

[82] A. Isaac, X. Zhang, P. Willett, and Y. Bar-Shalom, "A particle filter for tracking two closely spaced objects using monopulse radar channel signals," *Signal Processing Letters, IEEE*, vol. 13, no. 6, pp. 357–360, 2006.

[83] ReBEL, "Recursive Bayesian Estimation Library and Toolkit for Matlab," http://choosh.csee.ogi.edu/rebel/, 2011, [Online; accessed 19-Jun-2011].

[84] J. Fan, J. Ford, and L. Gonzalez, "Separation management approaches during periods of communication failure," 2010.

[85] J. Murray, C. Miner, N. NWS, and T. Ryan, "Environmental information for the next generation air transportation system," in *16th Conference on Satellite Meteorology and Oceanography*, 2009.

[86] H. Erzberger, "Transforming the nas: The next generation air traffic control system," in *Proceedings of the 24th Int. Congress of the Aeronautical Sciences (ICAS)*, 2004.

[87] R. Clothier, R. Walker, R. Baumeister, M. Brunig, J. Roberts, A. Duggan, and M. Wilson, "The smart skies project," *Aerospace and Electronic Systems Magazine, IEEE*, vol. 26, no. 6, pp. 14–23, 2011.

[88] O. Techakesari and J. Ford, "Automated centralised separation management with onboard decision support," 2010.

[89] A. Lacher, D. Maroney, and A. Zeitlin, "Unmanned aircraft collision avoidance–technology assessment and evaluation methods," in *The 7th Air Traffic Management Research & Development Seminar Barcelona, Spain*, 2007.

[90] R. Baumeister, R. Estkowski, G. Spence, and R. Clothier, "Test architecture for prototyping automated dynamic airspace control," 2009.